air

Refinement Study of Dry Deposition Inference Methods Used in Alberta

Alberta
Environment

Refinement Study of Dry Deposition Inference Methods Used in Alberta

Prepared for
Alberta Environment
Edmonton, AB

Final Report

By:
WBK & Associates Inc.
12 Hart Place
St Albert, AB T8N 5R1

June 2007

Publication Number:
ISBN: 978-0-7785-7585-6 (Printed)
ISBN: 978-0-7785-7586-3 (On-line)
Web Site: http://www.gov.ab.ca/env/

Any comments, questions, or suggestions regarding the content of this document may be directed to:

Air Policy Branch
Alberta Environment
11th Floor, Baker Centre
10025-106 Street
Edmonton, AB
T5J 1G4
Fax: (780) 644- 8946

Additional copies of this document may be obtained by contacting:

Information Centre
Alberta Environment
Main Floor, Oxbridge Place
9820 – 106th Street
Edmonton, Alberta T5K 2J6
Phone: (780) 427-2700
Fax: (780) 422-4086
Email: env.infocent@gov.ab.ca

FOREWORD

Acid deposition occurs when acidifying pollutants emitted from anthropogenic and other processes undergo chemical reactions in the atmosphere and fall to the earth as wet deposition (rain, snow, cloud, fog) or dry deposition (dry particles, gas). Acidic pollutants can be transported long distances in the atmosphere from their sources and eventually be deposited in ecosystems over broad regional scales and in locations far from the emission sources.

Dry deposition is generally more a local problem than wet deposition. Direct measurement of dry deposition rates is difficult. Dry deposition depends on many factors, including: meteorological conditions, characteristics of the pollutants being deposited (e.g. different gaseous chemical and particle size), and characteristics of the surface on which deposition occurs.

The most accepted and common method for estimating dry deposition is the so-called "inference method." The inferential method is a combination of measurement and modeling that involves indirect estimation of dry deposition rates on the basis of routinely measured air concentrations and meteorological parameters. The method is based on an assumed steady-state relationship $F = V_d C$, where the dry deposition flux or rate (F) is a product of the dry deposition velocity (V_d) and the concentration (C) of an airborne pollutant.

A series of studies have been initiated by AENV to evaluate the inference method and search for the most suitable and simple model for deposition rate estimations in Alberta. This report documents the third study in the series. Titles for the reports of the other studies are: "*Review and Assessment of Methods for Monitoring and Estimating Dry Deposition in Alberta*", and "*Dry Deposition Monitoring Method in Alberta*". It is anticipated that once all necessary information is gathered, an Alberta protocol for dry deposition measurement will be prepared.

Lawrence Cheng, Ph. D.
Air Policy,
Climate Change, Air and Land Policy Branch

SUMMARY

Environment Canada developed a dry deposition inference model to predict deposition of gaseous and particulate species onto land or water in Canada. Alberta Environment has developed a dry deposition inference model to similarly predict deposition of gaseous and particulate species onto land and water in Alberta. While numerous dry deposition inference models are used in practice in North America, uncertainty exists in results from these models because of an inability to take direct measurements to test their validity.

The objectives of this study were to examine the performance of the Alberta Environment inference model for predicting dry deposition in Alberta; and to identify and recommend changes to a number of assumptions and boundary conditions in the model to improve its performance relative to the Environment Canada inference model. The following findings and recommendations are noted:

1. The three most important species contributing to potential acid input among eleven species considered in the Alberta Environment model were SO_2, NO_2, and HNO_3.

2. Sensitivity testing of resistance factors (R_a, R_b, and R_c) used in Alberta Environment's model showed that step changes in the magnitude of R_c are much more important in influencing total deposition compared to step changes in R_a or R_b for all depositing species examined. This is generally consistent with scientific literature.

3. AENV model performance in terms of overall deposition flux of 11 species was observed to be closely dependent on deposition velocity modeling for SO_2 and NO_2; particularly with respect to selection of R_c values used to parameterize these gases. Relative to performance of the ENVC model, values used to represent R_c in the AENV model were less conservative for SO_2 in winter and spring and more conservative in summer and autumn. For NO_2, values used to represent R_c in the AENV model were less conservative in autumn and winter and more conservative in spring and summer. For HNO_3, deposition in the AENV model was driven by R_b. These differences do not necessarily imply problems in the AENV model. The ENVC inference model does not necessarily represent the best set of assumptions and conditions to parameterize dry deposition. In addition, AENV's parameterization of R_c originates from previously published values that are seasonal- and species-specific and, therefore, can be considered reasonable.

4. R_a is an indication of the mixing conditions in the atmosphere such that a very low R_a implies maximum mixing conditions (experienced during daytime). Setting a minimum value of 5 s/m for R_a in the Alberta Environment model had only a small positive change in model performance relative to the Environment Canada model. Although the effect of this change is small, it is recommended for future use because a minimum limit for R_a acknowledges that there is always some limit to mixing possible in an atmosphere.

5. Setting a maximum value of 1000 s/m for R_a in the Alberta Environment model resulted in better agreement in overall deposition flux of species relative to the Environment Canada model for the conditions tested. Very high R_a values would be associated with no mixing in the atmosphere (ideal stable night time conditions). An extremely high R_a value would not necessarily offer a reasonable representation of natural conditions. From a practical point of view, large or moderately large R_a values (and correspondingly small or moderately small deposition velocity and deposition fluxes) are unimportant. This upper limit is recommended for future use in the Alberta Environment model.

6. The Monin-Obukhov length is used in calculation of the stability function which is ultimately used to calculate R_a. Maximum and minimum values of -5 and 5 m for negative and positive limits are recommended for future use in the Alberta Environment model as small absolute Monin-Obukhov length values correspond to extremes which are not representative of natural conditions.

7. A minimum wind speed value of 1 m/s is recommended for future use in the Alberta Environment model.

8. As part of the calculation steps for R_a, minimum requirements discussed in more detail in this report are recommended on how to calculate surface roughness length (z_o) as a monthly average using hourly data where the wind speed is >6 m/s in the Alberta Environment model.

9. Wetness alters the characteristics of a surface to act a sink for depositing species (primarily gases). The Alberta Environment model requires an hourly measurement to represent the amount of wetness on a surface in determination of surface resistance (R_c). The model is set up to use field measurement data from surface wetness sensing equipment. However, past experience has indicated that this field equipment does not provide reliable measurement data in an Alberta setting due to the wide range of climatic conditions experienced. Alternatively, the model allows a relative humidity measurement cutoff (87%) to be used as an approximation to represent a surface as being wet. It is recommended that this criterion be maintained in the model for future use.

TABLE OF CONTENTS

FOREWORD i
SUMMARY ii
LIST OF TABLES vi
LIST OF FIGURES viii

1.0 Introduction 1
1.1 Background 1
1.2 Objectives 1
1.3 Report Organization 2

2.0 Acid Deposition Background 4
2.1 Introduction to Dry Deposition 4
2.2 Inferential Methods 4
2.3 Deposition Velocity 5
2.3.1 Gaseous Deposition 6
2.3.2 Particles 7
2.4 Dry Deposition Model Issues 10

3.0 Model Descriptions 12
3.1 Environment Canada (ENVC) Model 12
3.1.1 Gases 12
3.1.2 Particulates 14
3.1.3 Alberta Environment (AENV) Model 15
3.1.4 Gases 15
3.1.5 Particulates 15

4.0 Dry Deposition Modeling for ENVC and AENV Models 17
4.1 Model Methods for Coniferous Forest (Base Case) 17
4.1.1 Input Parameters for Modeling 17
4.1.2 Atmospheric Concentrations of Chemical Species 18
4.2 Model Results – Coniferous Forest 19
4.2.1 Deposition Flux 19
4.2.2 Deposition Velocities – Coniferous Forest 20
4.2.2.1 Deposition Behavior of Gases (SO_2, NO_2, HNO_3, HNO_2) 20
4.2.2.2 Fine Particle (SO_4^{2-}, NH_4^+) Deposition Behavior 24
4.2.2.3 Coarse Particle (NO_3^-, Na^+, K^+, Ca^{2+}, Mg^{2+}) Deposition Behavior 25
4.3 Model Methods for Other Land Use Categories 26
4.4 Model Results – Coniferous Forest 27
4.4.1 Deposition Flux 27
4.4.2 Resistance Factors and Deposition Velocities 35
4.4.2.1 Gaseous Deposition (SO_2, NO_2, HNO_3) 36
4.4.2.2 Fine and Coarse Particle Deposition (SO_4^{2-}, NH_4^+, NO_3^-, Na^+, K^+, Ca^{2+}, Mg^{2+}) 46

5.0 Model Evaluation **51**
5.1 Resistance Factors 51
5.1.1 Evaluation Methods *51*
5.1.2 Results 51
5.1.2.1 Dominant (Influential) Resistance Factors **51**
5.1.2.2 Sensitivity Testing of Resistance Factors **53**
5.1.2.3 Performance Indicators for AENV Model **55**
5.2 Parameter Boundary Conditions 56
5.2.1 Evaluation Methods *56*
5.2.2 Results 56
5.2.2.1 Aerodynamic Resistance **56**
5.2.2.2 Monin-Obukhov Length **59**
5.2.2.3 Minimum Wind Speed **60**
5.3 Non-Boundary Condition Components 62
5.3.1 Evaluation Methods *63*
5.3.1.1 Surface Roughness Length **63**
5.3.1.2 Surface Wetness and Relative Humidity **64**
5.3.1.3 Settling Properties of Large Particle Size Distributions **64**
5.3.2 Results 65
5.3.2.1 Surface Roughness Length **65**
5.3.2.2 Surface Wetness and Relative Humidity **67**
5.3.2.3 Particulate Size Distributions **74**

6.0 Findings and Recommendations **77**

7.0 References **82**

Appendix A Environment Canada Calculation Methods for Gases and Particulates **86**
Appendix B Alberta Environment Calculation Methods for Gases and Particulates **103**
Appendix C Monthly Average Species Concentrations **111**
Appendix D Tables for Monthly Deposition Velocities of Component Chemicals **113**
Appendix E Monthly Averaged Diurnal Deposition Velocities for SO_2, NO_2, and HNO_3 ..... **117**
Appendix F Counts for Resistance Factors **129**
Appendix G Breakdown of Chemicals Contributing to Differences in Deposition Caused by Percent Changes of Resistances (R_a, R_b, and R_c) **137**
Appendix H Deposition Contributions for Species associated with Large Particles **143**

LIST OF TABLES

Table 1 Boundary conditions evaluated during study..... 3

Table 2 Comparison of monthly summed deposition flux (kg H^+/ha) for 11 species to a coniferous forest cover using the AENV and ENVC models.....19

Table 3 Breakdown of magnitude of differences in monthly summed deposition flux in kg H^+/ha for individual species between deciduous forest and coniferous forest cover using the AENV model. 28

Table 4 Breakdown of magnitude of differences in monthly summed deposition flux in kg H^+/ha for individual species between wetland/swamp and coniferous forest cover using the AENV model. 29

Table 5 Breakdown of magnitude of differences in monthly summed deposition flux in kg H^+/ha for individual species between grassland and coniferous forest cover using the AENV model. 30

Table 6 Breakdown of magnitude of differences in monthly summed deposition flux in kg H+/ha for individual species between cropland and coniferous forest cover using the AENV model. 32

Table 7 Breakdown of magnitude of differences in monthly summed deposition flux in kg H+/ha for individual species between urban and coniferous forest cover using the AENV model. 33

Table 8 Breakdown of magnitude of differences in monthly summed deposition flux in kg H+/ha for individual species between water and coniferous forest cover using the AENV model. 34

Table 9 Breakdown of magnitude of differences in monthly summed deposition flux in kg H+/ha for individual species between snow/ice and coniferous forest cover using the AENV model. 36

Table 10 Monthly average relative humidity level (%) for data used to evaluate AENV model. 40

Table 11 Counts of hourly Ra values within a maximum of 1000 s/m for the AENV model run with an allowable upper limit of 1000 s/m for a coniferous forest cover.....57

Table 12 Comparison of monthly summed deposition flux (g H+/ha) for AENV model with minimum Ra limit of 5 s/m to AENV base case model and ENVC model results for coniferous forest cover.....58

Table 13 Comparison of monthly summed deposition flux (g H+/ha) for AENV model with maximum Ra limit of 1000 s/m to AENV base case conditions and ENVC model results for coniferous forest cover. 59

Table 14 Monthly summed deposition flux (g H+/ha) for 11 species showing changes with and without limits set on L with AENV base case conditions and ENVC model results for a coniferous forest cover. 61

Table 15 Comparison of AENV total deposition for 1 m/s minimum limit on wind speed with AENV base case conditions and ENVC model results for a coniferous forest cover..... 62

Table 16 Monthly average surface roughness length (zo, m), standard deviation, and sample size (number of hourly values) in which wind speed >6 m/s for calculation of monthly average surface roughness length for a coniferous forest cover.....65

Table 17 Monthly average re-calculated surface roughness length (zo) values (m), standard deviation, and sample size (number of hourly values) for different wind speed criteria used in the re-calculation for a coniferous forest cover.....68

Table 18 Monthly calculated surface roughness length (z_o) values (m) and standard deviation for different wind speed ranges for a coniferous forest cover.....70

Table 19 Recommended changes to AENV acid deposition inference model. 80

LIST OF FIGURES

Figure 1 Possible interactions for potential inclusion in third-generation dry deposition inference models (Peters et al., 1995). 5

Figure 2 Relative locations where dry deposition resistance factors R_a, R_b, and R_c apply..... 7

Figure 3 Deposition velocity of particles as function of size in a stable atmosphere for two different roughness lengths (z_o, cm), particle densities (ρ, kg/m^3), and horizontal wind speed of 5 m/s using model of Sehmel and Hodgson, 1980 (as cited in Ruijgrok et al., 1995). 9

Figure 4 Scheme of resistance analogy in Environment Canada dry deposition inference model (after Zhang et al. 2003)..... 13

Figure 5 Comparison of monthly summed deposition flux for 11 species to a coniferous forest cover using the AENV and ENVC models..... 20

Figure 6 Comparison of monthly average SO_2 deposition velocity for a coniferous forest cover using the AENV and ENVC model. 21

Figure 7 Comparison of monthly average NO_2 deposition velocity for a coniferous forest cover using the AENV and ENVC model. 22

Figure 8 Comparison of monthly average HNO_3 deposition velocity for a coniferous forest cover using the AENV and ENVC model. 23

Figure 9 Comparison of monthly average HNO_2 deposition velocity for a coniferous forest cover using the AENV and ENVC model. 24

Figure 10 Comparison of monthly average small particle deposition velocity for a coniferous forest cover using the AENV and ENVC model. 25

Figure 11 Comparison of monthly average large particle deposition velocity for a coniferous forest cover using the AENV and ENVC model. 26

Figure 12 Comparison of monthly summed deposition flux for 11 species to a deciduous forest and coniferous forest cover using the AENV model..... 27

Figure 13 Comparison of monthly summed deposition flux for 11 species to wetland/swamp and coniferous forest cover using the AENV model. 29

Figure 14 Comparison of monthly summed deposition flux for 11 species to grassland and coniferous forest cover using the AENV model. 30

Figure 15 Comparison of monthly summed deposition flux for 11 species to cropland and coniferous forest cover using the AENV model. 31

Figure 16 Comparison of monthly summed deposition flux for 11 species to urban and coniferous forest cover using the AENV model. 33

Figure 17 Comparison of monthly summed deposition flux for 11 species to water and coniferous forest cover using the AENV model. 34

Figure 18 Comparison of monthly summed deposition flux for 11 species to snow/ice and coniferous forest cover using the AENV model. 35

Figure 19 Comparison of SO2 monthly average surface resistance (Rc) for a deciduous forest and coniferous forest (base case) cover using the AENV model. 37

Figure 20 Comparison of SO2 monthly average surface resistance (Rc) for wetland/swamp and coniferous forest (base case) cover using the AENV model..... 38

Figure 21 Comparison of SO2 monthly average surface resistance (Rc) for a grassland and coniferous forest (base case) cover using the AENV model..... 38

Figure 22 Comparison of SO2 monthly average surface resistance (Rc) for a cropland and coniferous forest (base case) cover using the AENV model..... 39

Figure 23 Comparison of SO2 monthly average surface resistance (Rc) for urban and coniferous forest (base case) cover using the AENV model..... 40

Figure 24 Comparison of SO2 monthly average surface resistance (Rc) for a water and coniferous forest (base case) cover using the AENV model..... 41

Figure 25 Comparison of SO_2 monthly average surface resistance (R_c) for snow/ice and coniferous forest (base case) cover using the AENV model..... 41

Figure 26 Comparison of NO2 monthly average surface resistance (Rc) for deciduous forest and coniferous forest (base case) cover using the AENV model. 42

Figure 27 Comparison of NO_2 monthly average surface resistance (R_c) for wetland/swamp and coniferous forest (base case) cover using the AENV model..... 43

Figure 28 Comparison of NO2 monthly average surface resistance (Rc) for grassland and coniferous forest (base case) cover using the AENV model..... 43

Figure 29 Comparison of NO_2 monthly average surface resistance (R_c) for cropland and coniferous forest (base case) cover using the AENV model..... 44

Figure 30 Comparison of NO2 monthly average surface resistance (Rc) for urban and coniferous forest (base case) cover using the AENV model..... 44

Figure 31 Comparison of NO2 monthly average surface resistance (Rc) for water and coniferous forest (base case) cover using the AENV model..... 45

Figure 32 Comparison of NO_2 monthly average surface resistance (R_c) for snow/ice and coniferous forest (base case) cover using the AENV model..... 45

Figure 33 Comparison of monthly average deposition velocity of small and large particles for a deciduous forest and coniferous forest (base case) cover using the AENV model..... 47

Figure 34 Comparison of monthly average deposition velocity of small and large particles for a wetland/swamp and coniferous forest (base case) cover using the AENV model..... 47

Figure 35 Comparison of monthly average deposition velocity of small and large particles for grassland and coniferous forest (base case) cover using the AENV model. 48

Figure 36 Comparison of monthly average deposition velocity of small and large particles for cropland and coniferous forest (base case) cover using the AENV model. 48

Figure 37 Comparison of monthly average deposition velocity of small and large particles for urban and coniferous forest (base case) cover using the AENV model. 49

Figure 38 Comparison of monthly average deposition velocity of small and large particles for water and coniferous forest (base case) cover using the AENV model. 49

Figure 39 Comparison of monthly average deposition velocity of small and large particles for snow/ice and coniferous forest (base case) cover using the AENV model. 50

Figure 40 Monthly summed deposition flux for 11 species using AENV model showing influence of step changes in R_a for a coniferous forest cover. 53

Figure 41 Monthly summed deposition flux for 11 species using AENV model showing influence of step changes in R_b for a coniferous forest cover. 54

Figure 42 Monthly summed deposition flux for 11 species using AENV model showing influence of step changes in R_c for a coniferous forest cover. 55

Figure 43 Monthly summed deposition flux for 11 species using AENV model showing changes with and without (base case) minimum 5 s/m and maximum 1000 s/m limits to hourly R_a values for a coniferous forest cover..... 60

Figure 44 Monthly summed deposition flux for 11 species using AENV model showing influence with and without (base case) limits on L for a coniferous forest cover..... 61

Figure 45 Monthly summed deposition flux for 11 species using AENV model showing the influence of with and without (base case) a 1 m/s minimum limit on wind speed for a coniferous forest cover..... 63

Figure 46 Monthly summed deposition flux for 11 species using AENV model showing influence resulting from corrected z_o values for the months of February, March, and November for a coniferous forest cover..... 67

Figure 47 Annual average re-calculated surface roughness length (zo) values (m) for different wind speed criteria used in the re-calculation for a coniferous forest cover..... 69

Figure 48 Monthly summed deposition flux for 11 species using AENV model showing influence of using a different RH cutoff for establishing a surface as wet (base case RH = 0.87) for deciduous forest cover..... 71

Figure 49 Monthly summed deposition flux for 11 species using AENV model showing influence of using a different RH cutoff for establishing a surface as wet (base case RH = 0.87) for a coniferous forest cover. 71

Figure 50 Monthly summed deposition flux for 11 species using AENV model showing influence of using a different RH cutoff for establishing a surface as wet (base case RH = 0.87) for wetland/swamp cover..... 72

Figure 51 Monthly summed deposition flux for 11 species using AENV model showing influence of using a different RH cutoff for establishing a surface as wet (base case RH = 0.87) for grassland..... 72

Figure 52 Monthly summed deposition flux for 11 species using AENV model showing influence of using a different RH cutoff for establishing a surface as wet (base case RH = 0.87) for cropland. 73

Figure 53 Monthly summed deposition flux for 11 species using AENV model showing influence of using a different RH cutoff for establishing a surface as wet (base case RH = 0.87) for urban cover. 73

Figure 54 Monthly summed deposition flux for 11 species using AENV model showing influence of using a different RH cutoff for establishing a surface as wet (base case RH = 0.87) for snow/ice 74

Figure 55 Monthly summed deposition flux for 11 species for AENV model base case, ENVC model, and ENVC model corrected for large particle size distribution for a coniferous forest cover. 75

Figure 56 Monthly summed deposition flux for 11 species using modified AENV model compared to original AENV model and ENVC model for a coniferous forest cover. 81

1.0 INTRODUCTION

1.1 Background

Environment Canada (ENVC) developed a dry deposition inference model to predict deposition of gaseous and particulate species onto land or water in Canada (Zhang et al., 2003a, 2003b, 2002, 2001; Brook et al., 1999). Environment Canada's model uses pollutant and meteorological data collected from the Canadian Air and Precipitation Monitoring Network (CAPMoN) (Brook et al., 1999). Alberta Environment (AENV) has developed a dry deposition inference model (Cheng et al., 2001) to similarly predict deposition of gaseous and particulate species onto land and water in Alberta. Both approaches are a form of dry deposition inference modeling.

Dry deposition inferential models evolved from methods used by meteorologists and foresters to characterize H_2O, CO_2, heat, and momentum exchange between the atmosphere and plant canopies. While numerous dry deposition inference models are used in practice in North America and elsewhere, uncertainty exists in results from these models because of an inability to take direct measurements to test their validity (Lovett, 1994). Dry deposition inference models should have the capability to represent dry deposition of atmospheric pollutants in a manner that reflects current scientific understanding. Also important, results from any one approach should compare reasonably well with other approaches used to represent dry deposition. It has however been noted by Wesely and Hicks (2000) that further work on parameterizing inferential models is necessary before resultant dry deposition estimates can be considered reliable and this needs to be considered when interpreting and applying model outputs.

Alberta Environment is interested in developing their dry deposition inference model for wider use in Alberta. WBK & Associates Inc. (WBK, 2008) undertook initial testing of the ENVC and AENV models using a common set of meteorological and pollutant data to examine how they compared for predicting dry deposition of eleven gaseous and particulate species. Initial findings of this work indicated both models gave comparable results for amounts of dry deposition for gaseous and inorganic species on a monthly and annual basis. One of the recommendations from this study was to undertake further comparative testing of these two models to better understand reasons why model results departed from each other.

1.2 Objectives

Further investigation of the AENV and ENVC dry deposition inference models was undertaken as a follow-up to recommendations of WBK (2008). The objectives of this study were: i) to examine the performance of the Alberta Environment inference model relative to the ENVC model for predicting dry deposition in Alberta; and ii) to use this performance comparison to recommend changes for a number of assumptions and

boundary conditions in the AENV inference model to improve its performance. The ENVC inference model does not necessarily represent the best set of assumptions and conditions to characterize dry deposition. However, results from any one approach should compare reasonably well with other approaches used to characterize dry deposition.

1.3 Report Organization

Dry deposition is initially discussed and general modeling approaches of acid deposition are presented based upon current scientific literature. The ENVC modeling approach is presented in detail along with the AENV model. The discussion is split into gaseous and particulate deposition.

In general, the inference method involves indirect estimation of dry deposition rates on the basis of routinely measured air concentrations and meteorological parameters (WBK, 2006). The method is based on an assumed steady-state relationship $F = V_d C$, where dry deposition flux or rate (F) is a product of the dry deposition velocity (V_d) and the concentration (C) of an airborne pollutant. V_d is estimated on the basis of resistance models and is defined as – using an Ohm's law analogy – the inverse of the sum of multiple resistance factors (aerodynamic resistance (R_a), boundary-layer resistance (R_b), and surface resistance (R_c)) (Wesely and Hicks, 2000, 1977). Gaseous deposition is discussed according to the three major resistance pathways and particulate deposition is discussed according to important acidic species (sulfate, nitrate, and ammonium) and base cations (calcium, magnesium, potassium and sodium).

The AENV model was run using different boundary conditions for selected model parameters and the results were compared with the model run under original conditions for similar inputs. A number of the different boundary conditions were based on conditions set in the ENVC model. A summary of conditions evaluated is presented in Table 1. Finally, the AENV model was run using different boundary conditions and compared with the ENVC model run using similar inputs. Based upon comparisons of results for these sets of model runs, recommendations were made about how best to proceed with using assumptions and boundary conditions for operating the AENV model in the future.

Table 1 Boundary conditions evaluated during study.

Parameter	Units	Original Default	Revised Default Evaluated	Basis for Revision
R_a	s/m	upper limit undefined	upper limit capped at 1000 s/m (at 2000 s/m for water)	limit set in ENVC model
R_a	s/m	lower limit undefined	lower limit capped at 5 s/m	limit set in ENVC model
Monin-Obukhov length	m	undefined limit	upper limit of -5 m on negative side and lower limit of +5 m on positive side	limit set in ENVC model
wind speed	m/s	set to 0 m/s if less than 0.09 m/s	set to 1 m/s if less than 1 m/s	limit set in ENVC model

2.0 ACID DEPOSITION BACKGROUND

2.1 Introduction to Dry Deposition

Acid rain may contribute to acidification of terrestrial and aquatic systems (AENV, 1999). A portion of the deposited nitrogen may also contribute to terrestrial fertilization and/or aquatic eutrophication. Acid rain involves three processes including: transport, transformation, and deposition (Wesely and Hicks, 1977). Acid deposition can occur by wet and dry processes. Dry deposition is reported to represent about 40% of total deposition (Smith et al., 2000).

Increased industrialization in Alberta, particularly oil sands extraction and processing in north eastern Alberta and petroleum upgrading and refining activities in central Alberta, is raising awareness about potential acid deposition due to industrial activities. A critical load method is used in Alberta as a receptor-based approach for managing acid deposition (AENV, 1999). Since it is very difficult to directly measure dry deposition, models are essential for the estimation of the amount of dry deposition that a particular land type will experience given an atmospheric concentration of a depositing species.

Dry depositing species can be divided into sulfur compounds, nitrogen compounds, and base cations. Sulfur compounds of interest include a gaseous sulfur dioxide (SO_2) and particulate sulfate (SO_4^{2-}). Nitrogen compounds include several gases – nitrogen dioxide (NO_2), nitric acid (HNO_3), nitrous acid (HNO_2), nitric oxide (NO), and ammonia (NH_3). Particulate forms of nitrogen include nitrate (NO_3^-) and ammonium (NH_4^+). Base cations include particulate calcium (Ca^{2+}), sodium (Na^+), potassium (K^+), and magnesium (Mg^{2+}).

2.2 Inferential Methods

The inferential method refers to a method of approximating deposition processes with a resistance analogy (Hicks et al., 1987). The inferential method reflects the concept that different surfaces will experience different deposition. Early inference models approximated the entire canopy as one large surface and were referred to as a "big-leaf" method (Hicks et al., 1987). A two-big-leaf model evolved to emphasize separate treatment of sunlit and shaded portions of a canopy (Zhang et al., 2001a, 2001b).

Multi-layer models (MLMs) or second generation models have evolved that include integration of deposition along the canopy height of vegetation (Meyers et al., 1998). Peters et al. (1995) reported that third generation models will include interactions among chemistry, deposition processes, and meteorology; and may include physiological phenomena such as photosynthesis and CO_2 production (Niyogi et al., 2003). Consequently, third generation models will be highly complex. A schematic of possible interrelations showing this complexity is included in Figure 1.

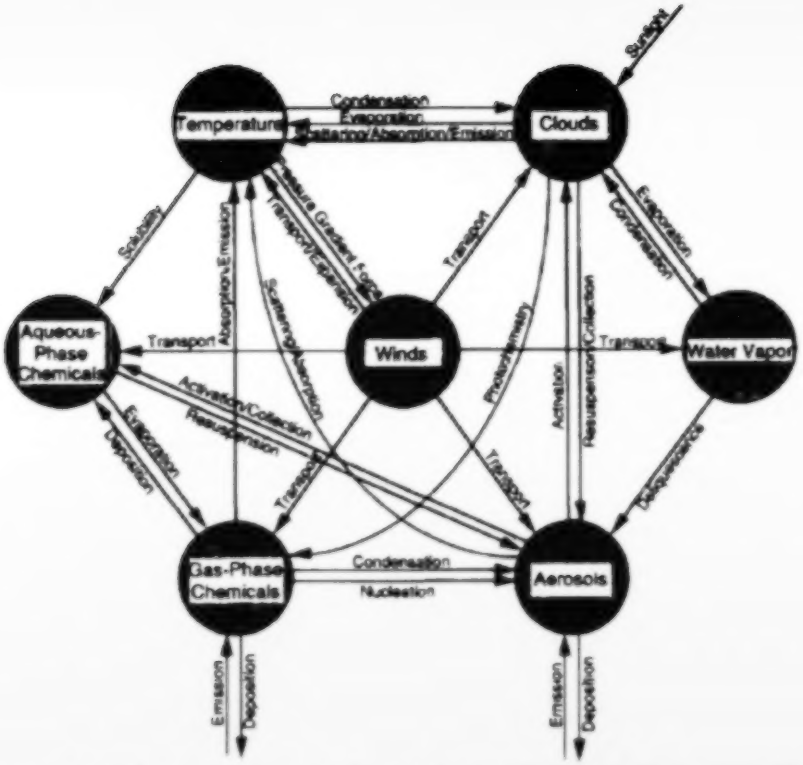

Figure 1 **Possible interactions for potential inclusion in third-generation dry deposition inference models (Peters et al., 1995).**

2.3 Deposition Velocity

Deposition velocity is a parameter multiplied by the concentration of a chemical in air in order to calculate chemical flux or deposition rate (Wesely and Hicks, 2000). Values for deposition velocities are reported to range from 0 cm/s for inert substances to about greater than 2 cm/s for reactive substances such as nitric acid (HNO_3) (Wesely and Hicks, 2000). Deposition velocities are quoted in several units including m/s, mm/s, or cm/s, the latter being the most commonly used. The behavior of gaseous ammonia near a soil surface is bidirectional as both deposition to and emission from soil occurs, depending upon ambient concentrations. The concept of deposition velocity should not be used for ammonia at very low ambient concentrations because it may originate from soil and it violates an assumption that the flux is unidirectional (towards the surface) (Hicks et al., 1987; Wesely and Hicks, 2000).

2.3.1 Gaseous Deposition

Deposition velocity is commonly modeled as three resistances in series (Hicks et al., 1987). These resistances include: aerodynamic resistance (R_a) associated with turbulent transfer, boundary layer resistance across the near-surface layer (R_b), and surface resistance involving the pollutant-surface interaction (R_c) (Voldner et al., 1986). Parameterization methods for representing these resistances in the Environment Canada and Alberta Environment inference methods are presented in detail in Appendix A and B, respectively.

Aerodynamic Resistance (R_a)

Parameters used for modeling aerodynamic resistance are meteorological-specific, including: wind speed, wind direction, and air temperature at two heights above the ground (usually 2 and 10 m). Modeled R_a values vary depending upon stability and surface roughness conditions, which are determined using these parameter inputs. Most inference methods represent surface roughness by using default values for different sets of surface roughness conditions (e.g., Voldner et al., 1986). Because the input parameters are meteorological- and not chemical-specific, the aerodynamic resistance term is independent of chemical species.

Boundary Layer Resistance (R_b)

The boundary layer is a thin layer next to the surface (refer to Figure 2). Molecular diffusion determines gas transfer while Brownian diffusion and inertial impact determine particle transfer (WBK, 2008). Parameters needed for this resistance term include: wind speed, roughness length, and temperature. R_b is usually smaller than aerodynamic resistance; which means it is usually less very important for deposition velocity calculations (Walcek et al, 1986).

Total Surface Resistance (R_c)

R_c includes all processes involving the actual surface and the particular chemical of interest (Hicks et al., 1987). Most of the difference between inference models is in the modeling of surface resistance. As models evolve to include more and more physiological phenomena, variables such as soil pH, surface wetness, and photo synthetically active radiation are required (Wesely and Hicks, 2000). These variables can be difficult or expensive to obtain (measure).

Sophisticated parameterizations of R_c have represented it as a series of multiple resistances and leaf area index of the canopy, for example (Zhang et al., 2003): stomatal resistance, mesophyll resistance, in-canopy aerodynamic resistance, ground resistance, and canopy cuticle resistance. Stomatal resistance involves a gas entering the leaf through the stomata. Mesophyll resistance involves resistance to a gas dissolving in the

mesophyll cells in the interior of the leaf. In-canopy aerodynamic resistance refers to meteorological issues within the canopy, including temperature gradients. Ground resistance includes resistance of soil, ground litter, and any water surface under the canopy.

Figure 2 **Relative locations where dry deposition resistance factors R_a, R_b, and R_c apply.**

For a water surface or even water on the surface of soil or vegetation, R_c parameterizations can include aspects of the nature of the water itself in terms of parameters such as: pH, concentration of the chemical already dissolved, and surface characteristics of the water (Zhang et al., 2003). Canopy cuticle resistance includes interaction with the cuticular surface of the plant. Alternatively, simpler parameterizations of R_c have represented it as a series of default values for different surface conditions represented by season, time of day, and surface wetness condition (Voldner et al., 1986).

2.3.2 Particles

Particles in the atmosphere containing chemical species or elements tend to have a range of sizes that can be represented as a log-normal distribution (Ruijgrok et al., 1995). Larger mass median elements tend to have a unimodal distribution while smaller mass median elements (≤2 µm in diameter) tend to have a bimodal distribution (Milford and Davidson, 1985). The general size distribution of a particle typically depends upon its origin. Particles can be divided into three size modes (Holsen and Noll, 1992):

- The largest mode (≥2.5µm) results from mechanical abrasion and wind erosion.
- Fine mode particles (0.1 to 2.5 µm) originate through coagulation processes and are primary aerosol emissions.
- The smallest particles (<0.1 µm) are secondary products of emissions.

Gases may also react with larger particles and be present in larger particles (Ruijgrok et al., 1995). This duality of origin may explain the bimodal shape of the size distribution. Atmospheric chemical reactions involving gaseous precursors to particulates can be affected by presence of other chemicals (Ruijgrok et al., 1995). Nitrate may reside on large particles as a result of reactions of nitric oxide with alkaline species of crustal origin (Ruijgrok et al., 1995; Wolff, 1984). If ammonia gas is present, which is common in animal feedlot areas, nitric oxide may react with it, resulting in nitrate (and ammonium) on small particles (Ruijgrok et al., 1995; Wolff, 1984).

When modeling particulate deposition, it is important that the size distributions are reasonable representations of conditions for an area being modeled. Neighboring salt water bodies (i.e., near coastal areas), animal feedlots, and soil types can all strongly influence size distribution of particulate matter. Thus particle size distributions may be different for different areas or different times of the year (Ruijgrok et al., 1997; Wiman and Agren, 1985; Whitby, 1978; Milford and Davidson, 1985; Hoff et al., 1983). Arimoto et al. (1997) stated that mass particle size distributions may never reach equilibrium. In addition, Hedin et al. (1994) stated that the amount of atmospheric cations may be declining over time.

Models that represent deposition based on particle size are considered process-oriented models; as opposed to bulk resistance-oriented models that do not distinguish for particle size (Ruijgrok et al., 1995). Particle deposition mechanisms include (Slinn, 1982): diffusion, interception, impaction, gravitational settling, and phoretic mechanisms. Brownian diffusion dominates small particle (<0.1 μm) deposition; whereas gravitational sedimentation dominates large particle (≥ 2.5 μm) deposition. Figure 3 illustrates that deposition velocities are highest for large particles and are controlled by sedimentation. Deposition velocities reach a minimum for particles from 0.1 to 1 μm in size.

Process-oriented models can be further increased in complexity by inclusion of phoretic effects; including electrophoresis, thermophoresis, and diffusiophoresis (Ruijgrok et al., 1995). Hygroscopic growth of particles can be an issue for high relative humidities (>80%) (Draaijers et al., 1997; Ruijgrok et al., 1995). For example, an inference model used by Erisman et al. (1997) includes cases for wet and dry surface conditions as well as for relative humidity above and below 80%. Another complication not commonly addressed in particle deposition models is that Brownian diffusion will decrease if a gas becomes attached to a particle (Sehmel, 1980). Finally, atmospheric stability issues may be a concern if a model was only designed for neutral stability conditions (Ruijgrok et al., 1995).

High deposition velocities related to sedimentation of large particles result in models that can be extremely sensitive to the method used to represent the large size end of the size distribution (Holsen and Noll, 1992). Solely using the mass median diameter (MMD) to represent particle size without integrating across the whole size distribution can cause large differences in model results (Ruijgrok et al., 1995). Ideally, it is very important to represent the distribution as divided into sufficiently small portions so that the full effects

of the large particle end of a distribution can be properly represented. For example, when using 1, 6, or 100 different diameters to represent the distribution for sodium-bound particulates (mean MMD of 6.5 µm); Dulac et al. (1987) calculated mean dry deposition fluxes as 915, 700, and 30,000 $\mu g/m^2$/day, respectively.

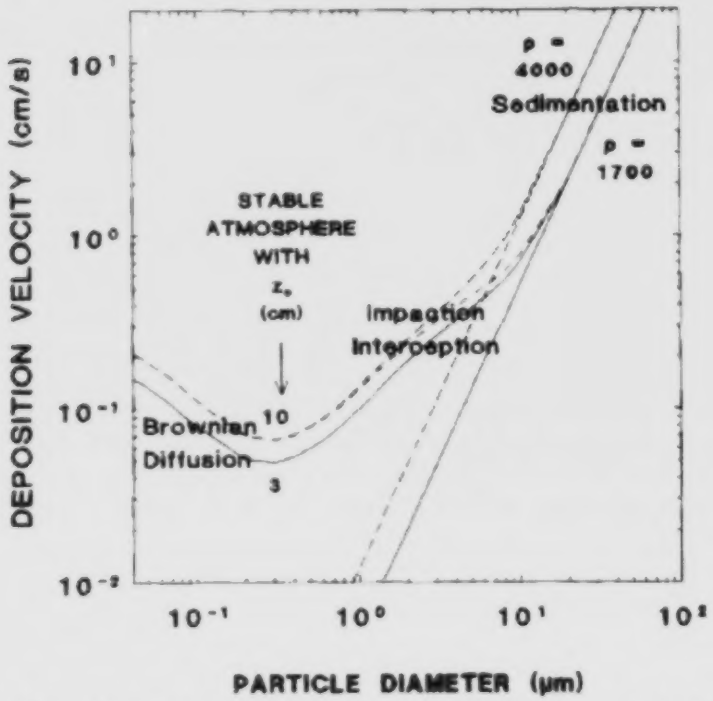

Figure 3 **Deposition velocity of particles as function of size in a stable atmosphere for two different roughness lengths (z_0, cm), particle densities (ρ, kg/m^3), and horizontal wind speed of 5 m/s using model of Sehmel and Hodgson, 1980 (as cited in Ruijgrok et al., 1995).**

Large particles, while rarer, can be responsible for more than 90% of the flux of a chemical because of large deposition velocities (Holsen and Noll, 1992). For large particles, process-oriented models using numerous size distributions are highly sensitive to selection of the largest particle size as well as to representativeness of the lognormal distribution (Holsen and Noll, 1992). Particles originating from crustal material tend to be large (≥60 to 100 µm) (Ruijgrok et al., 1995.) Given that larger particles mostly contain base cations which act to reduce the impact of acidic components, underestimating the amount of deposition of these larger particles may act as a safety factor in estimation of net total acid deposition or potential acid input (PAI).

2.4 Dry Deposition Model Issues

Dry deposition can be difficult to model because of scientific complexities and the limitations in approaches used to represent these complexities. Others have reported that it is not possible to incorporate all relevant physiological and atmospheric processes into an acid deposition model for several reasons (Lovett, 1994; Venkatram et al., 1988):

- Incomplete understanding of the processes involved.
- Limitations in computational capacity.
- Limitations in model validation, including limitations of measuring equipment.

Wesely and Hicks (2000) state that there is an extremely large number of processes involved in the transfer of a chemical from air to a surface. Phenomena that are currently difficult to represent in a deposition model include (Wesely and Hicks, 2000; Lovett, 1994; Venkatram et al., 1988): surface wetness, surface roughness, edge effects, in-canopy chemical reactions, and bi-directional chemical gradients.

Computational capacity is always an issue in modeling and models are usually designed up to the limits of the applicable computer processing speed and capacity (Venkatram et al., 1988). Modeling natural processes always involves approximating complicated relationships, including: interactions, thresholds, and feedback loops. In this study, the requirement to have a model that is relatively easy to use was an important priority so that others could readily employ it to estimate acid deposition behavior in Alberta.

Model validation is of particular concern in acid deposition. Current measurement equipment is not able to detect small concentrations rapidly enough to detect or to measure deposition phenomena. Eddy correlation techniques are reported to be the most sophisticated approaches for measuring dry deposition (Meyers et al., 1996; Lovett, 1994), however, this method requires sensitive anemometry and rapid-response pollutant monitoring equipment (Lovett, 1994). In addition, errors in measurement techniques are reported to frequently be higher than 40% (Businger, 1986). Finally, there is uncertainty as to whether deposition information gathered at one location in one time period can be applied to represent different locations or at different times.

Wesely and Hicks (2000) reported that quasi-comparisons of model results with deposition measurements have shown differences as large as +/-30%. These comparisons refer only to converting measured ambient concentrations into deposition estimates and not the element of computer dispersion modeling that translates emission estimates into ambient concentrations; which introduces another source of uncertainty into modeled deposition estimates.

In addition, Wesely and Hicks (2000) state that the Ohm's law analogy for representing deposition velocity is likely an oversimplification and that the role of plant physiological processes are not sufficiently incorporated into these models. For modeling gaseous deposition, possible modeling limitations can be due to a failure to adequately represent edge effects, heterogeneity of the landscape, and terrain complexity (Hicks et al., 1987).

Difficulties associated with modeling particle deposition mechanisms may result in underestimating particle deposition by as much as an order of magnitude (Holsen and Noll, 1992).

3.0 MODEL DESCRIPTIONS

3.1 Environment Canada (ENVC) Model

3.1.1 Gases

The gas module of the ENVC model calculates deposition velocity (V_d) as the inverse of the sum of three resistances (R_a, R_b, and R_c) as follows (Zhang et al. 2003):

$$V_d = \frac{1}{R_a + R_b + R_c} \tag{1}$$

Aerodynamic resistance (R_a) is calculated as:

$$R_a = \frac{1}{ku_*}\left[0.74\ln(z/z_0) - \psi_H\right] \tag{2}$$

using von Karman's constant (k), friction velocity (u_*), reference height (z), roughness length (z_o), and the stability function (ψ) (Brook et al. 1999). Further details regarding calculation of these parameters can be found in Appendix A.

Sublayer or boundary layer resistance (R_b) is calculated as:

$$R_b = \frac{5}{u_*}\left(\frac{Vi}{Di}\right)^{2/3} \tag{3}$$

using friction velocity (u_*), thermal diffusivity (V_i), and molecular diffusivity (D_i) (Brook et al. 1999).

Total surface resistance (R_c) of the ENVC model is represented by stomatal and non-stomatal resistances (Zhang et al. 2003). The stomatal resistance components include stomatal (R_{st}) and mesophyll (R_m) resistance, adjusted for stomatal blocking caused by wet conditions (W_{st}) (Zhang et al. 2003). Non-stomatal resistance components include in-canopy aerodynamic resistance (R_{ac}), ground resistance (R_g), and cuticle resistance (R_{cut}) (Zhang et al. 2003). The relationships between these resistances are illustrated in Figure 4.

Mathematically, the R_c portion of the model can be stated as follows (adapted from Zhang et al., 2003):

$$\frac{1}{R_c} = \frac{1 - Wst}{R_{st} + R_m} + \frac{1}{R_{ac} + R_g} + \frac{1}{R_{cut}} \tag{4}$$

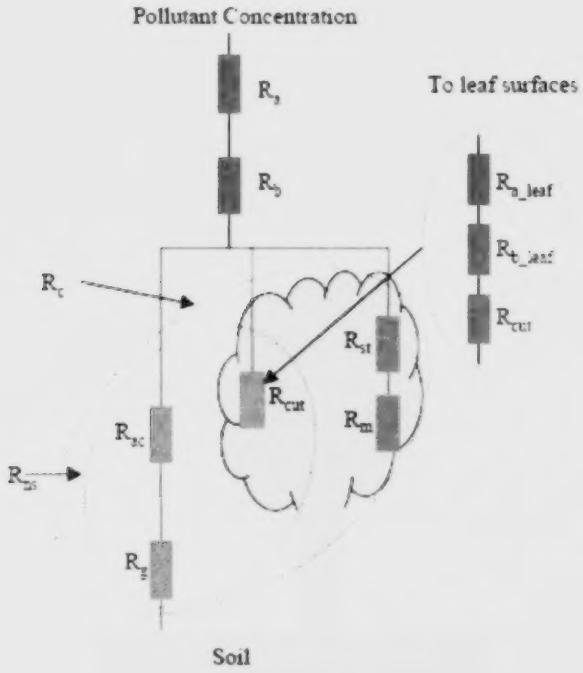

Figure 4 Scheme of resistance analogy in Environment Canada dry deposition inference model (after Zhang et al. 2003).

Stomatal resistance (R_{st}) includes four components (Zhang et al. 2003): unstressed leaf stomatal conductance ($Gs(PAR)$), conductance reducing effects of air temperature ($f(T)$), water-vapor pressure deficit ($f(D)$), and leaf water potential ($f(\psi)$). Mathematically, stomatal resistance can be stated as (Zhang et al. 2003):

$$R_{st} = \frac{1}{G_s(PAR) f(T) f(D) f(\psi) D_i / D_s} \tag{5}$$

Mesophyll resistance (R_m) is species dependent and Environment Canada represents this term as a series of default values for different chemical species (refer to Table A.3 in Appendix A) (Zhang et al. 2003).

Non stomatal resistances include (Appendix A): in-canopy aerodynamic resistance (R_{ac}), ground resistance (R_g), and canopy cuticle resistance (R_{cut}) (Zhang et al. 2003). In-canopy aerodynamic resistance is represented as a series of default values adjusted for

leaf area indices (LAIs) for different seasons. Ground resistance is represented as a series of default values adjusted for temperature, rain or dew conditions, and snow cover fraction (Zhang et al. 2003). Cuticle resistance is represented as a series of default values according to land use category and adjusted for temperature, rain or dew conditions, leaf area indices, and snow cover fraction (Zhang et al. 2003).

3.1.2 Particulates

The ENVC model uses a separate module for modeling particle deposition velocity (V_d); which includes components of gravitational settling (V_g), aerodynamic resistance (R_a), and surface resistance (R_s) in the following relationship (Zhang et al. 2001):

$$V_d = V_g + \frac{1}{R_a + R_s} \tag{6}$$

Gravitational settling velocity (V_g) includes the following variables: particle density (ρ), particle diameter (d_p), gravitational acceleration (g), viscosity (μ), and the Cunningham slip correction factor (C) in the following relationship (Zhang et al. 2001):

$$V_g = \frac{\rho d_p^2 g C}{18\mu} \tag{7}$$

Aerodynamic resistance (R_a) is calculated the same way as for gaseous deposition in the ENVC model (Zhang et al. 2001). Surface resistance (R_s) includes collection efficiency of Brownian diffusion (E_B), impaction (E_{IM}), interception (E_{IN}), a stickiness factor (R_1), friction velocity (u_*), and a constant (ε_0) as illustrated in the following relationship (Zhang et al. 2001):

$$R_s = \frac{1}{\varepsilon_0 u_* (E_B + E_{IM} + E_{IN}) R_1} \tag{8}$$

For actual application of the model, size distributions used for a particular particle group is divided into 40 incremental sizes using the following formula, where I is from 1 to 40:

$$size_increment = 0.001 * I^{2.5} \tag{9}$$

The resulting particle sizes range from 0.001 µm for I = 1; to 10 µm for I = 40. Once a size increment has been generated, it is used to calculate the deposition velocity associated with that size. The resulting deposition for each size increment is weighted according to the area under the curve for that size increment and then summed across the forty increment sizes for the total deposition velocity (Zhang et al. 2001). A similar process is used for the distribution of larger particles.

3.1.3 Alberta Environment (AENV) Model

3.1.4 Gases

A description of the AENV model is provided by Cheng et al. (2001) and WBK (2008) and briefly described here. The AENV model uses the same resistance analogy approach for calculation of deposition velocity (V_d) as the ENVC model, but calculates each of the three components differently (Appendix B) (WBK, 2008; Cheng et al. 2001). The AENV calculation for R_a involves calculating a value for the surface roughness length (z_o) as a monthly average using hourly data where the wind speed is >6 m/s:

$$z_o = z\, e^{-\left(\frac{0.4u}{u^*}\right)} \tag{10}$$

$$R_a = \frac{1}{ku^*}\left\{\ln\frac{z}{z_0} - \psi\left(\frac{z}{L}\right)\right\} \tag{11}$$

The AENV model calculates R_b based upon von Karman's constant (k), the friction velocity (u_*), the Schmidt number (Sc) for a chemical, and the Prandt number (Pr) for air in the following relationship (Cheng et al., 2001):

$$R_b = \frac{2}{ku_*}\left(Sc \times \frac{1}{\mathrm{Pr}}\right)^{2/3} \tag{12}$$

The AENV model represents R_c as default values that are seasonally adjusted for the gases SO_2 and NO_2. For HNO_2 and HNO_3, R_c is always 10 s/m. The default values for SO_2 and NO_2 are drawn from published literature as a function of surface type, surface wetness, and incident radiation; and as such address some of the variation in R_c caused by stomatal physiology. The AENV model incorporates differences for wet and dry surface conditions, weighted based on surface wetness (Appendix B). If surface wetness measurement data are unavailable, then relative humidity is used a surrogate for surface wetness. The model allows a minimum relative humidity (RH) measurement cutoff (87%) to be used as an approximation to represent a surface as being wet.

3.1.5 Particulates

The AENV model uses the same deposition velocity relationship for particulates as used by the gaseous model. Initially, use of this approach may appear to be quite different from that of the ENVC model. However, the two models are actually quite similar as the gravitational settling velocity component of the ENVC model is considered to be quite small.

For particulates, R_c is considered negligible and this resistance is assigned a value of 0. R_a is determined independent of chemical species. R_b is represented as default values for different species and are drawn from scientific literature and adjusted for dry/wet and seasonal conditions as a function of surface type and weighted according to average day length for each month at a mid-Alberta latitude location (54°N latitude).

4.0 DRY DEPOSITION MODELING FOR ENVC AND AENV MODELS

4.1 Model Methods for Coniferous Forest (Base Case)

The two dry deposition inference models in their original form, described in Appendices A and B, were run to establish a starting point from which to evaluate effects of changes made to the AENV model. Initially, results were shown for monthly deposition flux to permit a comparison of the overall performance of the two models for a coniferous forest land use category (LUC) and considering 11 species (SO_2, SO_4^{2-}, NO_2, HNO_3, HNO_2, NO_3^-, NH_4^+, Ca^{2+}, Na^+, K^+, and Mg^{2+}).

Results were further examined using deposition velocities (V_d) for each species involved in the calculation of monthly deposition flux. Since deposition velocities should be relatively constant for all chemical species for a given land use and set of meteorological conditions, comparisons with deposition velocity literature values were made for individual species. The behavior of the three most important individual species making up the largest difference in monthly deposition flux between the two models was further examined to better understand the importance of these species. These species included SO_2, NO_2, and HNO_3. Using the "contribution to total deposition flux" rather than "deposition velocity" of an individual species allowed an understanding of how important each species was in contributing to change in total deposition flux when modifications to the AENV model were made.

The original model form for the AENV model was also used to generate results for seven other LUCs for which the AENV model was designed. These results were compared with original results for a coniferous forest LUC. These comparisons were done for monthly deposition flux; as well as for surface resistance (R_c) values for gases and deposition velocity (V_d) values for particles. It is important to point out that inputs for meteorological parameters used in comparing the two dry deposition inference models were obtained from a setting consistent with a coniferous forest LUC.

These parameter inputs were used to make comparisons for the seven LUCs to better understand their general behavior for the AENV model. These parameter inputs are not necessarily representative of the settings for the seven LUCs because some meteorological parameters – such as roughness length and relative humidity – are affected by the respective surface conditions. As such, deposition velocities and surface resistance values cannot be fairly compared with literature values for these seven LUCs.

4.1.1 Input Parameters for Modeling

All of the modeling in this study was performed using measurements of hourly pollutant concentrations for 11 species and hourly values for meteorological parameters

made at the Wood Buffalo Environmental Association Fort MacKay air monitoring station for the year 2003. Gaseous species measured included SO_2, NO_2, HNO_3, and HNO_2. Particulate ions included SO_4^{2-}, NO_3^-, and NH_4^+. Base cations included K^+, Na^+, Ca^{2+}, and Mg^{2+}. Measured meteorological values included wind speed, standard deviation of wind direction, air temperature at 2 m and 10 m heights, and relative humidity. Inputs for solar zenith angle and solar radiation values used in the ENVC model were computed using a Visual Basic program developed during a previous study (WBK, 2008).

Quality assurance and quality control was performed on the input data. Input values found to be very uncommon were left in the input data set to allow performance of the models to be evaluated using actual data. Missing hourly data were replaced with the average of the value for the hours before and after the hour of the missing value if only one hour's value was missing. If two or more consecutive hours were missing, then the month's median value for each of those hours was used to represent the missing data for those hours. For species measured intermittently (24 hours every 6 days), the hourly average was used for all of the 144 hours (6 days) in that time period. Complete details of data collection, processing, and assumptions are described in WBK (2008).

4.1.2 Atmospheric Concentrations of Chemical Species

Deposition of a particular species is the product of species concentration and deposition velocity. From a practical point of view, it is important to understand those species having the greatest influence on acid deposition in terms of hydrogen ion equivalents. Monthly averages species concentrations are provided in Appendix C.

Concentrations of nitrogen compounds (NO_2, HNO_3, HNO_2, NO_3^-, and NH_4^+) tend to be higher in winter than summer months. Deposition velocities for NO_2, HNO_3, and HNO_2 tend to be lower in winter months. Species and respective concentration ranges were as follows for the 2003 data set:

- NO_2 was the species with the highest recorded hourly concentration (range 3.7 to 21.7 $\mu g/m^3$).
- SO_2 was the second most important species although hourly levels observed were much lower (range 1.0 to 4.9 $\mu g/m^3$).
- Calcium ion (Ca^{2+}) levels ranged from 0.2 to 1.9 $\mu g/m^3$. Calcium concentration maxima occurred in April, July, and November.
- Sulphate (SO_4^{2-}) ions ranged from 0.5 to 2.4 $\mu g/m^3$.
- HNO_3 concentration ranged from 0.2 to 1.5 $\mu g/m^3$.
- Levels of all other species were less than 1.0 $\mu g/m^3$ for all months of the year.

4.2 Model Results – Coniferous Forest

4.2.1 Deposition Flux

The first modeling was done using AENV and ENVC models in their original forms. Total monthly deposition flux values ranged from near 0 to 0.016 kg hydrogen ion per hectare (kg H^+/ha) for the AENV model and from 0.004 to 0.018 kg H^+/ha for the ENVC model (Table 2). Total deposition flux for the year was 0.141 kg H^+/ha for the AENV model and 0.153 kg H^+/ha for the ENVC model.

For total annual deposition, the difference between the two models was small at 0.012 kg H^+/ha, representing a difference of about 8%. As shown in Figure 5, months having the largest differences were November, July, and September – all of which the AENV model underestimated the ENVC model. May, October, April, and December showed moderate differences. Total deposition for the months of January, February, March, June, and August were similar for both models.

Table 2 Comparison of monthly summed deposition flux (kg H^+/ha) for 11 species to a coniferous forest cover using the AENV and ENVC models.

Month	AENV	ENVC	Difference
Month 1	0.016	0.016	0.000
Month 2	0.011	0.011	-0.001
Month 3	0.016	0.016	0.000
Month 4	0.016	0.017	-0.001
Month 5	0.014	0.012	0.002
Month 6	0.007	0.006	0.001
Month 7	0.007	0.011	-0.003
Month 8	0.013	0.013	0.000
Month 9	0.010	0.012	-0.003
Month 10	0.016	0.018	-0.002
Month 11	0.000	0.004	-0.004
Month 12	0.016	0.017	-0.001
Total	0.141	0.153	-0.012
Total % difference			8

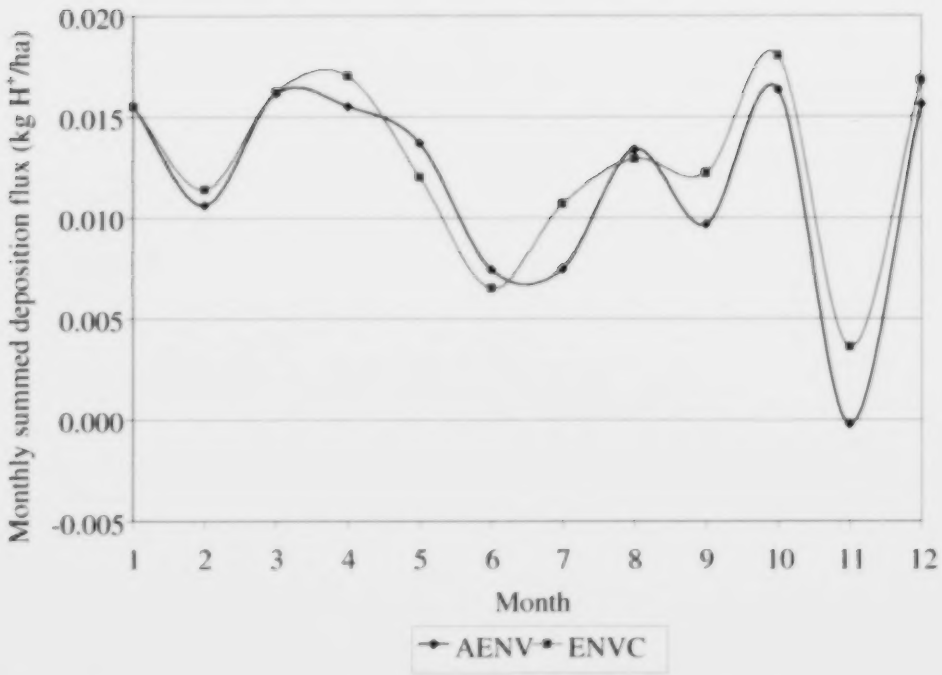

Figure 5 **Comparison of monthly summed deposition flux for 11 species to a coniferous forest cover using the AENV and ENVC models.**

4.2.2 Deposition Velocities – Coniferous Forest

The initial model results were broken out to show monthly average deposition velocities for each species in Figures 6 to 11. Tabular values associated with Figures 6 to 11 can be found in Appendix D.

4.2.2.1 Deposition Behavior of Gases (SO_2, NO_2, HNO_3, HNO_2)

SO_2

Resulting average deposition velocities (V_d) for SO_2 for the two models indicate that SO_2 deposition ranges from 0.09 to 0.49 cm/s across the year. The AENV model under represents the ENVC model in winter and spring months, but over represents it in summer months (Figure 6).

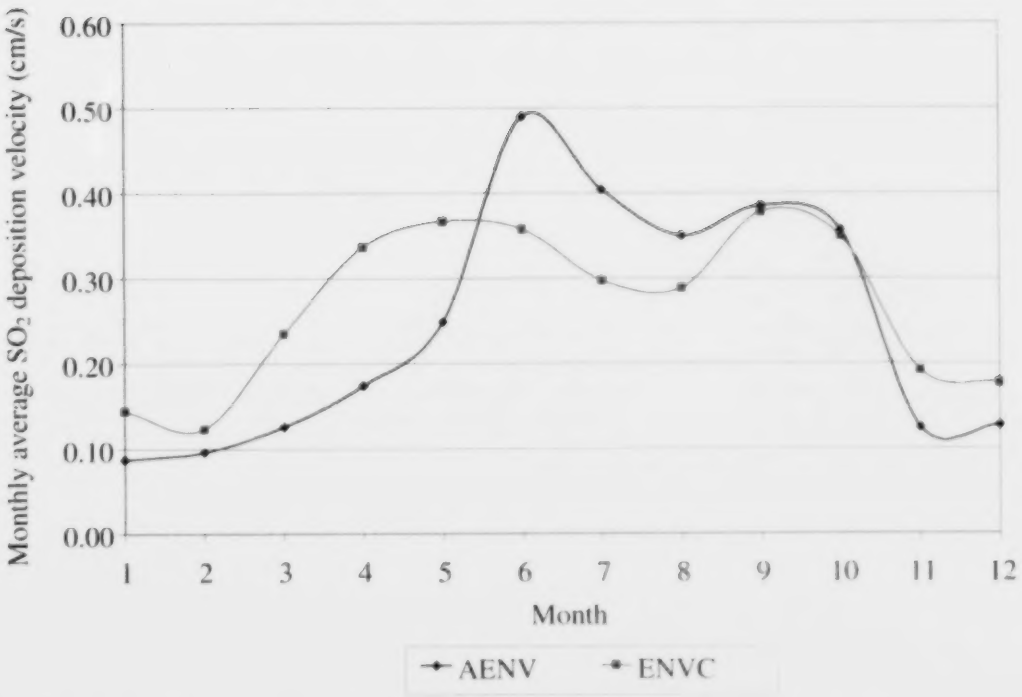

Figure 6 **Comparison of monthly average SO_2 deposition velocity for a coniferous forest cover using the AENV and ENVC model.**

In a study from literature, a U.S. National Dry Deposition Network (NDDN) model – which is reported to be similar to the ENVC model – was used to simulate acidic deposition at Ann Arbor, Michigan, for a land use combination of grass, water, and forest (Brook, 1996). Their model results indicated SO_2 monthly average deposition velocities ranged from 0.20 to 0.55 cm/s, with the peak in June (Brook, 1996).

NO_2

NO_2 monthly average deposition velocities are shown in Figure 7 and ranged from 0.04 to 0.25 cm/s with the AENV model under representing the ENVC model in winter and spring months while over representing it in summer. Generally, ENVC results were quite similar to AENV results.

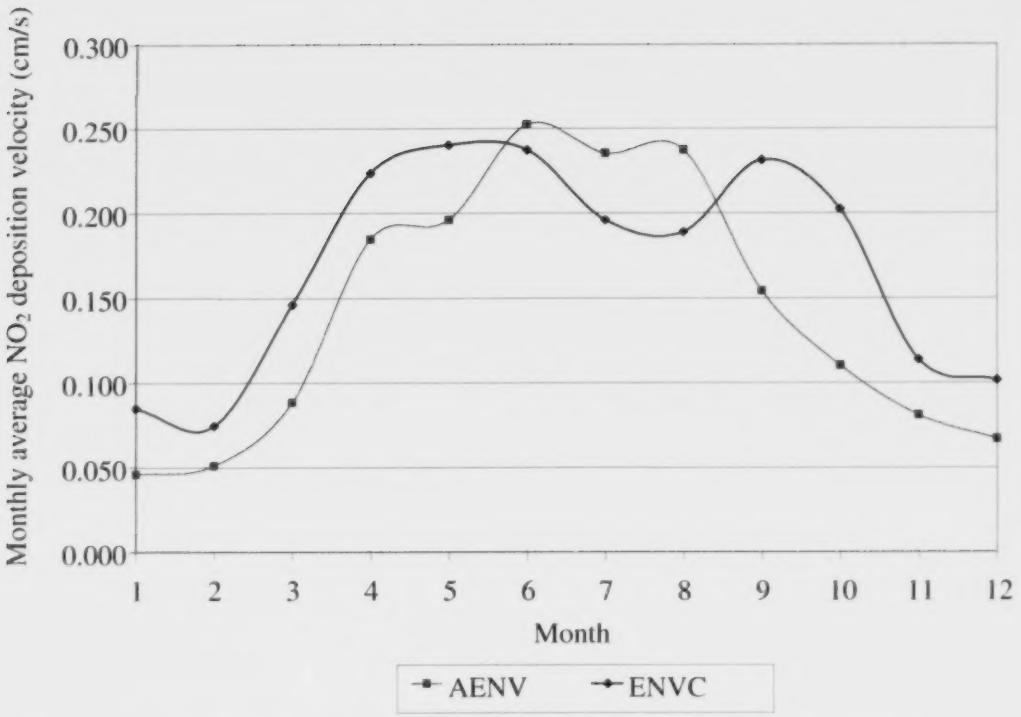

Figure 7 **Comparison of monthly average NO_2 deposition velocity for a coniferous forest cover using the AENV and ENVC model.**

HNO_3

Monthly average HNO_3 deposition velocities are shown in Figure 8 and they range from 0.8 to 2.1 cm/s with the AENV model over representing the ENVC model in all months except December. The two models produced similar trends with monthly average AENV deposition velocities being higher than those of the ENVC model. In the previously mentioned Ann Arbor study (Brook, 1996), the NDDN model produced HNO_3 deposition velocities ranging from 1.4 to 2.2 cm/s with peaks in April and December and troughs in August.

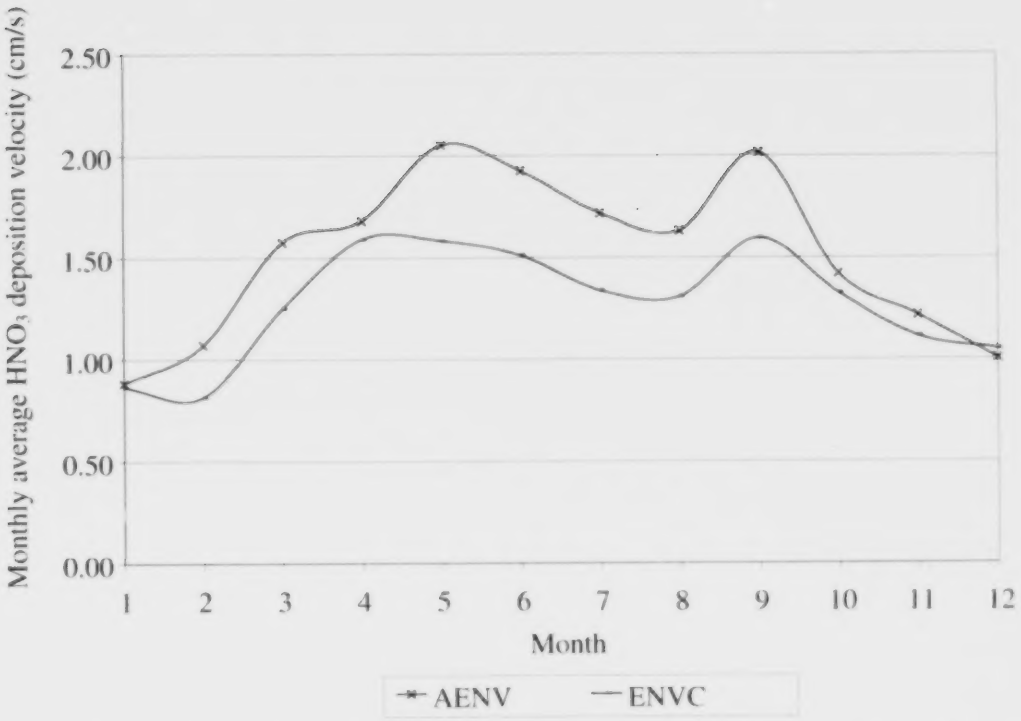

Figure 8 **Comparison of monthly average HNO_3 deposition velocity for a coniferous forest cover using the AENV and ENVC model.**

HNO_2

Monthly average HNO_2 deposition velocities are shown in Figure 9 and they ranged from 0.3 to 2.2 cm/s. The AENV model consistently over represented the ENVC model by two to three times. While this difference may seem substantial, the low concentration of HNO_2 in the atmosphere results in a relatively small contribution to total monthly deposition flux for both of the models.

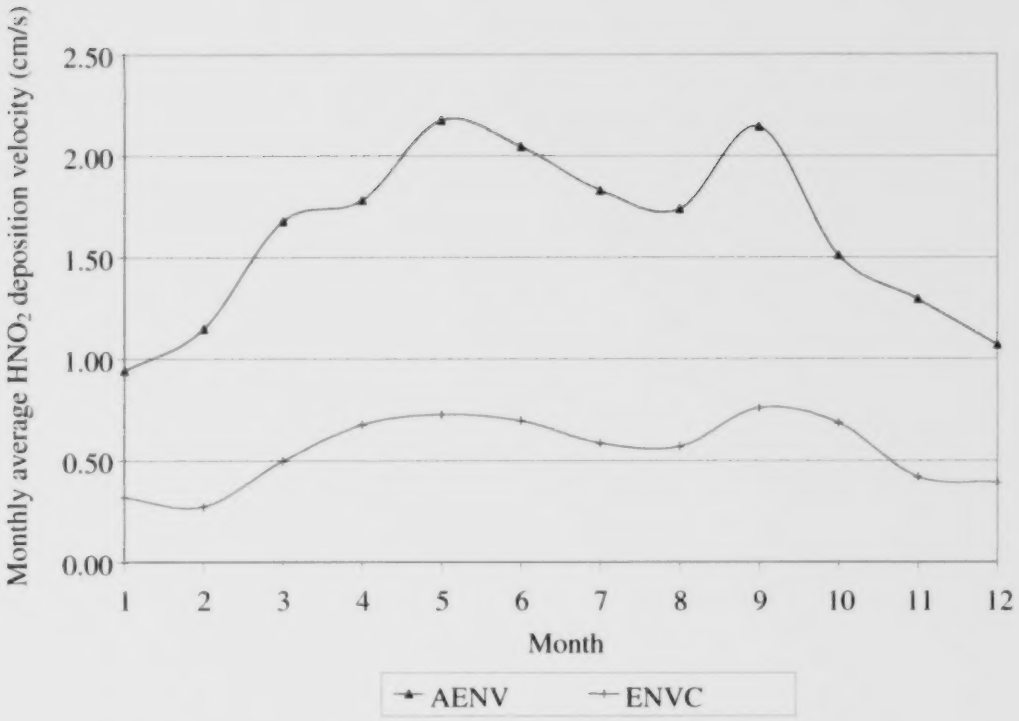

Figure 9 **Comparison of monthly average HNO_2 deposition velocity for a coniferous forest cover using the AENV and ENVC model.**

4.2.2.2 Fine Particle (SO_4^{2-}, NH_4^+) Deposition Behavior

Deposition velocities for smaller particles (SO_4^{2-} and NH_4^+) are shown in Figure 10 and they ranged from 0.09 to 0.35 cm/s with the AENV model over representing the ENVC model in every month. Particle deposition behavior in both models is mostly dominated by aerodynamic resistance (R_a) based on aerodynamic properties (diameter) of the particle and independent of individual species.

The AENV results showed a peak in summer months that was absent in the ENVC model. In the literature study in Ann Arbor (Brook, 1996), the NDDN model reported small-particle monthly average deposition velocities ranging from 0.07 to 0.15 cm/s with slightly higher values in May and a minimum in winter months.

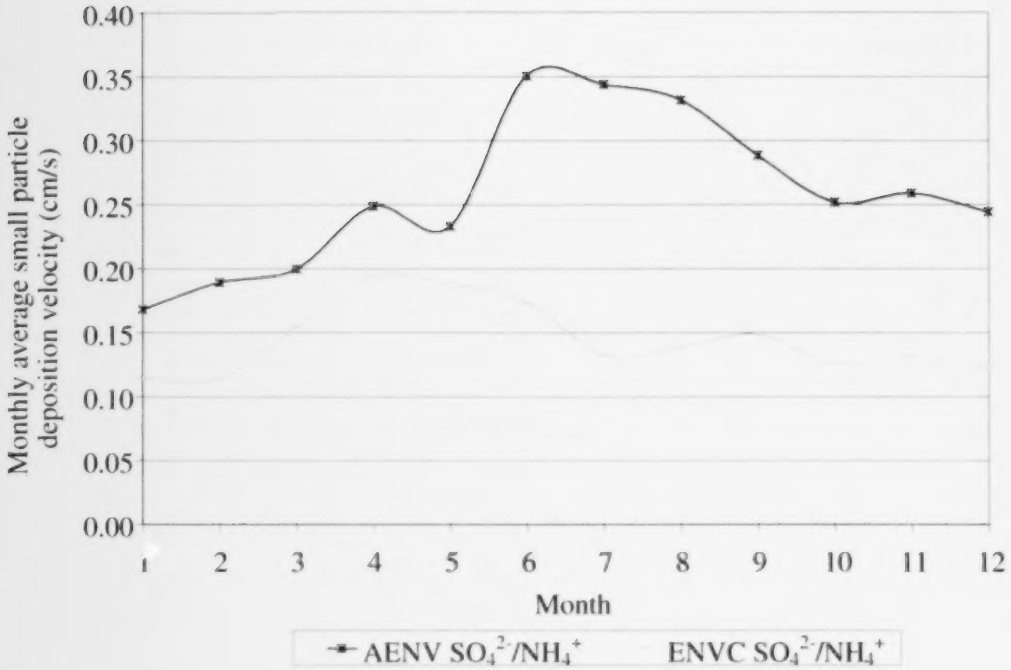

Figure 10 Comparison of monthly average small particle deposition velocity for a coniferous forest cover using the AENV and ENVC model.

4.2.2.3 Coarse Particle (NO_3^-, Na^+, K^+, Ca^{2+}, Mg^{2+}) Deposition Behavior

Again, particle deposition behavior in both models is mostly dominated by aerodynamic resistance (R_a) based on aerodynamic properties (diameter) and independent of individual species. Monthly average deposition velocities for larger (coarse) particles shown in Figure 11 and they ranged from 0.29 to 0.64 cm/s. Similar to Figure 10 (small particle deposition), monthly average deposition velocities for large particles showed a peak in summer months for the AENV model that did not occur in the ENVC model.

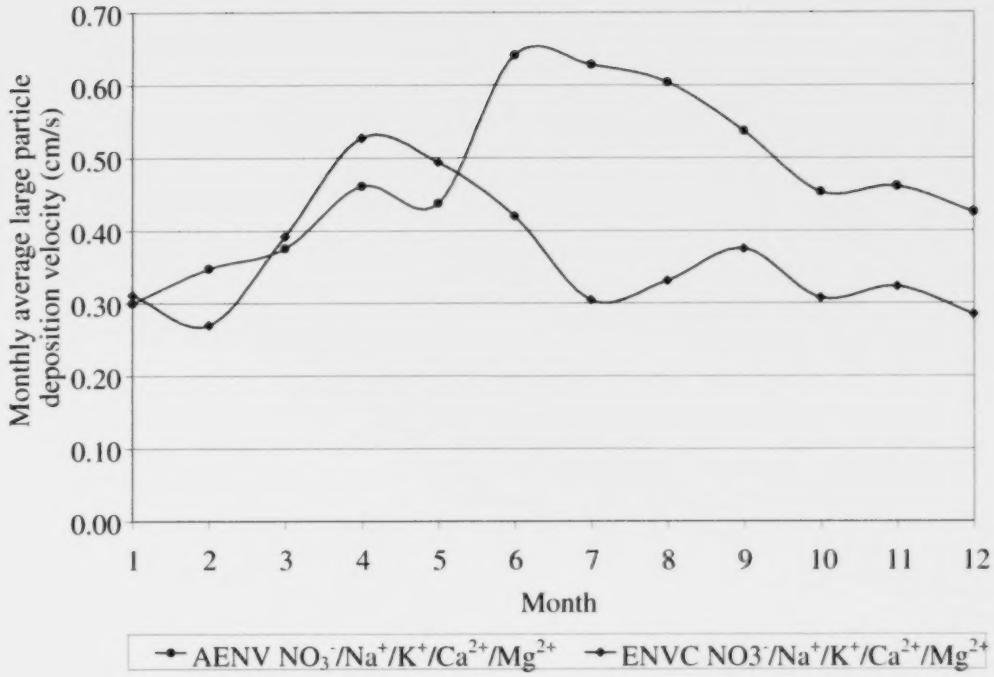

Figure 11 Comparison of monthly average large particle deposition velocity for a coniferous forest cover using the AENV and ENVC model.

Monthly averaged diurnal deposition velocities for the three most dominant species – SO_2, NO_2, and HNO_3 – were calculated and compared for each model. These comparisons are presented in Appendix E. In all cases, both models were similar and behaved as expected in that higher monthly averaged diurnal deposition velocities occurred during daytime heating hours and lower monthly averaged diurnal deposition velocities occurred during nighttime.

4.3 Model Methods for Other Land Use Categories

The AENV model was rerun for seven land uses that represent other land use categories (LUCs) for which the model was designed. Input data were the same as that used previously, the only change was the selection of LUC. Because calculation of roughness length (z_o) is based on the meteorological input data, roughness lengths used for these seven LUCs were the same as that used for a coniferous forest LUC.

4.4 Model Results – Coniferous Forest

4.4.1 Deposition Flux

Monthly summed deposition flux results for all of LUCs are compared with a coniferous forest surface cover in Figures 12 through 18 and detailed for individual species in Tables 3 through 9. A negative value in the tables indicates that the monthly average result for an individual species for the alternative LUC is less than for a coniferous forest surface (the value indicating the magnitude of the difference) and vice versa.

LUC 1 – Deciduous Forest Compared with Coniferous Forest

The differences in monthly summed deposition flux for a deciduous forest cover are shown in Figure 12. From Table 3, it is observed the largest differences are for NO_2 and Ca^{2+} deposition in winter and Ca^{2+} deposition in summer.

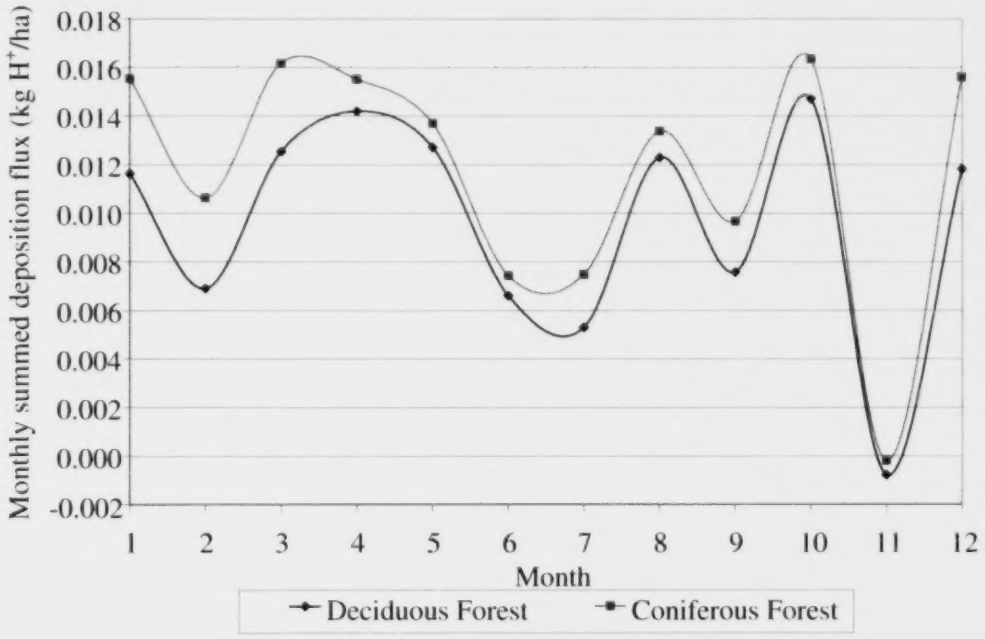

Figure 12 Comparison of monthly summed deposition flux for 11 species to a deciduous forest and coniferous forest cover using the AENV model.

Table 3 **Breakdown of magnitude of differences in monthly summed deposition flux in kg H^+/ha for individual species between deciduous forest and coniferous forest cover using the AENV model.**

Month	SO_2	NO_2	HNO_2	HNO_3	SO_4^{2-}	NH_4^+	NO_3^-	Na^+	K^+	Ca^{2+}	Mg^{2+}	Total
Month 1	-0.5	-2.5	0.0	0.0	-0.7	-1.2	-0.3	0.4	0.1	0.6	0.2	-3.9
Month 2	-0.7	-2.5	0.0	0.0	-0.8	-1.0	-0.2	0.3	0.0	0.9	0.2	-3.7
Month 3	-0.7	-1.8	0.0	0.0	-1.3	-1.0	-0.1	0.2	0.0	0.8	0.1	-3.6
Month 4	-0.6	-1.8	0.0	0.0	-0.6	-0.8	-0.1	0.2	0.0	2.2	0.2	-1.3
Month 5	-0.3	-1.1	0.0	0.0	-0.4	-0.5	0.0	0.1	0.0	1.0	0.2	-1.0
Month 6	0.0	0.0	0.0	0.0	0.4	0.5	0.0	-0.1	-0.1	-1.4	-0.2	-0.8
Month 7	0.0	0.0	0.0	0.0	0.4	0.4	0.1	-0.1	-0.1	-2.5	-0.3	-2.2
Month 8	0.0	0.0	0.0	0.0	0.5	0.6	0.1	-0.1	-0.1	-1.8	-0.4	-1.1
Month 9	-0.7	-1.5	0.0	0.0	-0.2	-0.3	0.0	0.1	0.0	0.4	0.1	-2.1
Month 10	-0.7	-1.7	0.0	0.0	-0.3	-0.4	0.0	0.1	0.0	1.2	0.1	-1.6
Month 11	-0.3	-2.5	0.0	0.0	-0.3	-0.6	-0.2	0.1	0.1	3.1	0.1	-0.6
Month 12	-1.2	-3.9	0.0	0.0	-0.8	-1.0	-0.6	0.4	0.2	2.6	0.4	-3.8

LUC 3 – Wetland/Swamp Compared with Coniferous Forest

The differences in monthly summed deposition flux for a wetland/swamp are shown in Figure 13. From Table 4, it is observed that the largest differences are for NO_2 deposition being low across the year because of wet surface conditions representative of wetland/swamp and SO_2 deposition being higher in spring and summer months because of wet surface conditions representative of wetland/swamp compared to winter months.

LUC 4 – Grassland as Compared with Coniferous Forest

The differences in monthly summed deposition flux for grassland are shown in Figure 14. The trend in monthly summed deposition flux for this surface type was similar to that for a wetland/swamp cover (Figure 13). Importance of individual species and underlying conditions contributing to these differences can be understood from Table 5. Again, the largest differences are for SO_2 and NO_2 deposition.

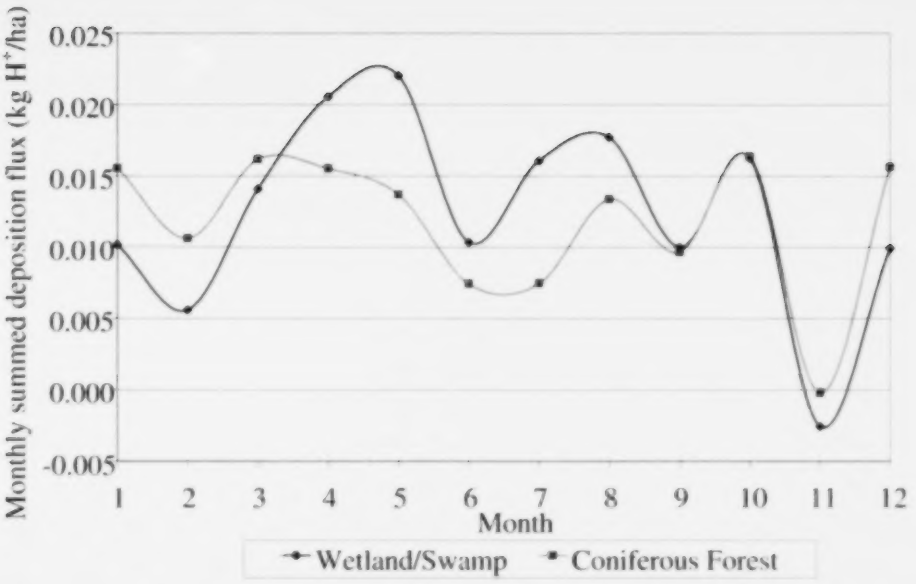

Figure 13 **Comparison of monthly summed deposition flux for 11 species to wetland/swamp and coniferous forest cover using the AENV model.**

Table 4 **Breakdown of magnitude of differences in monthly summed deposition flux in kg H^+/ha for individual species between wetland/swamp and coniferous forest cover using the AENV model.**

Month	SO_2	NO_2	HNO_2	HNO_3	SO_4^{2-}	NH_4^+	NO_3^-	Na^+	K^+	Ca^{2+}	Mg^{2+}	Total
Month 1	-0.3	-4.2	0.0	0.0	-0.7	-1.2	-0.3	0.4	0.1	0.6	0.2	-5.4
Month 2	-0.4	-4.2	0.0	0.0	-0.8	-1.0	-0.2	0.3	0.0	1.0	0.2	-5.1
Month 3	3.8	-5.2	0.0	0.0	-0.7	-0.6	-0.1	0.1	0.0	0.5	0.1	-2.1
Month 4	11.2	-6.8	0.0	0.0	-0.3	-0.5	-0.1	0.1	0.0	1.2	0.1	5.0
Month 5	12.8	-4.7	0.0	0.0	-0.2	-0.3	0.0	0.1	0.0	0.6	0.1	8.3
Month 6	6.1	-3.8	0.0	0.0	-0.2	-0.3	0.0	0.0	0.0	0.9	0.1	2.9
Month 7	12.4	-5.3	0.0	0.0	-0.2	-0.3	-0.1	0.1	0.1	1.6	0.2	8.6
Month 8	10.5	-6.9	0.0	0.0	-0.3	-0.4	0.0	0.1	0.0	1.1	0.2	4.3
Month 9	4.1	-3.9	0.0	0.0	-0.2	-0.3	0.0	0.1	0.0	0.4	0.1	0.3
Month 10	3.7	-4.5	0.0	0.0	-0.3	-0.4	0.0	0.1	0.0	1.2	0.1	-0.1
Month 11	0.2	-4.8	0.0	0.0	-0.3	-0.6	-0.2	0.1	0.1	3.1	0.1	-2.4
Month 12	-0.7	-6.4	0.0	0.0	-0.8	-1.0	-0.6	0.4	0.2	2.7	0.4	-5.7

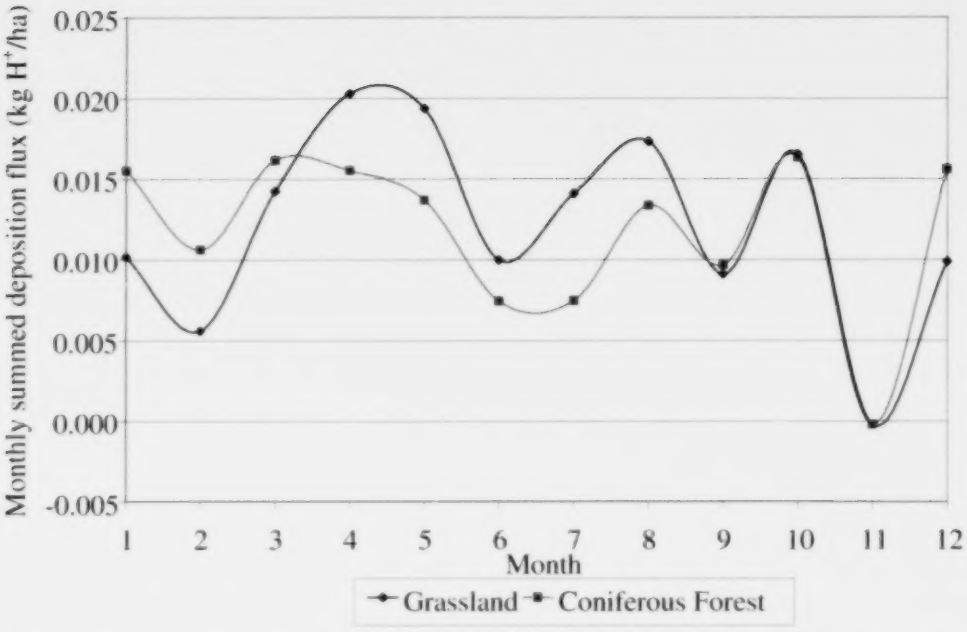

Figure 14 **Comparison of monthly summed deposition flux for 11 species to grassland and coniferous forest cover using the AENV model.**

Table 5 **Breakdown of magnitude of differences in monthly summed deposition flux in kg H^+/ha for individual species between grassland and coniferous forest cover using the AENV model.**

Month	SO_2	NO_2	HNO_2	HNO_3	SO_4^{2-}	NH_4^+	NO_3^-	Na^+	K^+	Ca^{2+}	Mg^{2+}	Total
Month 1	-0.3	-4.2	0.0	0.0	-0.7	-1.2	-0.3	0.4	0.1	0.6	0.2	-5.4
Month 2	-0.4	-4.2	0.0	0.0	-0.8	-1.0	-0.2	0.3	0.0	1.0	0.2	-5.1
Month 3	1.8	-2.5	0.0	0.0	-1.3	-1.0	-0.1	0.3	0.0	0.8	0.1	-1.9
Month 4	5.8	-2.1	0.0	0.0	-0.6	-0.8	-0.1	0.2	0.0	2.3	0.2	4.8
Month 5	6.4	-1.1	0.0	0.0	-0.4	-0.6	0.0	0.1	0.0	1.1	0.2	5.7
Month 6	2.9	-1.4	0.0	0.0	-0.5	-0.6	-0.1	0.1	0.1	1.7	0.3	2.6
Month 7	5.9	-2.0	0.0	0.0	-0.5	-0.5	-0.1	0.2	0.1	3.2	0.4	6.6
Month 8	5.1	-2.6	0.0	0.0	-0.6	-0.8	-0.1	0.2	0.1	2.2	0.4	4.0
Month 9	1.8	-2.5	0.0	0.0	-0.4	-0.6	-0.1	0.2	0.1	0.8	0.2	-0.6
Month 10	1.7	-3.0	0.0	0.0	-0.6	-0.7	-0.1	0.1	0.1	2.3	0.3	0.2
Month 11	0.0	-4.2	0.0	0.0	-0.5	-1.2	-0.4	0.3	0.1	5.8	0.3	0.0
Month 12	-0.7	-6.4	0.0	0.0	-0.8	-1.0	-0.6	0.4	0.2	2.7	0.4	-5.7

LUC 5 – Cropland as Compared with Coniferous Forest

Monthly summed deposition flux for cropland is shown in Figure 15 and, as expected, it shows a large increase in the spring (growing) season. It should be noted that the scale in this figure has been changed to fit the large increase associated with growing season conditions. From Table 6, it can be seen that this increase is solely a result of changes (increases) in SO_2 deposition. Monthly summed deposition fluxes are comparable to that of a coniferous forest surface for other months of the year.

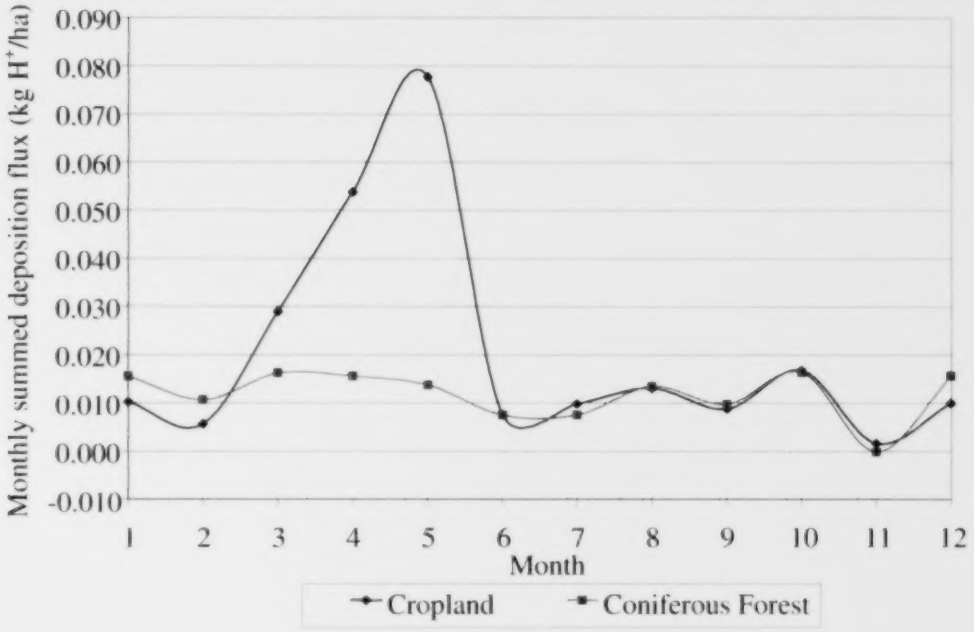

Figure 15 Comparison of monthly summed deposition flux for 11 species to cropland and coniferous forest cover using the AENV model.

LUC 6 – Urban as Compared with Coniferous Forest

Conditions representing an urban surface resulted in similar monthly summed deposition fluxes during winter and lower values during other periods compared to a coniferous forest cover (Figure 16). From Table 7, differences in monthly summed deposition fluxes from March through October can be seen to be largely a result of differences in NO_2 deposition.

Table 6 **Breakdown of magnitude of differences in monthly summed deposition flux in kg H^+/ha for individual species between cropland and coniferous forest cover using the AENV model.**

Month	SO_2	NO_2	HNO_2	HNO_3	SO_4^{2-}	NH_4^+	NO_3^-	Na^+	K^+	Ca^{2+}	Mg^{2+}	Total
Month 1	-0.3	-4.2	0.0	0.0	-0.7	-1.2	-0.3	0.4	0.1	0.6	0.2	-5.4
Month 2	-0.4	-4.2	0.0	0.0	-0.8	-1.0	-0.2	0.3	0.0	1.0	0.2	-5.1
Month 3	16.9	-2.5	0.0	0.0	-1.8	-1.4	-0.2	0.4	0.0	1.2	0.2	12.8
Month 4	38.8	-2.1	0.0	0.0	-0.8	-1.2	-0.2	0.3	0.1	3.1	0.2	38.2
Month 5	64.5	-1.1	0.0	0.0	-0.6	-0.8	-0.1	0.2	0.0	1.5	0.3	63.9
Month 6	1.4	-2.3	0.0	0.0	-0.5	-0.6	-0.1	0.1	0.1	1.7	0.3	0.1
Month 7	2.7	-3.3	0.0	0.0	-0.5	-0.5	-0.1	0.2	0.1	3.2	0.4	2.3
Month 8	2.4	-4.3	0.0	0.0	-0.6	-0.8	-0.1	0.2	0.1	2.2	0.4	-0.4
Month 9	1.8	-3.0	0.0	0.0	-0.6	-0.8	-0.1	0.3	0.1	1.1	0.3	-0.9
Month 10	1.7	-3.5	0.0	0.0	-0.8	-1.0	-0.1	0.2	0.1	3.3	0.4	0.3
Month 11	0.0	-4.4	0.0	0.0	-0.7	-1.7	-0.6	0.4	0.1	8.3	0.4	1.7
Month 12	-0.7	-6.4	0.0	0.0	-0.8	-1.0	-0.6	0.4	0.2	2.7	0.4	-5.7

LUC 7 – Water as Compared with Coniferous Forest

As shown in Figure 17, water has the ability to receive much greater acid input than a coniferous forest cover. From Table 8, it is observed that this is largely a result of differences in deposition of SO_2, NO_2, SO_4^{2-}, NH_4^+, NO_3^-, Na^+, Ca^{2+}, and Mg^{2+}. In general, water is far more susceptible to SO_2 deposition and less susceptible to NO_2 deposition than a coniferous forest surface. Small particle deposition (SO_4^{2-}, NH_4^+) is characteristically higher over water compared to a coniferous forest cover. Because water has little or no resistance to SO_2 or particle deposition, total deposition is largely dependent on atmospheric concentration of these species.

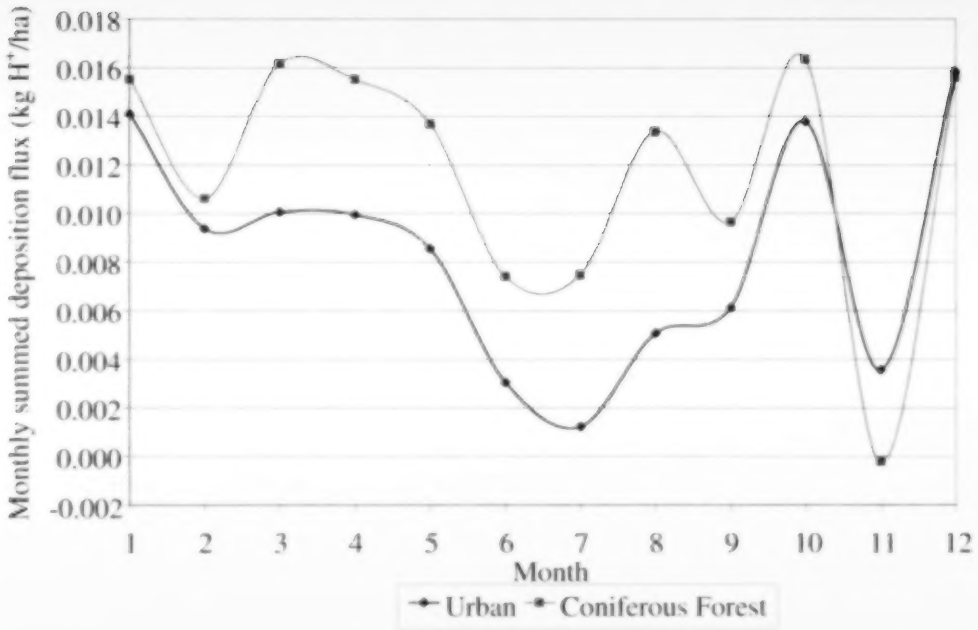

Figure 16 **Comparison of monthly summed deposition flux for 11 species to urban and coniferous forest cover using the AENV model.**

Table 7 **Breakdown of magnitude of differences in monthly summed deposition flux in kg H^+/ha for individual species between urban and coniferous forest cover using the AENV model.**

Month	SO_2	NO_2	HNO_2	HNO_3	SO_4^{2-}	NH_4^+	NO_3-	Na^+	K^+	Ca^{2+}	Mg^{2+}	Total
Month 1	-0.5	0.0	0.0	0.0	-0.8	-1.3	-0.3	0.5	0.1	0.6	0.2	-1.4
Month 2	-0.7	0.0	0.0	0.0	-0.9	-1.1	-0.2	0.3	0.0	1.0	0.2	-1.2
Month 3	-1.0	-3.3	0.0	0.0	-1.9	-1.5	-0.2	0.4	0.0	1.3	0.2	-6.1
Month 4	-1.7	-5.5	0.0	0.0	-0.9	-1.3	-0.2	0.3	0.1	3.4	0.2	-5.6
Month 5	-1.5	-4.3	0.0	0.0	-0.7	-0.8	-0.1	0.2	0.1	1.6	0.3	-5.1
Month 6	-1.3	-3.6	0.0	0.0	-0.2	-0.3	0.0	0.0	0.0	0.9	0.1	-4.4
Month 7	-2.6	-5.1	0.0	0.0	-0.2	-0.3	-0.1	0.1	0.1	1.6	0.2	-6.2
Month 8	-2.4	-6.6	0.0	0.0	-0.3	-0.4	0.0	0.1	0.0	1.1	0.2	-8.3
Month 9	-0.3	-3.5	0.0	0.0	-0.6	-0.7	-0.1	0.2	0.1	1.0	0.3	-3.5
Month 10	-0.5	-4.0	0.0	0.0	-0.7	-0.8	-0.1	0.2	0.1	2.9	0.3	-2.6
Month 11	-0.3	-1.4	0.0	0.0	-0.7	-1.5	-0.6	0.3	0.1	7.4	0.4	3.8
Month 12	-1.2	0.0	0.0	0.0	-0.8	-1.1	-0.6	0.4	0.2	2.9	0.4	0.2

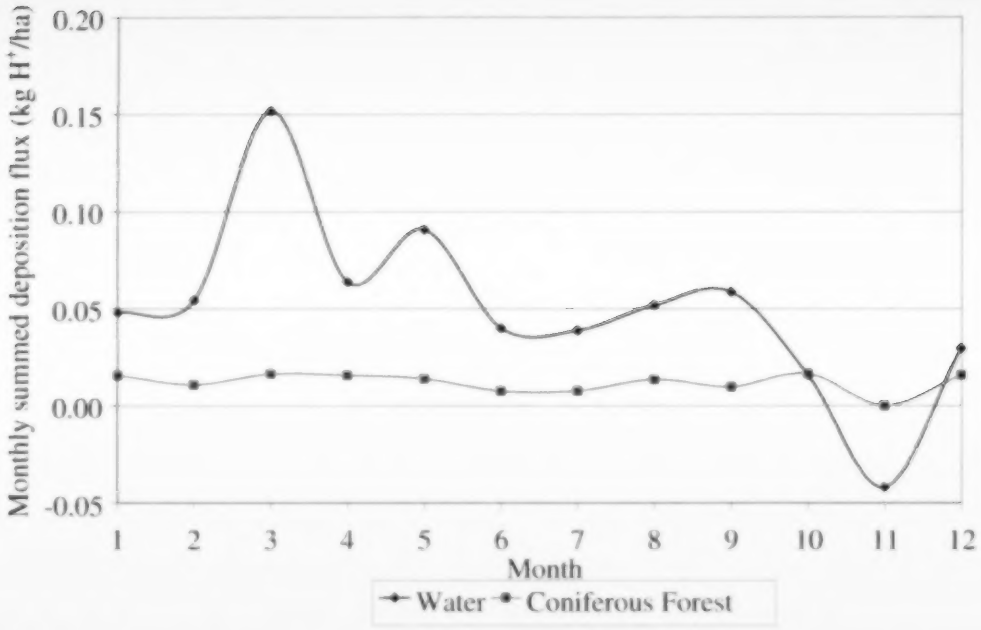

Figure 17 **Comparison of monthly summed deposition flux for 11 species to water and coniferous forest cover using the AENV model.**

Table 8 **Breakdown of magnitude of differences in monthly summed deposition flux in kg H^+/ha for individual species between water and coniferous forest cover using the AENV model.**

Month	SO_2	NO_2	HNO_2	HNO_3	SO_4^{2-}	NH_4^+	NO_3^-	Na^+	K^+	Ca^{2+}	Mg^{2+}	Total
Month 1	15.1	-4.6	0.0	0.0	12.7	21.0	3.1	-5.0	-1.1	-6.6	-2.3	32.4
Month 2	25.3	-4.5	0.0	0.0	16.4	20.8	1.8	-3.3	-0.3	-10.4	-2.3	43.7
Month 3	40.6	-6.3	0.0	0.0	75.5	61.2	4.1	-8.0	-0.6	-27.1	-4.2	135.3
Month 4	52.2	-8.6	0.0	0.0	22.4	32.0	2.2	-3.8	-0.7	-44.6	-3.0	48.2
Month 5	64.6	-6.1	0.0	0.0	30.5	37.8	1.6	-4.1	-1.2	-38.9	-7.1	77.0
Month 6	42.2	-4.7	0.0	0.0	16.5	20.0	1.2	-1.4	-1.4	-34.1	-5.9	32.4
Month 7	75.8	-6.5	0.0	0.0	14.2	17.5	1.8	-2.8	-2.1	-58.9	-8.0	31.0
Month 8	52.7	-8.6	0.0	0.0	19.0	23.6	1.4	-2.7	-1.3	-38.0	-7.8	38.3
Month 9	39.5	-5.1	0.0	0.0	22.2	29.1	1.5	-5.6	-1.7	-24.6	-6.7	48.7
Month 10	19.2	-6.0	0.0	0.0	23.3	27.9	1.5	-3.0	-1.1	-56.1	-6.2	-0.5
Month 11	9.4	-5.5	0.0	0.0	12.4	30.0	6.1	-3.9	-1.4	-85.1	-3.8	-41.9
Month 12	25.5	-6.9	0.0	0.0	7.3	9.2	2.8	-2.1	-1.1	-18.5	-2.3	13.8

LUC 8 – Snow/Ice as Compared with Coniferous Forest

For a snow/ice-covered surface, the months of January and February are repeated at the end of the year in Figure 18 to allow for continuity of the data. Snow/ice cover results in lower monthly summed deposition fluxes compared to a coniferous forest cover. From Table 9, it can be seen that difference are largely driven by SO_2, NO_2, and small particle deposition.

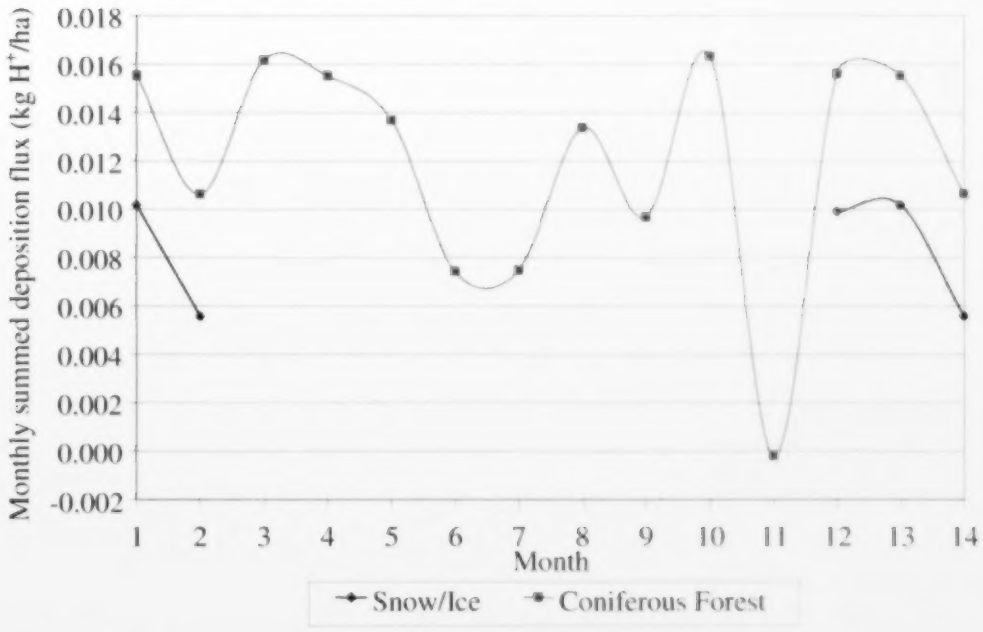

Figure 18 Comparison of monthly summed deposition flux for 11 species to snow/ice and coniferous forest cover using the AENV model.

4.4.2 Resistance Factors and Deposition Velocities

Aerodynamic resistance (R_a) is dependent on meteorological conditions and independent of deposition species for all LUCs in the AENV model. Calculation of boundary layer resistance (R_b) for gases is dependent on meteorological conditions and individual species and independent of the surface (i.e. LUC); consequently there are no differences in R_b values from one LUC to another for individual species. Finally, surface (canopy) resistance (R_c) is dependent upon individual species and surface type. Model results for

R_c for major depositing gases (SO_2, NO_2, and HNO_3) are examined more closely in the following section.

Table 9 Breakdown of magnitude of differences in monthly summed deposition flux in kg H^+/ha for individual species between snow/ice and coniferous forest cover using the AENV model.

Month	SO_2	NO_2	HNO_2	HNO_3	SO_4^{2-}	NH_4^+	NO_3-	Na^+	K^+	Ca^{2+}	Mg^{2+}	Total
Month 1	-0.3	-4.2	0.0	0.0	-0.7	-1.2	-0.3	0.4	0.1	0.6	0.2	-5.4
Month 2	-0.4	-4.2	0.0	0.0	-0.8	-1.0	-0.2	0.3	0.0	1.0	0.2	-5.1
Month 3												
Month 4												
Month 5												
Month 6												
Month 7												
Month 8												
Month 9												
Month 10												
Month 11												
Month 12	-0.7	-6.4	0.0	0.0	-0.8	-1.0	-0.6	0.4	0.2	2.7	0.4	-5.7

4.4.2.1 Gaseous Deposition (SO_2, NO_2, HNO_3)

Surface Layer Resistance (R_c) for SO_2

The calculation of R_c for SO_2 in the AENV method is done using default values such that it represents a total "dry" condition, total "wet" condition, or "weighted wet" condition using relative humidity (RH) and/or surface wetness (SW) measurement data for a specific LUC and season (Appendix A). For the input meteorological data set used in this study, the absence of surface wetness data resulted in the wetness condition being based upon whether the relative humidity was above or below 87%. Seasons are classified as winter (December to February), spring (March to May), summer (June to August), and autumn (September to November). The exception to this seasonal designation is that if the temperature for any hour is below 0°C during any season, then R_c for that hour is represented by the corresponding wet/dry value for winter for that species.

LUC 1 – Deciduous Forest

Monthly average R_c values for a deciduous forest surface cover (shown in Figure 19) are higher in winter and early spring/late autumn than for a coniferous forest surface cover. This would be expected due to an absence of leaves during these periods. Monthly average R_c values for both covers are similar during the leafy season (June, July, August).

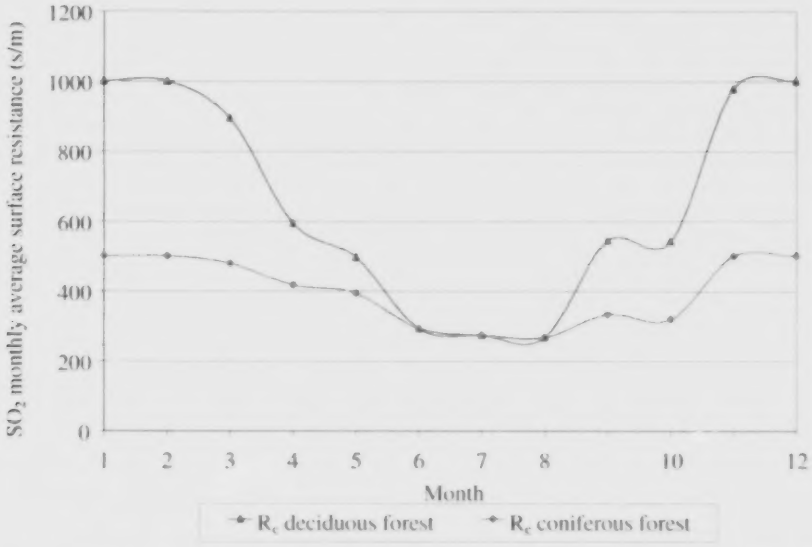

Figure 19 **Comparison of SO_2 monthly average surface resistance (R_c) for a deciduous forest and coniferous forest (base case) cover using the AENV model.**

LUC 3, 4, and 5 – Wetland/Swamp, Grassland, and Cropland

Monthly average R_c values for wetlands/swamp (Figure 20), grassland (Figure 21), and cropland (Figure 22) are all similar because of the nature of the growing season of vegetation representing these cover types in Alberta. Monthly average R_c values are the same for all three LUCs for the winter season; and they are all greater in winter compared to that for a coniferous forest cover which maintains more of its leaves (needles) during winter. During spring and summer months, monthly average R_c values for a wetland/swamp become much lower than those of the coniferous forest cover because of the growing season and lushness of vegetation.

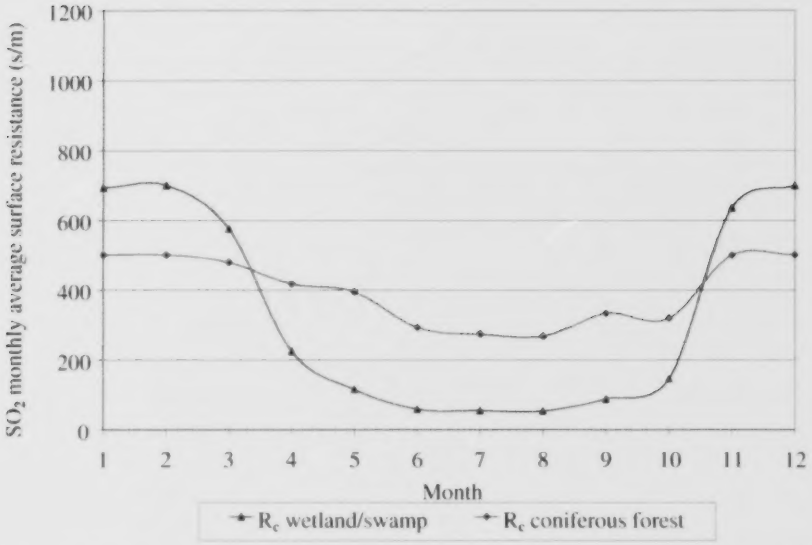

Figure 20 **Comparison of SO_2 monthly average surface resistance (R_c) for wetland/swamp and coniferous forest (base case) cover using the AENV model.**

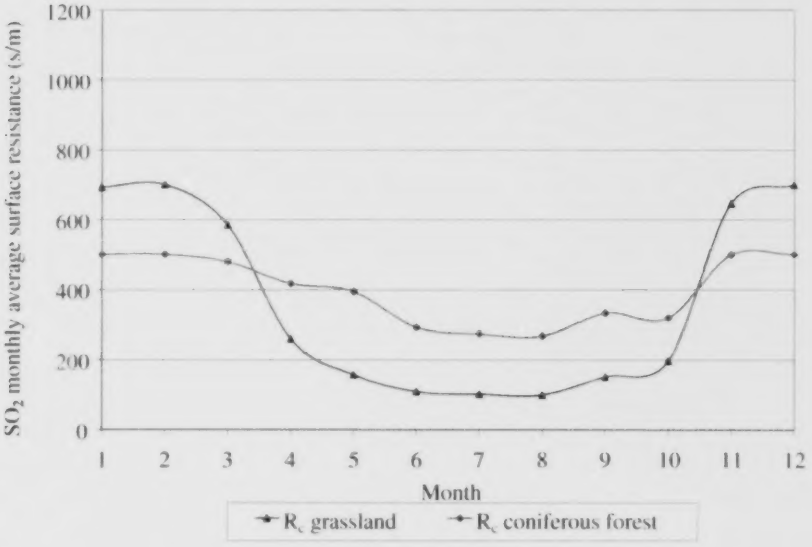

Figure 21 **Comparison of SO_2 monthly average surface resistance (R_c) for a grassland and coniferous forest (base case) cover using the AENV model.**

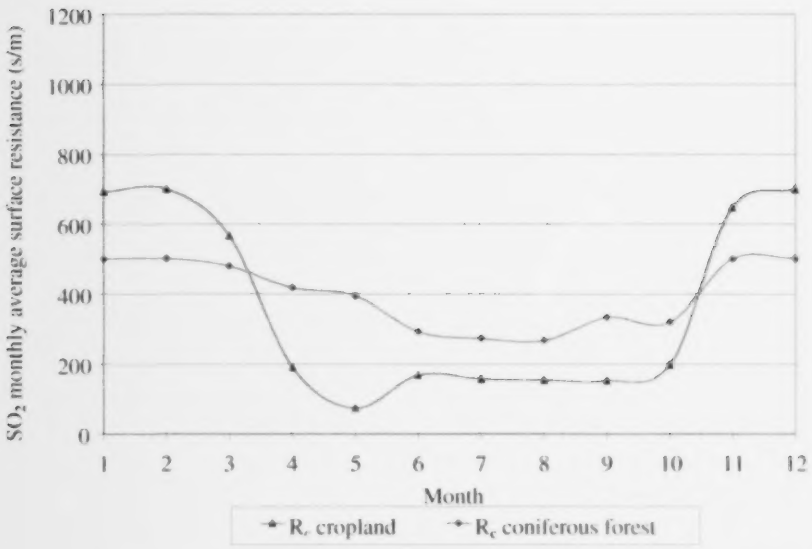

Figure 22 **Comparison of SO_2 monthly average surface resistance (R_c) for a cropland and coniferous forest (base case) cover using the AENV model.**

LUC 6 – Urban

Monthly average R_c values for urban land (shown in Figure 23) are higher than those for a coniferous forest cover; which may be a result of building and road surfaces which are not as interactive to atmospheric SO_2 as is vegetation. The declining resistance as summer progresses to autumn is mostly associated with increasing relative humidity; which is illustrated in Table 10.

LUC 7 – Water

Monthly average R_c values for water are constant and set at zero throughout a year (Figure 24).

LUC 8 – Snow/Ice

Monthly average R_c values for a snow/ice cover are shown in Figure 25. These values are similar as those for a snow-covered grassland, cropland, or wetland/swamp surface.

Table 10 **Monthly average relative humidity level (%) for data used to evaluate AENV model.**

month	Average
Month 1	69.2
Month 2	68.3
Month 3	63.3
Month 4	53.7
Month 5	55.5
Month 6	61.9
Month 7	67.1
Month 8	68.0
Month 9	75.4
Month 10	78.6
Month 11	73.6
Month 12	77.1

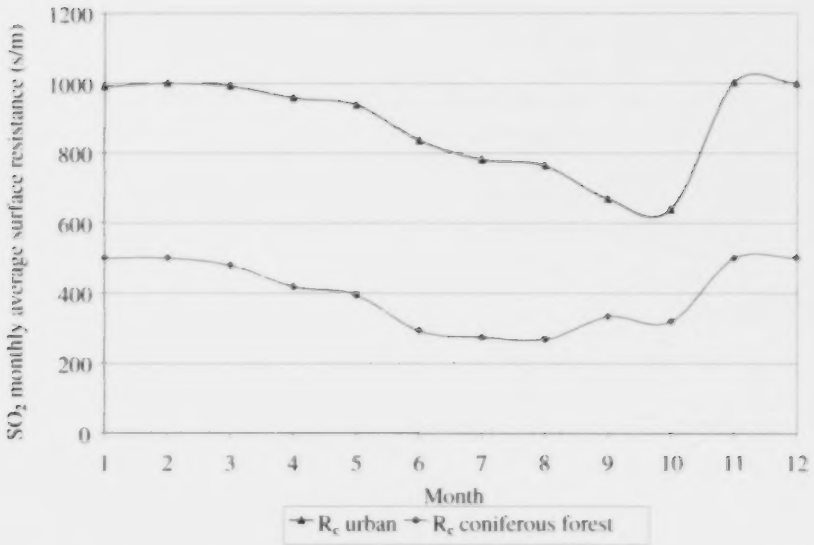

Figure 23 **Comparison of SO_2 monthly average surface resistance (R_c) for urban and coniferous forest (base case) cover using the AENV model.**

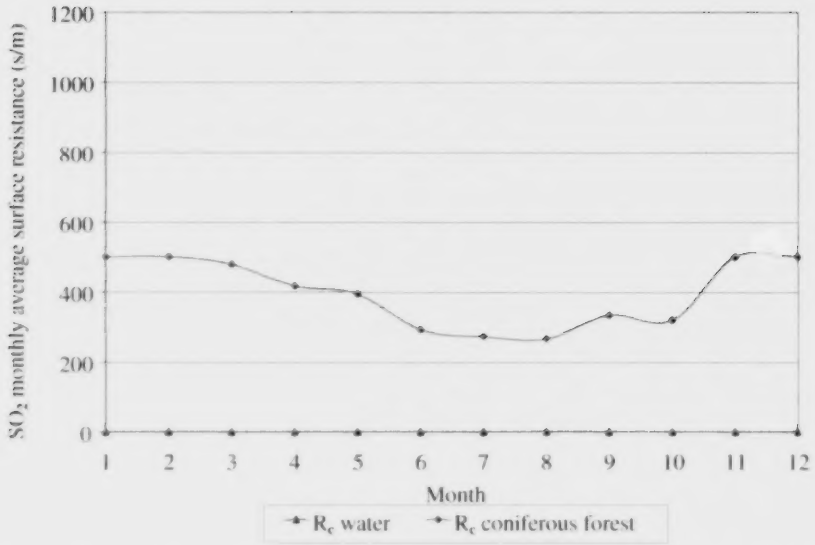

Figure 24 **Comparison of SO_2 monthly average surface resistance (R_c) for a water and coniferous forest (base case) cover using the AENV model.**

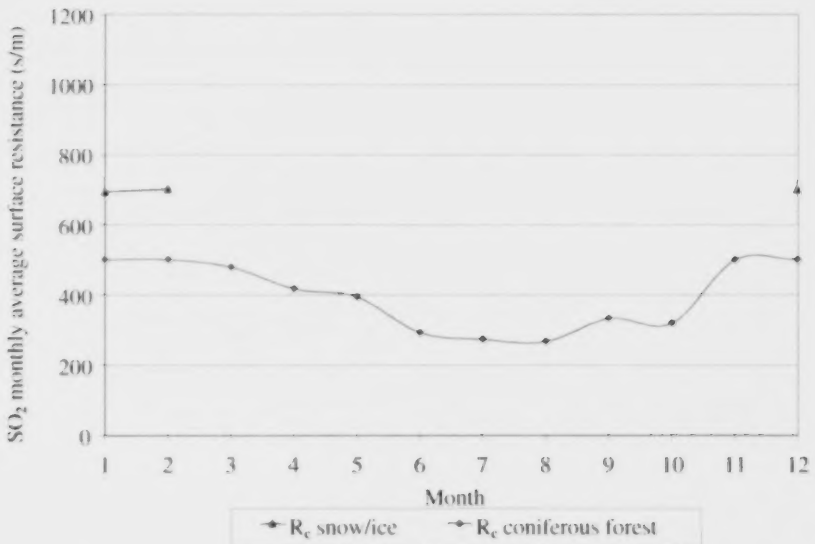

Figure 25 **Comparison of SO_2 monthly average surface resistance (R_c) for snow/ice and coniferous forest (base case) cover using the AENV model.**

Surface Layer Resistance (R_c) for NO_2

Similar to SO_2, R_c for NO_2 is dependent upon LUC, season, and wetness condition. Again, the wetness condition used in this study was based upon whether relative humidity was above 87%. The relationships between monthly average R_c values for NO_2 for different land uses are shown in Figures 26 to 32. The relationships for monthly average R_c values for NO_2 were similar to those for SO_2 except that values for NO_2 were generally much higher. Monthly average R_c values for NO_2 are more sensitive to differences between wet and dry conditions as compared to SO_2. Increases in monthly average R_c values for NO_2 across spring and summer months generally observed for all surface types reflects increasing relative humidity (as shown in Table 10). Even though November is classified as an autumn month, the presence of numerous hourly temperatures less than 0°C results in November behaving as a winter month.

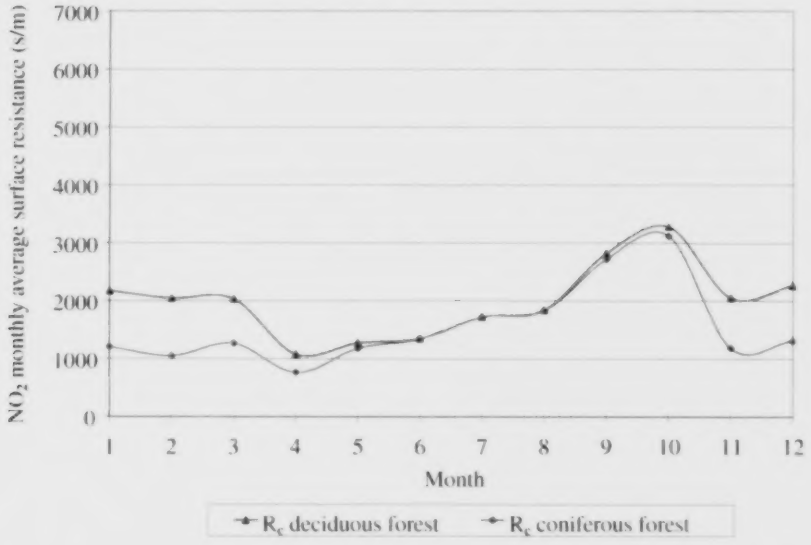

Figure 26 **Comparison of NO_2 monthly average surface resistance (R_c) for deciduous forest and coniferous forest (base case) cover using the AENV model.**

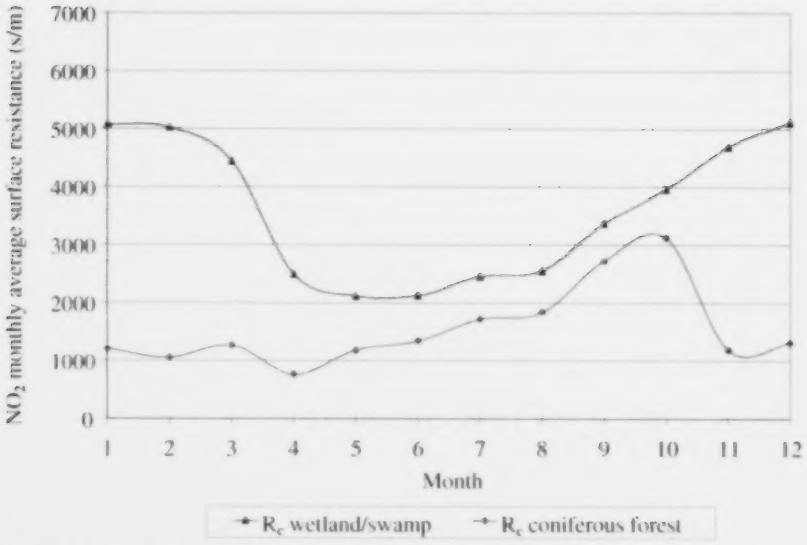

Figure 27 **Comparison of NO_2 monthly average surface resistance (R_c) for wetland/swamp and coniferous forest (base case) cover using the AENV model.**

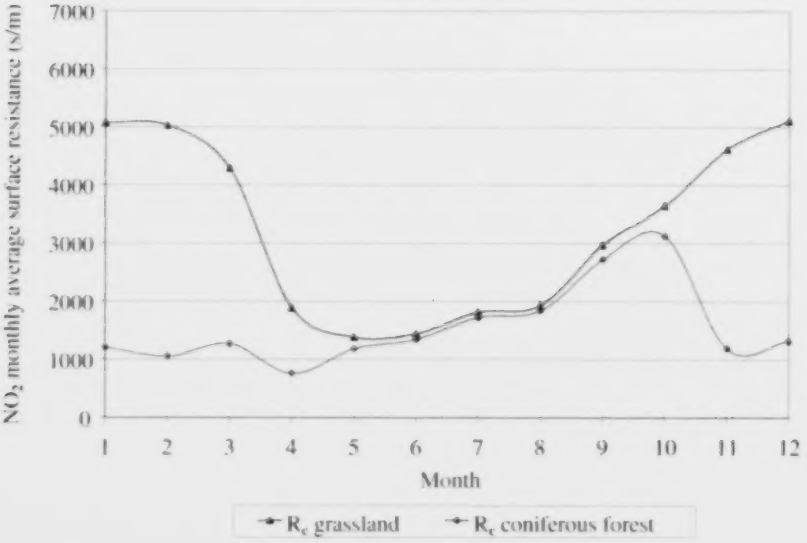

Figure 28 **Comparison of NO_2 monthly average surface resistance (R_c) for grassland and coniferous forest (base case) cover using the AENV model.**

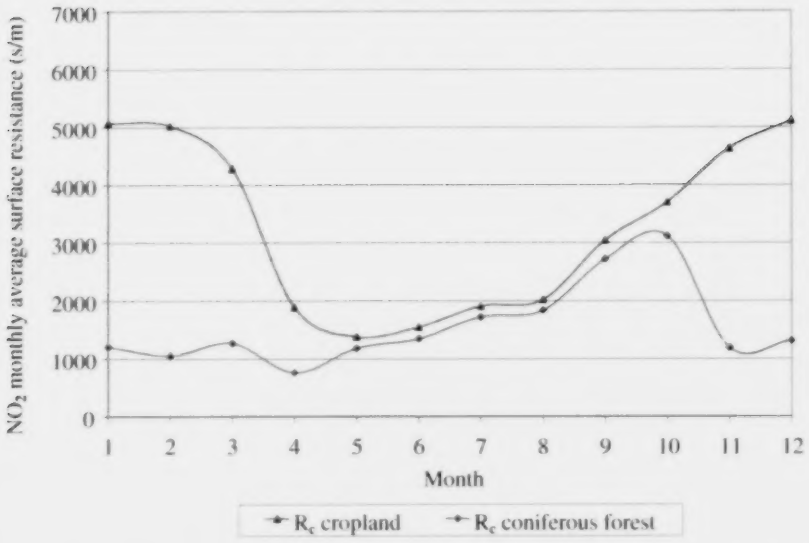

Figure 29 **Comparison of NO_2 monthly average surface resistance (R_c) for cropland and coniferous forest (base case) cover using the AENV model.**

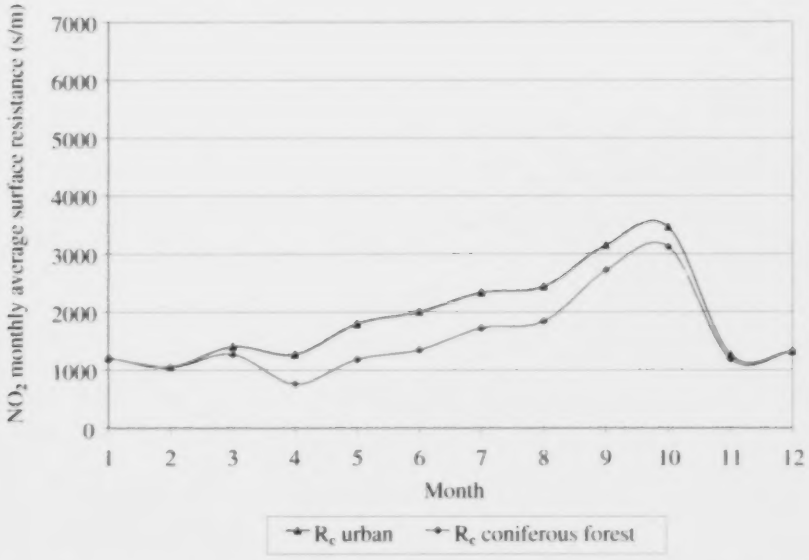

Figure 30 **Comparison of NO_2 monthly average surface resistance (R_c) for urban and coniferous forest (base case) cover using the AENV model.**

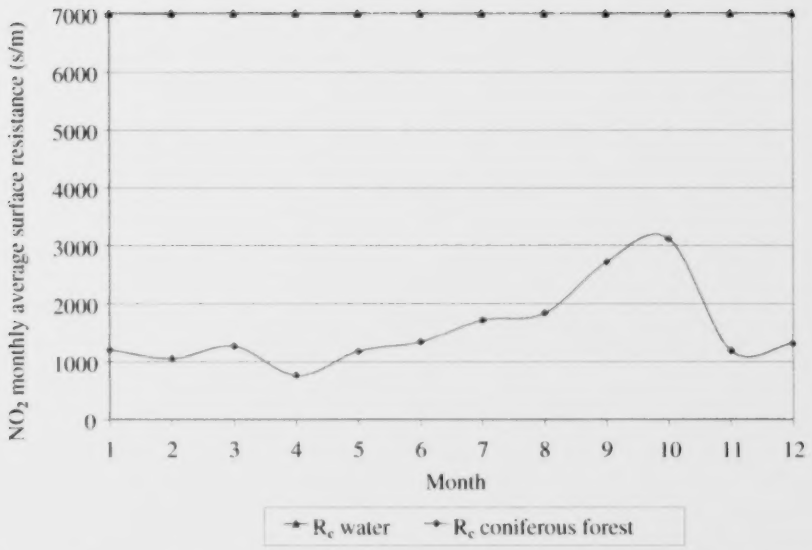

Figure 31 **Comparison of NO_2 monthly average surface resistance (R_c) for water and coniferous forest (base case) cover using the AENV model.**

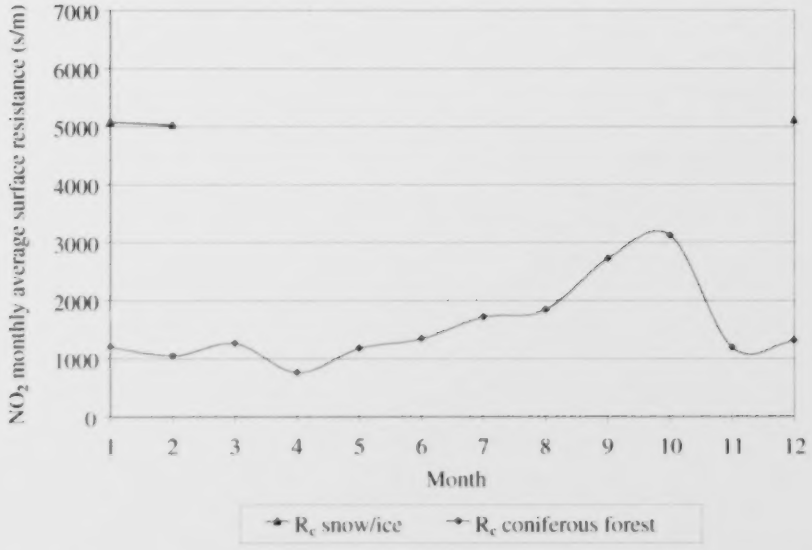

Figure 32 **Comparison of NO_2 monthly average surface resistance (R_c) for snow/ice and coniferous forest (base case) cover using the AENV model.**

Surface Layer Resistance (R_c) for HNO_3

Values for HNO_3 surface resistance (R_c) are treated as a constant (10 s/m) for all seasons and all surface types.

4.4.2.2 Fine and Coarse Particle Deposition (SO_4^{2-}, NH_4^+, NO_3^-, Na^+, K^+, Ca^{2+}, Mg^{2+})

The AENV model classifies SO_4^{2-} and NH_4^+ as fine (small) particle species; and NO_3^-, Na^+, K^+, Ca^{2+}, and Mg^{2+} as course (large) particle species. As stated previously, particle species deposition behavior is mostly dominated by aerodynamic resistance (R_a) based on aerodynamic diameter of a particle and independent of individual species. Boundary layer resistance (R_b) is treated as being constant within a season and a LUC. Surface (canopy) resistance (R_c) is treated as being negligible for particulate ions and is always zero. Therefore, deposition velocity for particles is treated as the inverse of the sum of R_a and R_b (Appendix B). Since it is not informative to examine R_a or R_b independently, deposition velocity for particles for the different LUCs was compared:

- Deciduous forest cover versus coniferous forest cover (base case) – In summer, monthly average deposition velocities for small and large particles for a deciduous forest cover are higher than those for a coniferous forest cover (base case) as shown Figure 33.
- Wetland/swamp versus coniferous forest cover – In Figure 34, it can be seen that monthly average small and large particle deposition velocities are lower for wetland/swamp compared to a coniferous forest cover (base case).
- Grassland versus coniferous forest cover – In Figure 35, small and large particle deposition velocities are even lower than those for wetland/swamp.
- Cropland versus coniferous forest cover – In Figure 36, a summer peak remains at the same level as that for grassland, however spring and autumn deposition velocities are clearly lower.
- Urban surface versus coniferous forest cover – In Figure 37, a summer peak is similar and higher compared to cropland and the spring and autumn deposition velocities are lower.
- Water versus coniferous forest cover is shown in Figure 38.
- Snow/ice versus coniferous forest cover – In Figure 39, deposition velocities are low and similar to those of a wetland/swamp, grassland, or cropland surface.

Tables summarizing all the monthly values used for Figures 33 to 39 for the eight LUCs are included in Appendix D.

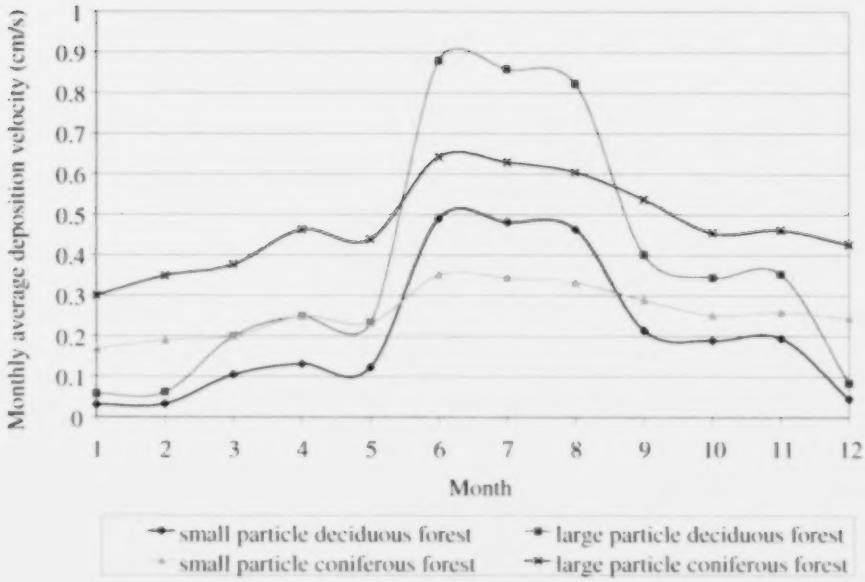

Figure 33 **Comparison of monthly average deposition velocity of small and large particles for a deciduous forest and coniferous forest (base case) cover using the AENV model.**

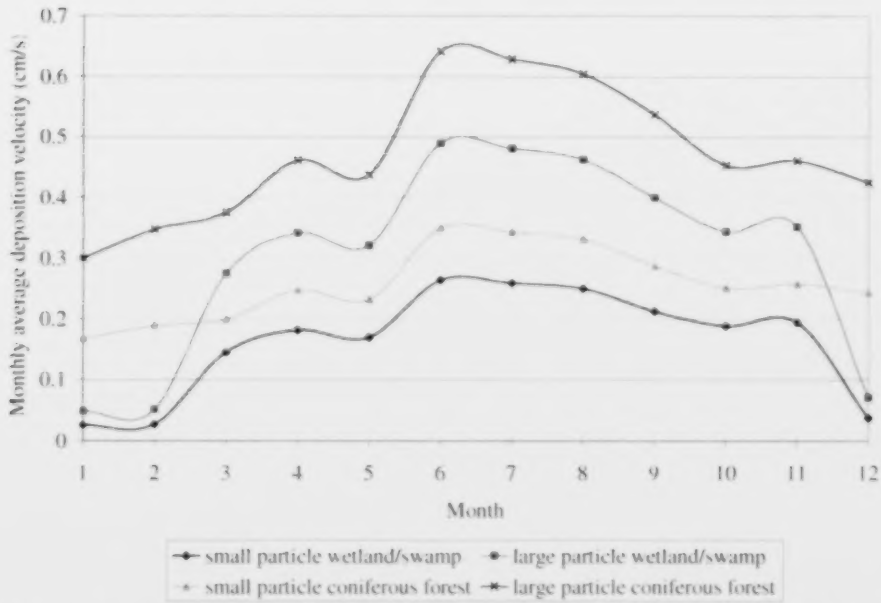

Figure 34 **Comparison of monthly average deposition velocity of small and large particles for a wetland/swamp and coniferous forest (base case) cover using the AENV model.**

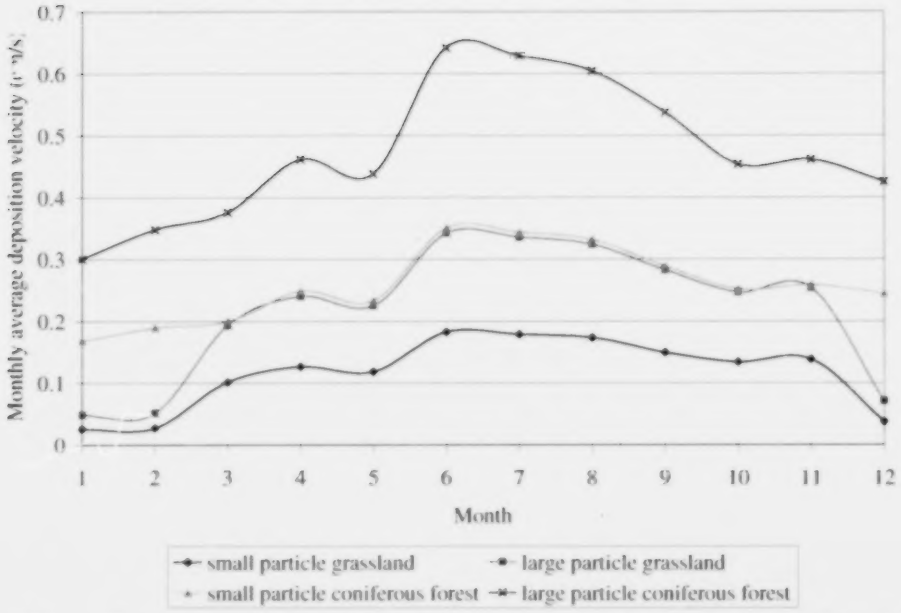

Figure 35 **Comparison of monthly average deposition velocity of small and large particles for grassland and coniferous forest (base case) cover using the AENV model.**

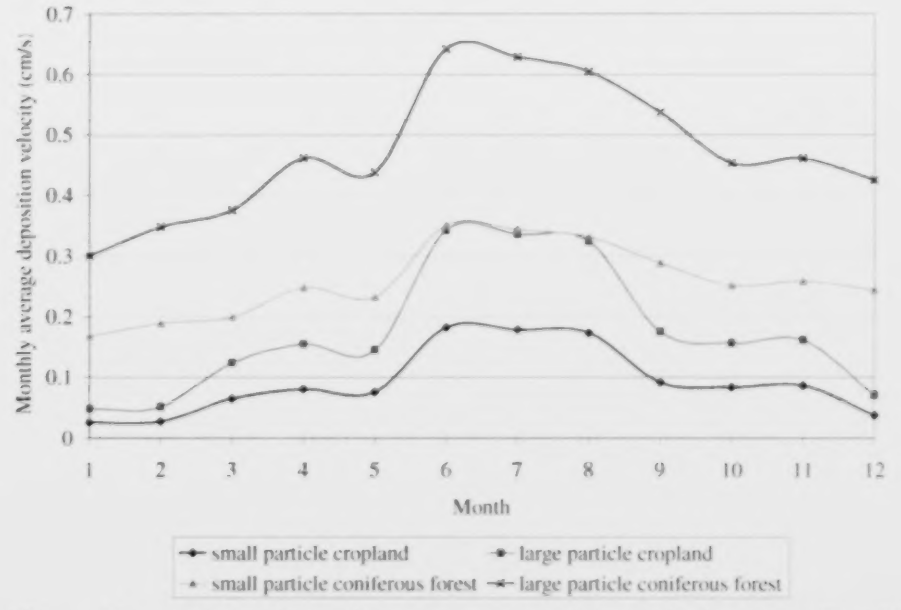

Figure 36 **Comparison of monthly average deposition velocity of small and large particles for cropland and coniferous forest (base case) cover using the AENV model.**

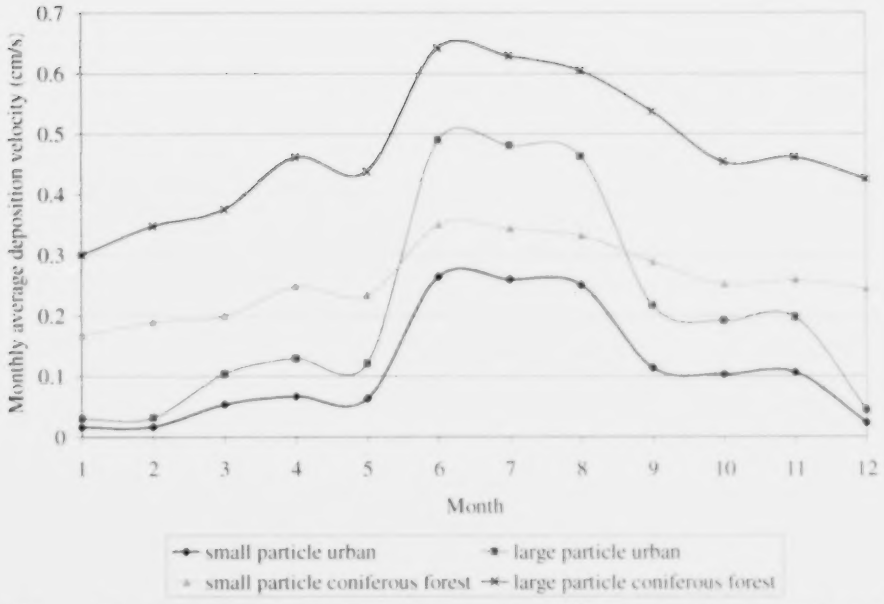

Figure 37 **Comparison of monthly average deposition velocity of small and large particles for urban and coniferous forest (base case) cover using the AENV model.**

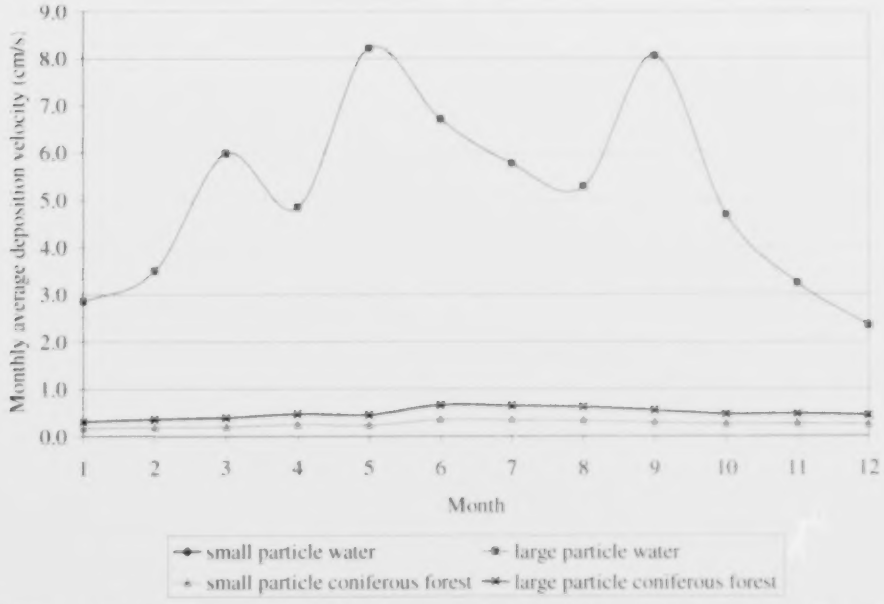

Figure 38 **Comparison of monthly average deposition velocity of small and large particles for water and coniferous forest (base case) cover using the AENV model.**

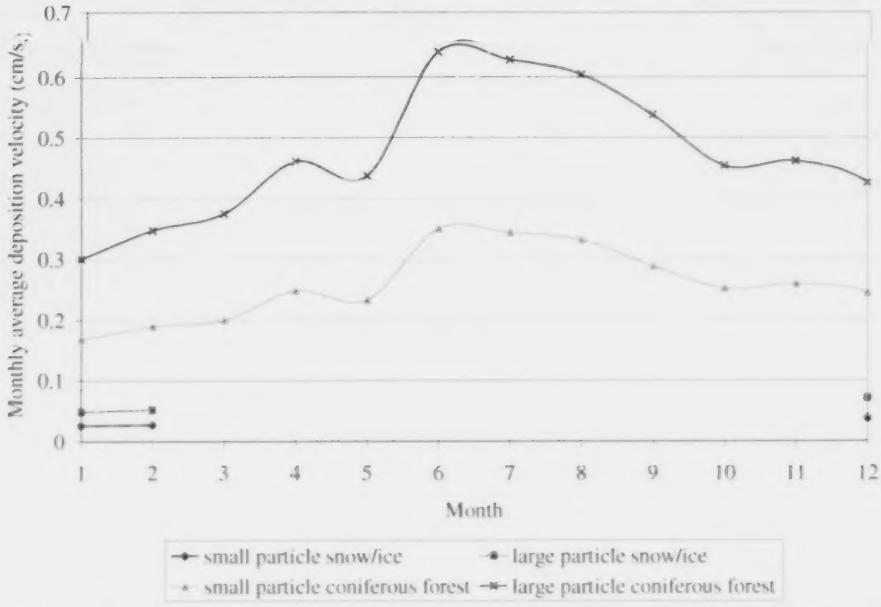

Figure 39 **Comparison of monthly average deposition velocity of small and large particles for snow/ice and coniferous forest (base case) cover using the AENV model.**

5.0 MODEL EVALUATION

5.1 Resistance Factors

5.1.1 Evaluation Methods

Deposition velocity (V_d) is calculated as the inverse of the sum of three resistances (R_a + R_b + R_c) on an hourly basis. In terms of potential acid deposition impacts, greater concern exists for species with higher deposition velocities. Because resistances are added before the sum is inverted, resistance factors with the largest magnitude of the three will dominate determination of deposition velocity. Therefore, influence of the largest resistance factor is the most important in terms of deposition velocity.

Two methods were used to evaluate behavior of the three resistance factors derived in the AENV model. In the first method, total resistance results (s/m) for each hour for the three most important depositing acidic species (SO_2, NO_2, and HNO_3) derived from both models were divided into the following ranges: i) less than 10, ii) 10 to 100, iii) 100 to 300, iv) 300 to 1000, and v) >1000 s/m. Within each range, the number of times that each of the three resistances was largest (or dominant) was counted. For HNO_3, size ranges less than 100 s/m were further broken down and similarly analyzed. These counts are summarized in Appendix F.

In the second method, a sensitivity analysis was conducted on the AENV model by separately increasing and decreasing each of the three resistances by a magnitude of 10% and 50% and observing the resulting changes in monthly summed deposition flux for 11 species.

5.1.2 Results

5.1.2.1 Dominant (Influential) Resistance Factors

The number of hourly occurrences in which each of the individual resistances was the dominant resistance was counted for SO_2, NO_2, and HNO_3 for each model and complete results are presented in Appendix F. For SO_2 in the ENVC model, R_c dominated in every instance; while in the AENV model, R_c usually dominated, but there were instances when R_a and R_b dominated.

SO_2

For example, for SO_2 deposition in October, there were 96 occurrences in which total resistance was between 10 and 100 s/m (Appendix F). Of these 96 occurrences, R_a

was dominant 20 times, R_b was dominant in 28, and R_c was dominant in 48. In contrast, for the ENVC model for this month, there were only 12 occurrences in which total resistance was between 10 and 100 s/m and all of which were R_c dominated (Appendix F). This difference suggests that AENV's approach for representing R_c values has a tendency to be less conservative relative to the ENVC approach for October conditions.

In January, there were no occurrences in which total resistance was less than 300 s/m for the AENV model (Appendix F), but there were 71 occurrences in the ENVC model in which total resistance was less than 300 s/m (three of which were between 10 s/m and 100). This difference suggests that AENV's approach for representing R_c values has a tendency to be more conservative realtive to the ENVC approach for January conditions and in the winter months (December through February). R_b was observed to be dominant in several instances in summer and autumn months in the AENV model.

NO_2

For NO_2, R_c dominated in every instance for the ENVC model for all ranges presented; while in the AENV model, R_c was observed to usually dominate, but there were instances where R_a dominated (Appendix F). This difference suggests that AENV's model for representing R_c values for NO_2 has a tendency to be less conservative compared to the ENVC approach. In spring and summer months, there was a greater occurrence of smaller total resistance values in the AENV model than in the ENVC model (Appendix F). This difference suggests that again AENV's model for representing R_c values for NO_2 has a tendency to be less conservative compared to the ENVC approach spring and summer months.

HNO_3

For HNO_3, R_c dominated in most instances in the ENVC model, but there were instances in which R_a or R_b was more dominant (Appendix F). In the AENV model, R_b dominated most often, followed by R_a and then R_c (Appendix F). Recall that R_c for HNO_3 is take as a constant equal to 10 s/m for all seasons and all surfaces.

The lowest total resistance range (10 to 100 s/m) was separated into smaller sections (shown in Appendix F) to allow for a more detailed comparison of the two models. In the 15 to 25 s/m range, R_c was always the dominant resistance for both models, but there were far more occurrences when this was the case for the AENV model than for the ENVC model.

In the 25 to 100 s/m range, R_b was the most common resistance factor that dominated in the AENV model; while R_c was the most common resistance factor that dominated in the ENVC model. These differences suggest that AENV's model for representing R_c values for HNO_3 has a tendency to be less conservative compared to the ENVC approach spring and summer months.

5.1.2.2 Sensitivity Testing of Resistance Factors

The other method to examine the relative importance of the three resistance factors was to check the influence of increasing and decreasing of magnitude of each of the resistances on monthly summed deposition flux.

Percent Change in R_a

The influence of a ten and fifty percent change (increase and decrease) in R_a on monthly summed deposition flux (kg H^+/ha) is shown in Figure 40. Months that were most influenced by the change in R_a were January, April, October, and December. The most important species that were responsible for these changes were HNO_2 (December) and HNO_3 (January, April, and October). Details of deposition quantities for these two species are tabulated in Appendix G.

Percent Change in R_b

The influence of a ten and fifty percent change (increase and decrease) in R_b on monthly summed deposition flux is shown in Figure 41. The months that were most influenced by the change in R_b were January, February, March, July, and November.

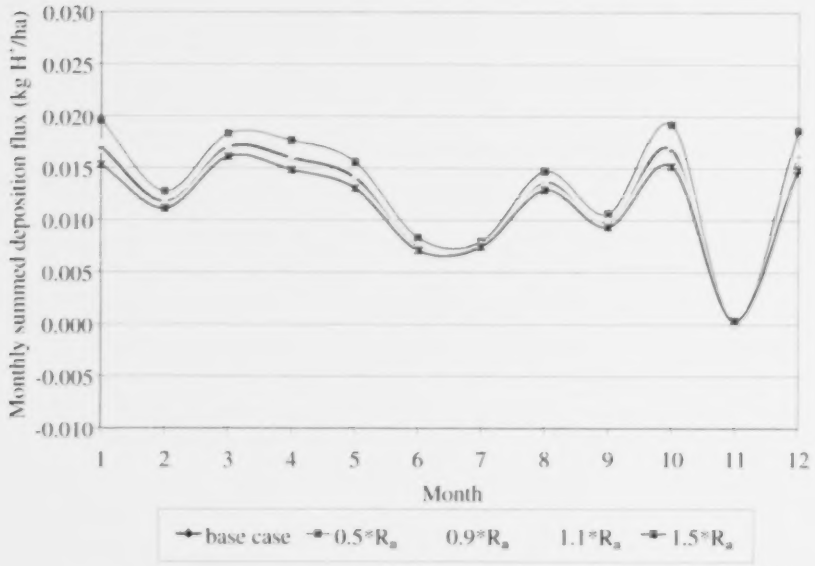

Figure 40 Monthly summed deposition flux for 11 species using AENV model showing influence of step changes in R_a for a coniferous forest cover.

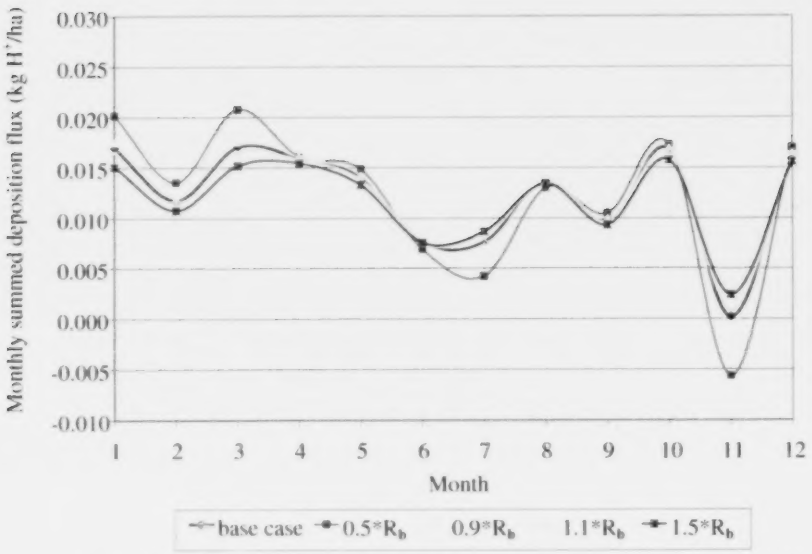

Figure 41 Monthly summed deposition flux for 11 species using AENV model showing influence of step changes in R_b for a coniferous forest cover.

A change in R_b values has more impact on total deposition than does an equivalent percent change in R_a, but not necessarily in the same months. The most important species that were responsible for changes were HNO_3 (January and October), SO_4^{2-} (March), NH_4^+ (March), and Ca^{2+} (July and November). The changes observed in February were caused by an absence of the neutralizing effect of calcium. Details of deposition quantities for these species are tabulated in Appendix G.

Percent Change in R_c

The influence of a ten and fifty percent change (increase and decrease) in R_c on monthly summed deposition flux is shown in Figure 42. Figure 42, when compared with Figures 40 and 41 shows that similar step changes in the magnitude of R_c are much more important in influencing total deposition than step changes in either R_a or R_b. The influence of changes in R_c is independent of month of the year although April and August had the greatest changes. The most important species that were responsible for changes were SO_2 (April, July, and August) and NO_2 (April, August, and December). Details of deposition quantities for these two species are tabulated in Appendix G.

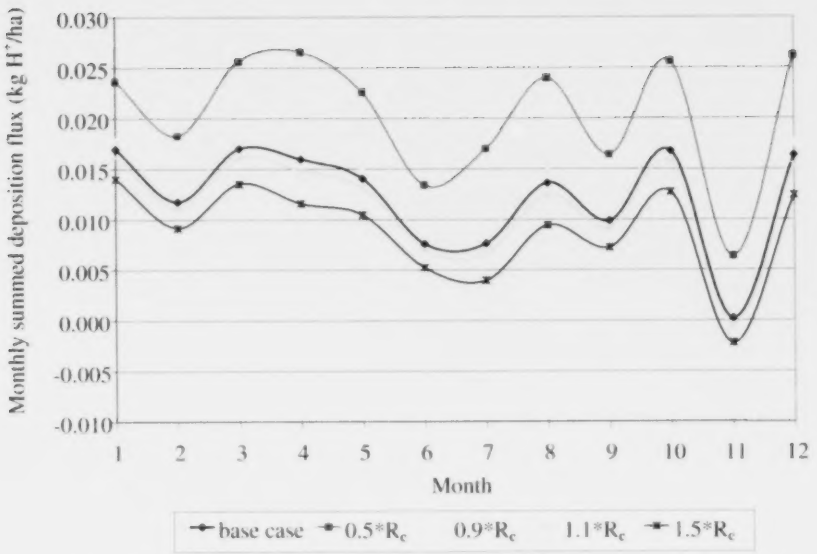

Figure 42 **Monthly summed deposition flux for 11 species using AENV model showing influence of step changes in R_c for a coniferous forest cover.**

5.1.2.3 Performance Indicators for AENV Model

Results presented in the previous sections suggest that AENV model performance is closely dependent on deposition velocity modeling for NO_2 and SO_2; particularly with respect to selection of surface (canopy) resistance (R_c) values used to parameterize NO_2 and SO_2 deposition. Relative to performance of the ENVC model, there are indications that values used for parameterizing R_c in the AENV model are less conservative for SO_2 in winter and spring and more conservative in summer and autumn. For NO_2, R_c values used for parameterizing R_c in the AENV model are less conservative in the autumn and winter and more conservative in the spring and summer. For HNO_3, deposition in the AENV model is driven by R_b.

It was stated previously that the ENVC inference model does not necessarily represent the best set of assumptions and conditions to parameterize dry deposition. In addition, AENV's parameterization of R_c originates from previously published values that are seasonal- and species-specific and, therefore, can be considered reasonable. Thus while there are apparent differences in how both models parameterize R_c, the evaluation results presented above only show where the models depart in their treatment of surface (canopy) resistance.

5.2 Parameter Boundary Conditions

One of the recommendations put forward by WBK (2008) was that performance of the AENV model may be improved relative to performance of the ENVC model by adopting some of the boundary conditions used for specific parameters in the ENVC model and including them in the AENV model. Specific boundary conditions in the ENVC model that are currently not used in the AENV model include:

- A defined range limit for R_a (minimum of 5; maximum of 1000 s/m (2000 s/m over water).
- A defined range limit for the Monin-Obukhov length (L) used as a measure of instability ($L = -5$ if $-5 < L < 0$ and $L = 5$ if $0 < L < 5$; as specified in the ENVC model, Appendix A).
- Establishing a minimum wind speed of 1 m/s for wind speeds recorded below this level.

5.2.1 Evaluation Methods

The AENV model was run several times, each time with a modification to include a separate boundary condition used by the ENVC model using a coniferous forest cover and hourly pollutant concentration and meteorological data from the Fort MacKay air monitoring station. Results were compared to original AENV model results (base case).

5.2.2 Results

5.2.2.1 Aerodynamic Resistance

Minimum of 5 s/m for R_a

In the ENVC model, aerodynamic resistance (R_a) is limited to a minimum of 5 and a maximum of 1000 s/m for all land use categories except for water; which has an upper limit of 2000 s/m. R_a is an indication of the mixing conditions of atmosphere such that a very low R_a implies maximum mixing conditions. The purpose of a minimum limit acknowledges that, inferentially, there is always some limit to mixing possible in a natural atmosphere. Because R_a is added to R_b and R_c in the determination of deposition velocity for a pollutant, a minimum R_a value will only have an important effect on deposition velocity if values for R_b and R_c for that hour are also small.

The number of times hourly R_a values were within certain ranges within a maximum of 1000 s/m were counted and summarized in Table 11 for the AENV model modified to run R_a with an allowable upper limit of 1000 s/m. Model conditions were for a coniferous forest cover and using hourly pollutant concentration and meteorological data from the Fort MacKay air monitoring station. From Table 11, it can be seen that May

was the month with the greatest number of hourly occurrences with the smallest computed R_a value (i.e., 0 to 10 s/m); which implies that it should be the month with the largest difference in corresponding deposition flux.

The AENV model was modified and rerun using an allowable lower value of 5 s/m for R_a and results (monthly summed deposition flux for all 11 species) were compared to the model run under base case conditions and to ENVC model results. Results are presented in Table 12. As shown in Table 12, May did in fact show the largest change of 0.06 g H^+/ha in deposition flux, although this difference only represented less than a 0.5% change in total deposition. This indicates that the overall effect of setting this minimum limit on R_a in the AENV model is anticipated to be small.

Table 11 Counts of hourly R_a values within a maximum of 1000 s/m for the AENV model run with an allowable upper limit of 1000 s/m for a coniferous forest cover.

Ra (s/m)	≤ 10	≤ 20	≤ 30	≤ 40	≤ 50	≤ 60	≤ 70	≤ 80	≤ 90	≤ 100
Jan	58	105	58	28	16	9	7	4	8	8
Feb	72	150	55	18	11	8	4	2	6	2
Mar	209	113	35	10	8	4	5	3	2	2
Apr	102	221	82	41	25	15	0	6	2	2
May	293	91	22	12	15	9	5	6	1	2
Jun	212	167	52	14	12	5	9	5	5	3
Jul	164	199	70	31	12	9	12	3	3	2
Aug	140	210	70	18	14	16	4	3	3	7
Sep	260	128	31	21	8	6	5	5	3	3
Oct	139	135	45	37	19	15	13	5	5	2
Nov	29	182	92	55	20	18	11	13	5	7
Dec	7	89	142	94	35	23	22	9	12	11

Ra (s/m)	≤ 200	≤ 300	≤ 400	≤ 500	≤ 600	≤ 700	≤ 800	≤ 900	≤ 1000
Jan	26	10	9	6	6	5	5	3	372
Feb	11	10	7	6	1	1	1	1	330
Mar	12	5	8	2	2	2	1	6	291
Apr	16	7	4	3	2	1	0	0	191
May	19	12	4	4	11	2	1	2	233
Jun	25	13	6	6	5	4	1	6	170
Jul	15	11	8	6	3	2	4	3	187
Aug	21	8	4	6	2	5	4	2	207
Sep	22	13	9	2	11	2	2	2	187
Oct	31	19	14	5	5	7	5	3	240
Nov	29	14	7	5	3	3	2	5	220
Dec	54	16	10	9	15	2	0	2	192

Note: Ranges presented include the following increments – ≤10 = 0 to 10 s/m, ≤20 = 10 to 20 s/m, etc.

Maximum of 1000 s/m for R_a

Just as a very low R_a value would not necessarily offer a reasonable representation of natural conditions during daytime; neither would an extremely high R_a value. A very high R_a value would be associated with no mixing in the atmosphere (ideally stable night

time conditions). From a practical point of view, very large aerodynamic resistances are not much different than moderately large aerodynamic resistances since deposition velocity involves the inverse of the sum of all three resistances ($R_a + R_b + R_c$). When hourly deposition values for a month are summed, it is the hourly conditions with small summed values for the three resistance factors (and hence correspondingly large deposition velocity and deposition flux values) that are important and drive the overall monthly summed deposition flux. Hence very large or moderately large aerodynamic resistance values (and correspondingly very small or moderately small deposition velocity and deposition flux values) are unimportant.

Table 12 Comparison of monthly summed deposition flux (g H^+/ha) for AENV model with minimum R_a limit of 5 s/m to AENV base case model and ENVC model results for coniferous forest cover.

	AENV w/ limit	AENV w/out limit	ENVC	difference w/limit in AENV model	closer to ENVC model
Month 1	15.5	15.5	15.5	-0.02	+
Month 2	10.6	10.6	11.4	0.00	0
Month 3	16.1	16.1	16.2	-0.02	+
Month 4	15.5	15.5	17.0	0.00	0
Month 5	13.6	13.7	12.0	-0.06	+
Month 6	7.4	7.4	6.5	-0.02	+
Month 7	7.5	7.5	10.7	0.00	0
Month 8	13.4	13.4	12.9	0.00	0
Month 9	9.6	9.6	12.2	-0.02	-
Month 10	16.3	16.3	18.0	-0.03	-
Month 11	-0.2	-0.2	3.6	0.00	0
Month 12	15.6	15.6	16.8	0.00	0
total	140.9	141.0	152.8	-0.2	-

An upper limit on R_a might be expected to have an effect where a monthly summed deposition flux results from the sum of a large number of small hourly deposition flux values (corresponding to large number of large hourly deposition velocity values perhaps influenced by large R_a values). As can be seen from Table 11, January had a large number of high R_a values between 900 and 1000 s/m (372) and few small R_a values (58 between 0 and 10 s/m). This is in contrast to the month of September; which had a small number of high R_a values between 900 and 1000 s/m (187) and numerous small R_a values (290 between 0 and 10 s/m). It would be expected that the month of January would show a greater response to the presence of a maximum limit set to R_a compared with September.

This is demonstrated to be the case in Table 13. The AENV model was rerun using a maximum value of 1000 s/m for R_a and results (monthly summed deposition flux) for all

11 species) were compared to the model run under the base case conditions and to ENVC model results. January shows the greatest change relative to the base case conditions. In addition, the direction of change caused by using a maximum value of 1000 s/m for R_a was to bring AENV model results closer to ENVC model results. In comparison with the AENV base case, using a maximum value of 1000 s/m for R_a in the AENV model resulted in an overall increase of 7 g H^+/ha in total annual deposition flux. This represents a 5% difference. Monthly deposition is shown graphically in Figure 43.

Table 13 Comparison of monthly summed deposition flux (g H^+/ha) for AENV model with maximum R_a limit of 1000 s/m to AENV base case conditions and ENVC model results for coniferous forest cover.

	AENV w/ limit	AENV w/out limit	ENVC	difference w/limit in AENV model	closer to ENVC model
Month 1	17.0	15.5	15.5	1.5	-
Month 2	11.3	10.6	11.4	0.7	+
Month 3	17.1	16.1	16.2	1.0	-
Month 4	16.0	15.5	17.0	0.5	+
Month 5	14.3	13.7	12.0	0.6	-
Month 6	7.7	7.4	6.5	0.2	-
Month 7	7.5	7.5	10.7	0.1	+
Month 8	13.7	13.4	12.9	0.3	-
Month 9	9.9	9.6	12.2	0.3	+
Month 10	17.0	16.3	18.0	0.7	+
Month 11	0.3	-0.2	3.6	0.5	+
Month 12	16.5	15.6	16.8	0.9	+
total	148.3	141.0	152.8	7.2	+

5.2.2.2 Monin-Obukhov Length

In the ENVC model, the Monin-Obukhov length (L) is limited to a maximum and minimum value of -5 and 5 for negative and positive values, respectively. L is used in the calculation of the stability function which is ultimately used in calculation of R_a. L represents the height above the surface in which convectively driven turbulence dominates over mechanically driven turbulence and it is indirectly a measure of the convective instability generated by the vertical heat flux through the surface layer. L is only meaningful in daytime convectively driven boundary layers.

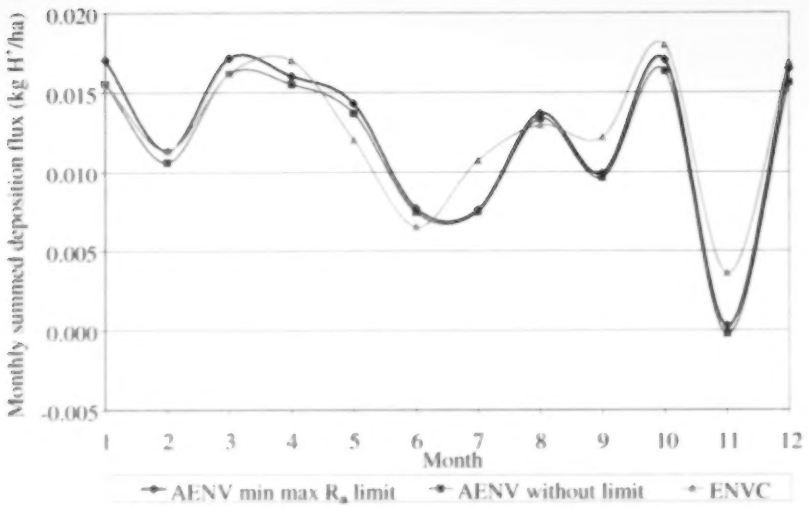

Figure 43 **Monthly summed deposition flux for 11 species using AENV model showing changes with and without (base case) minimum 5 s/m and maximum 1000 s/m limits to hourly R_a values for a coniferous forest cover.**

A negative value for L represents atmospheric instability and a positive value represents stability. Small absolute values for L represent extremes which are not representative in nature. In general, as L approaches zero, R_a becomes larger and corresponding deposition velocity is smaller. The result of applying the limit to L is a slightly lower R_a and a slightly higher corresponding deposition velocity. Since it is higher R_a values that are affected, the nature of the change should be similar to that of setting an upper limit on R_a. The effects of using limits to L are shown in Table 14 and Figure 44.

Annual summed deposition flux was increased by 5 g H^+/ha which represents a 4% difference in total deposition. The direction of change caused by using limits to L was to bring AENV model results closer to ENVC model results (the same general effect caused by setting an upper limit or 1000 s/m to R_a).

5.2.2.3 Minimum Wind Speed

Wind speed values in the AENV model are allowed to vary to a minimum of 0.09 m/s, below which they are assigned a value of 0 m/s. In the ENVC model, wind speed values are allowed to vary to a minimum of 1 m/s, below which they are assigned a value of 1 m/s. The effects of using a 1 m/s limit on wind speed in the ENVC model is shown in Table 15 and Figure 45. Annual deposition flux was increased by 6 g H^+/ha which represents a 4% difference in total deposition. The direction of change caused by using a

1 m/s limit to wind speed was to bring AENV model results closer to ENVC model results.

Table 14 **Monthly summed deposition flux (g H^+/ha) for 11 species showing changes with and without limits set on L with AENV base case conditions and ENVC model results for a coniferous forest cover.**

	AENV w limit	AENV w/out limit	ENVC	difference w/limit in AENV model	closer to ENVC model
Month 1	16.4	15.5	15.5	0.9	-
Month 2	11.0	10.6	11.4	0.4	+
Month 3	16.6	16.1	16.2	0.4	-
Month 4	15.9	15.5	17.0	0.4	+
Month 5	14.4	13.7	12.0	0.7	-
Month 6	7.7	7.4	6.5	0.3	-
Month 7	7.6	7.5	10.7	0.1	+
Month 8	13.6	13.4	12.9	0.2	-
Month 9	9.8	9.6	12.2	0.2	+
Month 10	16.9	16.3	18.0	0.6	+
Month 11	0.3	-0.2	3.6	0.5	+
Month 12	16.1	15.6	16.8	0.5	+
total	146.2	141.0	152.8	5.1	+

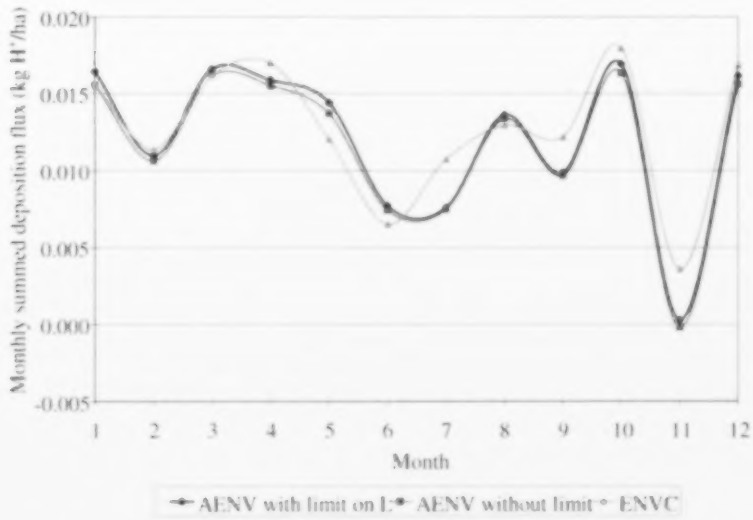

Figure 44 **Monthly summed deposition flux for 11 species using AENV model showing influence with and without (base case) limits on L for a coniferous forest cover.**

Table 15 Comparison of AENV total deposition for 1 m/s minimum limit on wind speed with AENV base case conditions and ENVC model results for a coniferous forest cover.

	AENV with 1 m/s wind speed limit	AENV without limit	ENVC	difference w/limit in AENV model	closer to ENVC model
Month 1	17.9	15.5	15.5	2.4	0
Month 2	11.2	10.6	11.4	0.6	+
Month 3	16.6	16.1	16.2	0.5	-
Month 4	15.6	15.5	17.0	0.1	+
Month 5	13.8	13.7	12.0	0.2	-
Month 6	7.5	7.4	6.5	0.1	-
Month 7	7.6	7.5	10.7	0.1	+
Month 8	13.7	13.4	12.9	0.3	-
Month 9	10.0	9.6	12.2	0.4	+
Month 10	16.9	16.3	18.0	0.6	+
Month 11	-0.3	-0.2	3.6	-0.1	-
Month 12	16.5	15.6	16.8	0.9	+
total	147.3	141.0	152.8	6.2	+

Wind speed is involved in the calculation of both R_a (for gases and particulates) and R_b (for gases). Using a minimum wind speed limit would be expected to affect months that have a large number of low hourly wind speeds, resulting in low R_a and R_b. Similar to a maximum limit set for R_a, as discussed previously, January would be expected to show the largest difference. Table 15 indicates that January shows the greatest change relative to the base case conditions.

5.3 Non-Boundary Condition Components

Three non-boundary issues were examined during this study. In the AENV model, two issues were further analyzed: i) calculation of surface roughness length (z_o), and ii) use of relative humidity (RH) as a surrogate parameter to define wetness conditions of a surface instead of a surface wetness measurement. In the ENVC model, treatment of the particle distribution for particle deposition was further analyzed.

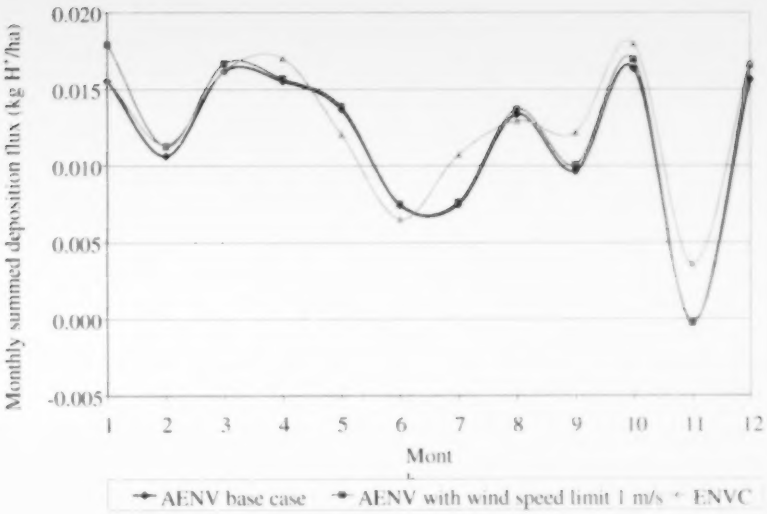

Figure 45 Monthly summed deposition flux for 11 species using AENV model showing the influence of with and without (base case) a 1 m/s minimum limit on wind speed for a coniferous forest cover.

5.3.1 Evaluation Methods

5.3.1.1 Surface Roughness Length

One potential limitation of the AENV method is a requirement to calculate surface roughness length (z_o) as a monthly average using hourly data where the wind speed is >6 m/s. At issue is a situation where only a small number of hourly values exist during the month in which the wind speed is >6 m/s. This results in greater uncertainty in the calculated average z_o value when computed from a small number of hourly values in which the wind speed is >6 m/s during the month.

The AENV model was rerun using modified criteria to establish representative values for z_o based on a minimum requirement that at least seven hourly data points must be used in the calculation of an average z_0 for that month:

- If one consecutive month did not have at least seven hourly data points to be used in the calculation of the z_o (e.g., November data in this case); then an average monthly z_o computed from for the two adjacent months (October and December in this case) are to be used.
- If two or more consecutive months did not have at least seven hourly data points to be used in calculation of z_o (e.g., February and March in this case); then an average annual value computed from z_o values for all months that had at least seven hourly data points was used to represent these months. This could be

applicable to surface cover characteristics that are not expected to undergo substantial change from season to season (e.g., a coniferous forest canopy).

- Resulting deposition flux values were then compared with original results.

Changing the minimum wind speed criterion (>6 m/s) in which to calculate a monthly z_o value was also examined by evaluating the relationship between different minimum wind speed criteria above and below 6 m/s and corresponding calculated monthly z_o values.

5.3.1.2 Surface Wetness and Relative Humidity

Wetness alters the characteristics of a surface to act a sink for depositing species (primarily gases). The AENV model requires an hourly measurement to represent the amount of wetness on a surface in determination of surface resistance (R_c). The model is set up to use field measurement data from surface wetness sensing equipment. However, past experience has indicated that this field equipment does not provide reliable measurement data in an Alberta setting due to the wide temperature ranges experienced. Alternatively, the AENV model can use relative humidity (RH) as a surrogate criterion for surface wetness (Bates, 1996). The AENV method uses a lower limit for RH of 87.4% in classifying a surface as being wet for the full hour after Bates (1996).

The effect of using different limits for RH was examined. The original AENV model was modified to set the RH value as 80% for the cutoff in determination of a wet/dry condition for selection of the R_c value for SO_2 and NO_2 for each of land use category. Similarly, the original AENV model was modified to use a RH value of 92% as the cutoff. Results in terms of monthly summed deposition flux for all species were compared to original results for each land use category.

5.3.1.3 Settling Properties of Large Particle Size Distributions

The ENVC model has an inherent limitation in the way that it treats settling properties of species associated with large particles (i.e., NO_3^-, Na^+, K^+, Ca^{2+}, and Mg^{2+}). The model forces the treatment settling properties for >24% of these particles (by mass) as being similar to settling properties of fine particles. This results in an underestimate of the neutralization capacity offered by depositing particulates containing base cations; and an overestimate in total deposition flux to a surface when all depositing species are taken into account. This limitation was further investigated to show how large this effect was for the ENVC model. In essence, because the ENVC model tends to estimate higher total deposition fluxes compared to the AENV model, better agreement among these two models would be achieved.

5.3.2 Results

5.3.2.1 Surface Roughness Length

One potential issue with the AENV model is the way surface roughness length (z_o) is calculated. The AENV model requires that hourly data to be used in calculation of z_o during a particular month be initially based on a monthly average z_o value using hourly data where the wind speed is >6 m/s in that month (WBK, 2008). For the 2003 meteorological data used in this study, the month of February did not have a single hourly wind speed value >6 m/s (shown in Table 16) such that it was necessary to use an average z_o value of the two surrounding months. In general, there was a lack of hourly values for several months (e.g., February, March, and November) for use in calculation of z_0 given the 6 m/s minimum wind speed cutoff value. The number of hourly values used for calculating each of the monthly average z_0 values ranged from 0 to 42 (shown in Table 16).

Table 16 Monthly average surface roughness length (z_o, m), standard deviation, and sample size (number of hourly values) in which wind speed >6 m/s for calculation of monthly average surface roughness length for a coniferous forest cover.

Month	z_0	Standard Deviation	Sample Size
January	1.24	0.40	19
February			0
March	1.50	0.54	6
April	0.67	0.18	42
May	1.46	0.75	29
June	1.26	0.45	26
July	1.20	0.49	10
August	1.11	0.52	13
September	1.61	0.89	9
October	1.30	0.64	10
November	0.72	0.24	2
December	0.50	0.16	7
	1.12	Weighted Annual Average	

For months with too few hours in which to calculate z_0, it would perhaps be more suitable if monthly wind speed data from another meteorological year could be used to supplement the number of observations used in the initial calculation of a z_o value for that that month at a site-specific location. Unfortunately, these data would not be applicable

for a location undergoing changes in surrounding land use. The approach taken here was to establish a requirement for the minimum number of hourly observations in which wind speed >6 m/s for calculating z_0 for a particular month:

- Seven was the number selected as the minimum number of observations in which to use.
- The average z_0 value of two surrounding months was established for any month in which an insufficient number of observations existed.
- If consecutive months data have an insufficient number of observations for a surface cover whose characteristics are not expected to undergo substantial change from season to season (e.g., a coniferous forest canopy), then an annual average should be used for these months. (Alternatively, if consecutive months have an insufficient number of observations for a surface cover whose characteristics are not expected to undergo substantial change within a season, then an average for the month within the season could be used for to represent these months.)

These changes were incorporated into the AENV model and results presented in Figure 46. Figure 46 is a plot of monthly summed deposition flux for 11 species using the AENV model showing the influence resulting from use of surrogate z_0 values for the months of February, March, and November versus the base case. z_0 used for November was taken as the average of October and December and the z_0 value used for February and March was taken as the annual average value shown in Table 16. Figure 46 shows that these substitutions only result in slightly higher deposition fluxes in February and March; while the difference in November is negligible.

Another potential issue with calculation of z_0 in the AENV model is that there was a wide variation computed for different months across the year. In theory, a mature coniferous forest should have a similar surface roughness length across the year because the foliage does not change seasonally. The ENVC model (Appendix A) assumes that the surface roughness length (z_0) for an evergreen needle leaf forest is consistent throughout the year at a value of 0.9 m. In the AENV model in this study, z_0 ranged from 0.5 m in December to 1.6 meters in October (Table 16).

Even within a particular month, z_0 was variable as seen in standard deviations for the AENV model (shown in Table 16). It has been observed by others that values for z_0 can change for different wind speeds if the surface cover is such that it can bend with the wind, thereby reducing the roughness length (Marht, 2001).

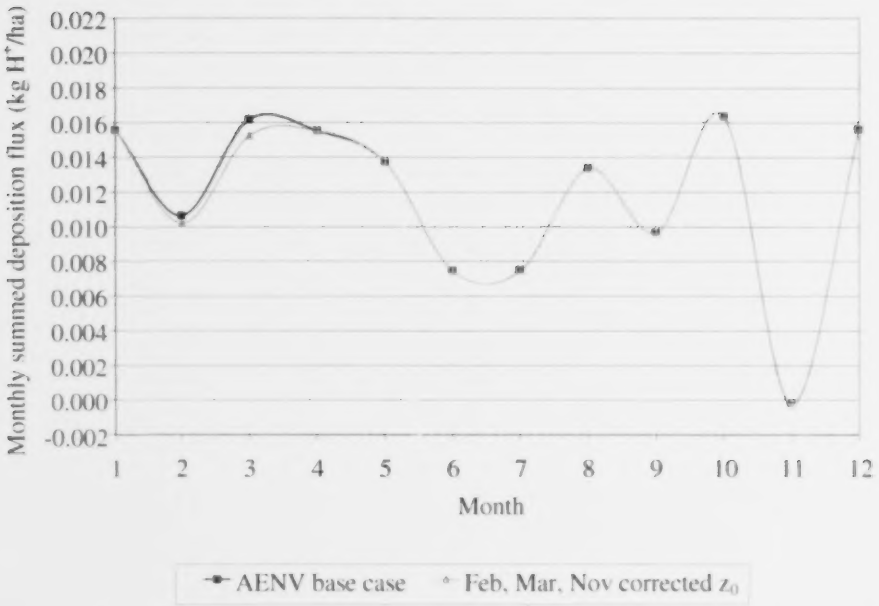

Figure 46 Monthly summed deposition flux for 11 species using AENV model showing influence resulting from corrected z_0 values for the months of February, March, and November for a coniferous forest cover.

With respect to the dependence of z_0 upon wind speed, it was found that if the value of the wind speed criterion used to calculate a monthly value for z_0 was decreased from 6 m/s, the monthly re-calculated mean z_0 value and corresponding standard deviation increased. This is shown in Table 17.

Weighted annual average z_0 values were computed and plotted in Figure 47 for each wind speed criterion listed in Table 17. This figure shows a linear change in weighted annual average z_0 for different wind speeds cutoffs used. If wind speeds are further separated into specific ranges and a corresponding z_0 value calculated for each range, as was done in Table 18, it is seen that z_0 values are highly variable among the ranges shown. Wind direction has also been found to affect calculation of z_0 as a result of differences in landscape features in different directions from a monitoring station (CEC, 1993).

5.3.2.2 Surface Wetness and Relative Humidity

Surface wetness is difficult to measure and it is very difficult to generalize data from one area to an entire area (Panofsky, 1974). Surface wetness data are required for the AENV model; however experience has shown that these data are frequently unavailable due to problems with surface wetness sensing equipment in the field. Consequently, the AENV model allows a minimum relative humidity (RH) measurement cutoff (87%) to be used as an approximation torepresent a surface as being wet. The selection of the RH value

cutoff was further examined to assess the sensitivity of this AENV model criterion. The current cutoff in the model is 87% and two alternative values – 80% and 92% – were assessed.

Table 17 Monthly average re-calculated surface roughness length (z_o) values (m), standard deviation, and sample size (number of hourly values) for different wind speed criteria used in the re-calculation for a coniferous forest cover.

Wind speed greater than or equal to	January			February			March			April			May			June		
(m/s)	Mean	St Dev	Sample Size	Mean	St Dev	Sample Size	Mean	St Dev	Sample Size	Mean	St Dev	Sample Size	Mean	St Dev	Sample Size	Mean	St Dev	Sample Size
1.5	1.76	1.26	347	1.84	1.27	350	1.93	1.25	517	1.89	1.34	578	2.32	1.26	601	2.37	1.17	573
2	1.49	1.09	210	1.68	1.21	215	1.80	1.19	394	1.77	1.27	476	2.28	1.19	506	2.41	1.09	447
2.5	1.18	0.95	133	1.59	1.10	124	1.66	1.15	287	1.69	1.25	374	2.20	1.08	398	2.35	1.02	354
3	1.05	0.85	95	1.66	1.04	68	1.60	1.11	211	1.45	1.20	286	2.10	1.01	309	2.17	0.96	259
3.5	1.19	0.84	64	1.69	1.01	37	1.48	1.06	161	1.30	1.13	227	2.10	0.96	236	2.11	0.93	178
4	1.27	0.74	44	1.47	0.99	16	1.25	0.95	108	1.00	0.91	169	2.05	0.96	183	1.99	0.89	122
4.5	1.42	0.71	36	2.15	0.94	6	1.03	0.75	58	0.85	0.71	137	1.97	0.92	125	1.80	0.85	78
5	1.45	0.66	27	2.00	1.39	2	0.96	0.67	29	0.70	0.40	96	1.99	0.93	84	1.59	0.70	54
5.5	1.46	0.64	25				1.26	0.54	14	0.68	0.30	66	1.65	0.91	51	1.45	0.63	38
6	1.24	0.40	19				1.50	0.54	6	0.67	0.28	42	1.46	0.75	30	1.26	0.45	25
7	1.20	0.41	14							0.61	0.23	16	0.97	0.43	10	1.03	0.30	16
8	1.13	0.14	7							0.50	0.13	4	0.75	0.11	6	0.95	0.22	10
9	1.22	0.19	3										0.77	0.12	5			

Wind speed greater than or equal to	July			August			September			October			November			December		
(m/s)	Mean	St Dev	Sample Size	Mean	St Dev	Sample Size	Mean	St Dev	Sample Size	Mean	St Dev	Sample Size	Mean	St Dev	Sample Size	Mean	St Dev	Sample Size
1.5	2.22	1.22	433	2.36	1.16	473	1.77	1.12	437	1.50	1.00	435	1.29	1.12	442	1.41	1.35	503
2	2.07	1.10	314	2.31	1.05	341	1.67	1.05	348	1.47	0.95	311	1.07	0.97	322	1.14	1.17	325
2.5	1.94	1.04	226	2.29	1.04	248	1.59	0.96	274	1.46	0.90	222	0.92	0.88	238	0.97	0.96	175
3	1.89	1.03	157	2.21	1.01	167	1.59	0.90	220	1.36	0.84	155	0.78	0.70	164	0.98	0.98	97
3.5	1.74	0.97	110	2.08	0.98	112	1.59	0.83	162	1.37	0.80	103	0.76	0.69	111	1.15	0.95	45
4	1.64	0.85	73	1.96	0.97	60	1.63	0.77	124	1.43	0.78	66	0.77	0.59	56	1.04	0.73	22
4.5	1.56	0.78	49	1.83	1.00	40	1.66	0.71	85	1.52	0.77	46	0.91	0.60	31	0.77	0.47	14
5	1.45	0.76	33	1.76	0.99	28	1.76	0.72	41	1.54	0.77	25	1.34	0.55	13	0.55	0.17	9
5.5	1.32	0.57	19	1.53	0.91	21	1.84	0.76	20	1.38	0.69	16	0.95	0.36	7	0.52	0.16	8
6	1.20	0.49	10	1.11	0.52	13	1.61	0.89	9	1.30	0.64	10	0.72	0.24	2	0.50	0.16	7
7	1.22	0.52	5	1.04	0.46	10										0.40	0.12	4
8				0.66	0.20	3												
9																		

Wetness affects surface resistance (R_c) for SO_2 and NO_2 in the AENV model. Default values used to represent R_c in the AENV model for SO_2 are generally lower when a surface is considered wet as opposed to dry (refer to Appendix B). Thus wetness will enhance the contribution of SO_2 deposition to a surface. On the other hand, default values used to represent R_c in the AENV model for NO_2 are generally higher when a surface is considered wet as opposed to dry (Appendix B). Thus wetness will decrease the contribution of NO_2 deposition to a surface.

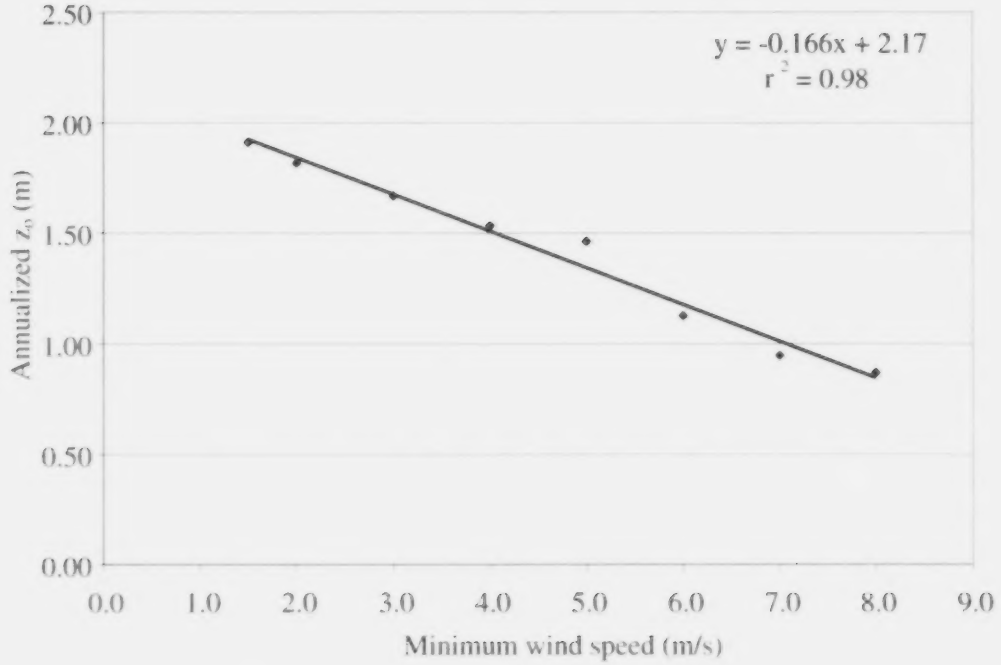

Figure 47 **Annual average re-calculated surface roughness length (z_o) values (m) for different wind speed criteria used in the re-calculation for a coniferous forest cover.**

Table 18 **Monthly calculated surface roughness length (z_o) values (m) and standard deviation for different wind speed ranges for a coniferous forest cover.**

Wind speed range	January		February		March		April		May		June	
(m/s)	Mean	St Dev	Mean	St Dev	Mean	St Dev	Mean	St Dev	Mean	St Dev	Mean	St Dev
$2 \le u < 3$	1.85	1.14	1.69	1.29	2.02	1.25	2.25	1.24	2.56	1.39	2.73	1.18
$3 \le u < 4$	0.86	0.90	1.72	1.06	1.97	1.15	2.10	1.26	2.17	1.08	2.34	0.99
$4 \le u < 5$	0.99	0.80	1.40	0.97	1.35	1.01	1.38	1.20	2.09	0.99	2.30	0.90
$5 \le u < 6$	1.96	0.88	2.00	1.39	0.82	0.64	0.73	0.48	2.28	0.89	1.87	0.76
$6 \le u < 7$	1.36	0.36			1.50	0.54	0.70	0.30	1.71	0.76	1.67	0.38
$7 \le u < 8$	1.27	0.58					0.64	0.25	1.30	0.54	1.16	0.38
$8 \le u < 9$	1.07	0.07					0.50	0.13	0.74	0.13	0.95	0.22
$9 \le u$	1.22	0.19							0.77	0.12		

Wind speed range	July		August		September		October		November		December	
(m/s)	Mean	St Dev	Mean	St Dev	Mean	St Dev	Mean	St Dev	Mean	St Dev	Mean	St Dev
$2 \le u < 3$	2.24	1.15	2.41	1.08	1.79	1.26	1.57	1.03	1.36	1.12	1.21	1.23
$3 \le u < 4$	2.12	1.11	2.35	1.01	1.54	1.04	1.31	0.88	0.79	0.75	0.97	1.05
$4 \le u < 5$	1.79	0.90	2.14	0.92	1.57	0.79	1.36	0.79	0.60	0.49	1.38	0.78
$5 \le u < 6$	1.55	0.83	2.33	0.96	1.81	0.68	1.70	0.83	1.45	0.51	0.71	0.08
$6 \le u < 7$	1.19	0.53	1.32	0.76	1.61	0.89	1.30	0.64	0.72	0.24	0.62	0.13
$7 \le u < 8$	1.22	0.52	1.21	0.45							0.40	0.12
$8 \le u < 9$			0.66	0.20								
$9 \le u$												

The effects of changing the surface wetness cutoff for all the land use categories, except water, on monthly summed deposition flux for 11 species are shown in Figures 48 to 54 below. Water had no change associated with it. These figures show that there is very little change in monthly summed deposition flux for 11 species caused using a different RH cutoff to represent a surface as being wet (e.g., 80%, 92% , or the base case of 87%).

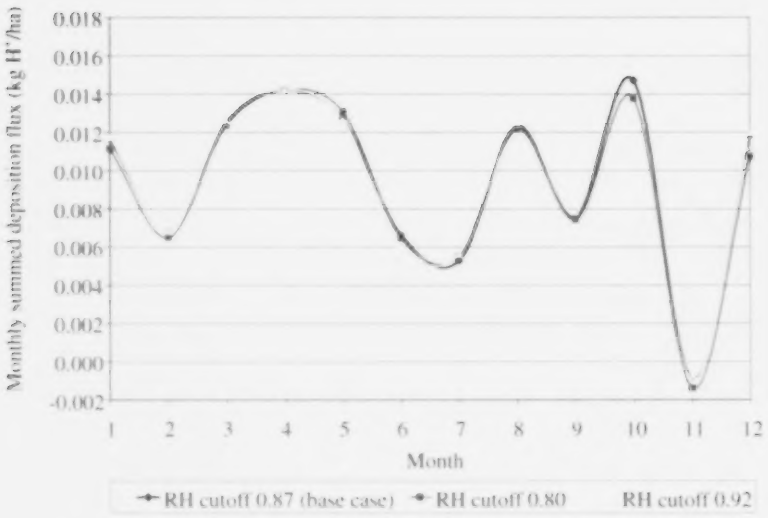

Figure 48 **Monthly summed deposition flux for 11 species using AENV model showing influence of using a different RH cutoff for establishing a surface as wet (base case RH = 0.87) for deciduous forest cover.**

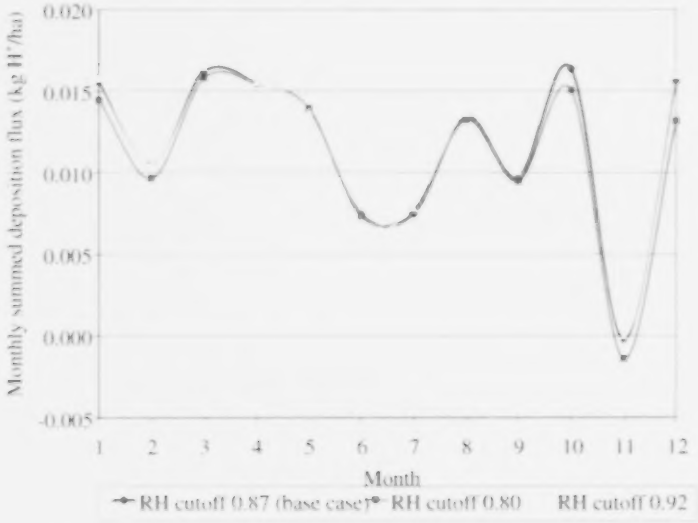

Figure 49 **Monthly summed deposition flux for 11 species using AENV model showing influence of using a different RH cutoff for establishing a surface as wet (base case RH = 0.87) for a coniferous forest cover.**

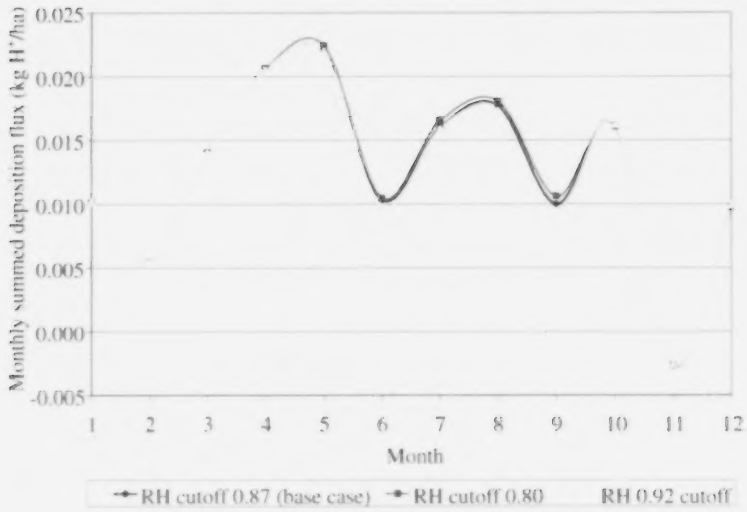

Figure 50 **Monthly summed deposition flux for 11 species using AENV model showing influence of using a different RH cutoff for establishing a surface as wet (base case RH = 0.87) for wetland/swamp cover.**

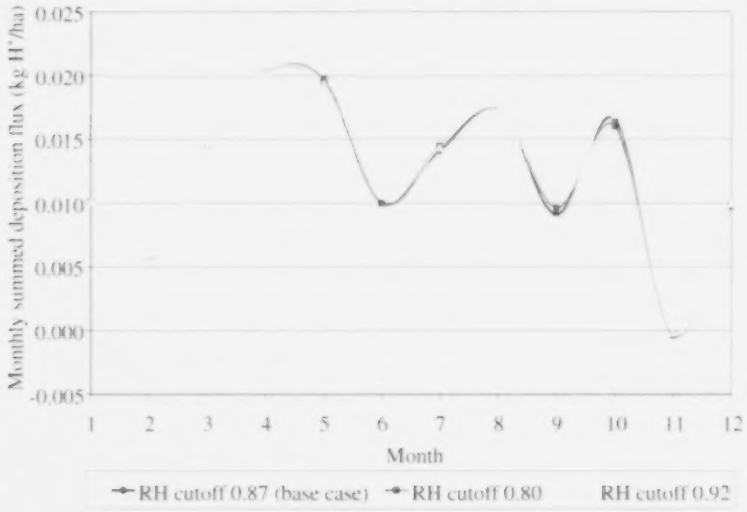

Figure 51 **Monthly summed deposition flux for 11 species using AENV model showing influence of using a different RH cutoff for establishing a surface as wet (base case RH = 0.87) for grassland.**

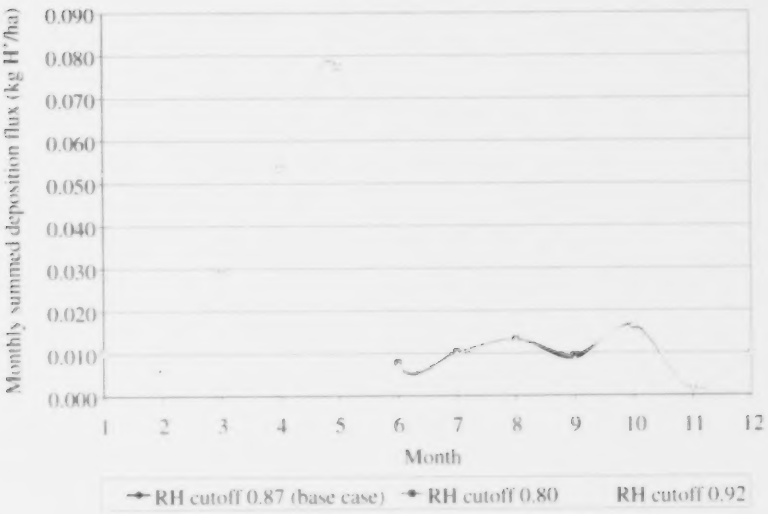

Figure 52 **Monthly summed deposition flux for 11 species using AENV model showing influence of using a different RH cutoff for establishing a surface as wet (base case RH = 0.87) for cropland.**

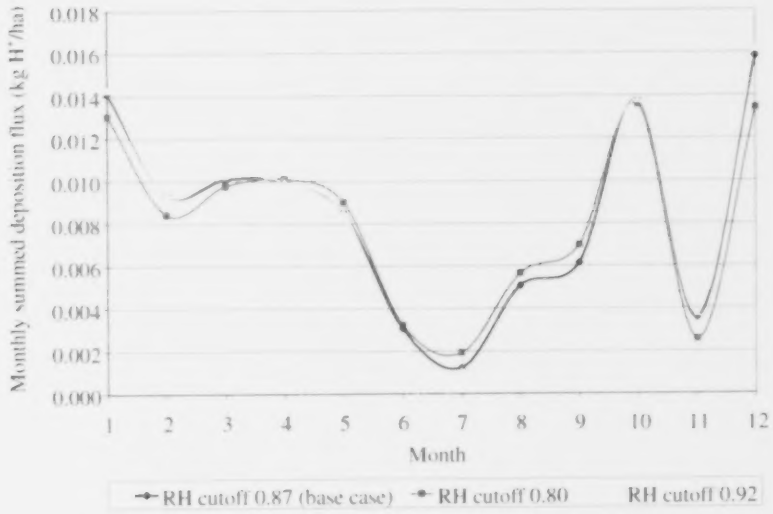

Figure 53 **Monthly summed deposition flux for 11 species using AENV model showing influence of using a different RH cutoff for establishing a surface as wet (base case RH = 0.87) for urban cover.**

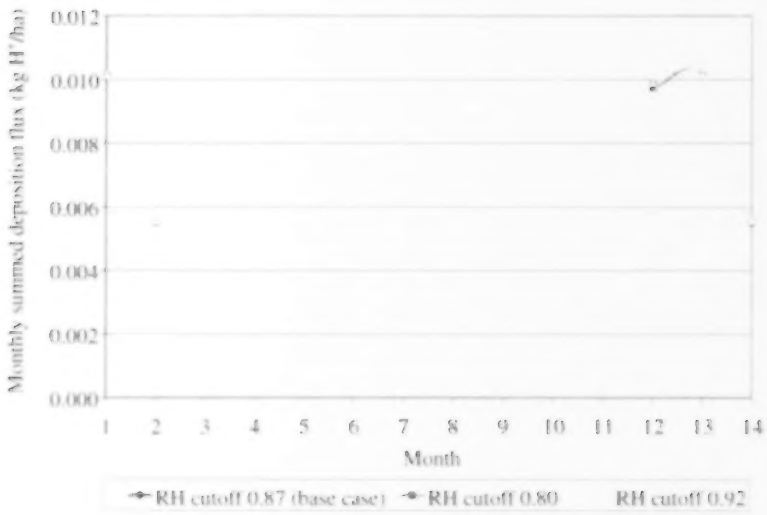

Figure 54 **Monthly summed deposition flux for 11 species using AENV model showing influence of using a different RH cutoff for establishing a surface as wet (base case RH = 0.87) for snow/ice.**

5.3.2.3 Particulate Size Distributions

Differences exist between the AENV and ENVC models in terms of how they predict large particle deposition. In the original design of the ENVC model – which only addressed SO_4^{2-} and NH_4^+ deposition associated with small particles – 40 aerodynamic sizes (referred to as binsizes by ENVC) were used to represent an overall particle size distribution in calculation of the deposition velocity for species associated with small particles. The largest size encompasses particles up to 10 µm in diameter; which matches the maximum size of particles classified as PM_{10}. This number of binsizes (40) encompasses almost 100% of a typical small particle distribution having a geometric mean of 0.5 µm and a standard deviation of 2.0 µm.

When the ENVC model was modified to include calculation of deposition velocity for species associated with large particles (i.e., NO_3^-, Na^+, K^+, Ca^{2+}, and Mg^{2+}), the number of binsizes remained at 40 so as to limit the largest particle size to that detected as PM_{10} (i.e., 10 µm) for determining deposition flux of these species. The size distribution of sodium (Na^+) was used as a conservative representation for the distribution of all large particles (NO_3^-, Na^+, K^+, Ca^{2+}, and Mg^{2+}) in the ENVC model. However a typical sodium particle distribution has a geometric mean of 0.5 µm and a standard deviation of 2.0 µm, and only 75.86% of this size distribution is encompassed within the first 40 binsizes to a diameter of 10 µm.

Thus >24% of the particle sizes for this distribution are greater than 10 µm and are unaccounted for in the ENVC model. These larger sized particles, >10 µm in diameter, are base cation species with increased settling properties as a result of their large size

compared to fine particles. The net results of taking larger sizes into account in the calculation would be a greater overall buffering effect; or more importantly a net decrease in acid deposition flux when all species are considered in the calculation. One possible way to correct for this limitation is to divide each binsize diameter used in the ENVC model by 0.7586 (75.86%/100%) to standardize and better represent the more likely settling properties of species associated with larger particles. When this adjustment is made, corrected ENVC model results (Figure 55) show much better agreement with AENV model results than previously presented.

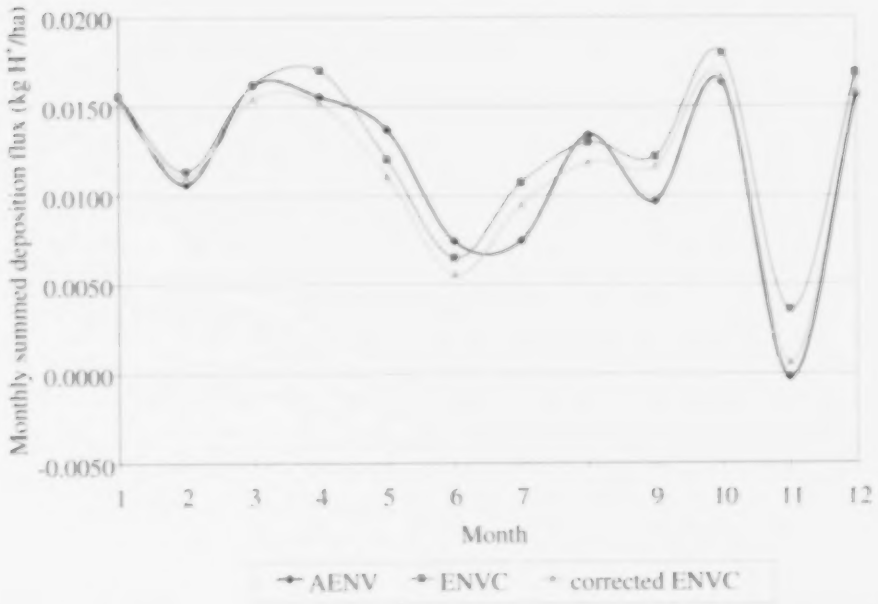

Figure 55 **Monthly summed deposition flux for 11 species for AENV model base case, ENVC model, and ENVC model corrected for large particle size distribution for a coniferous forest cover.**

The net difference in annual deposition flux for 11 species between the AENV model (base case) and corrected ENVC model was 1.2%; as opposed to a 7.7% difference without a correction (Table 2). As expected, the largest difference was observed in November. A breakdown of the influence of the ENVC model corrected for large particle size distribution on monthly summed deposition flux for NO_3^-, Na^+, K^+, Ca^{2+}, and Mg^{2+} for coniferous forest cover is provided in Appendix H.

Increasing the number of bins to capture larger particle sizes in the distribution (i.e., >10 μm) is typically not done because of uncertainty in extrapolating the amount of nitrate in particles larger than those detected by PM_{10} measurements. Current use of a truncated

distribution for large particles in ENVC's model produces a conservative estimate of deposition flux when considering all species. Because a majority of base cations is associated with large particle deposition, underestimating deposition of large particles results in an underestimation of the neutralization capacity of base cations.

6.0 FINDINGS AND RECOMMENDATIONS

An evaluation of the analytical basis of the Alberta Environment (AENV) and Environment Canada (ENVC) inference models for predicting dry deposition of 11 species was undertaken. These species included SO_2, NO_2, HNO_3, HNO_2, SO_4^{2-}, NH_4^+, NO_3^-, Na^+, K^+, Ca^{2+}, and Mg^{2+}. Important findings and recommends include:

1. The three most important species contributing to potential acid input were SO_2, NO_2, and HNO_3.

2. Sensitivity testing of resistance factors R_a, R_b, and R_c used in AENV's model showed that step changes in the magnitude of R_c were much more important in influencing total deposition compared to step changes in either R_a or R_b for all species examined. The influence of changes in R_c was independent of month of the year.

3. AENV model performance in terms of overall deposition flux of 11 species was observed to be closely dependent on deposition velocity modeling for SO_2 and NO_2; particularly with respect to selection of R_c values used to parameterize these gases. Relative to performance of the ENVC model, values used to represent R_c in the AENV model were less conservative for SO_2 in winter and spring and more conservative in summer and autumn. For NO_2, values used to represent R_c in the AENV model were less conservative in autumn and winter and more conservative in spring and summer. For HNO_3, deposition in the AENV model was driven by R_b. These differences do not necessarily imply problems in the AENV model. The ENVC inference model does not necessarily represent the best set of assumptions and conditions to parameterize dry deposition. In addition, AENV's parameterization of R_c originates from previously published values that are seasonal- and species-specific and, therefore, can be considered reasonable.

4. R_a is an indication of the mixing conditions in the atmosphere such that a very low R_a implies maximum mixing conditions experienced during daytime conditions. Setting a minimum value of 5 s/m for R_a in the AENV model had only a small positive change in model performance relative to the ENVC model. Although the effect of this change is small, it is recommended for future use in the AENV model. The purpose of a minimum limit for R_a acknowledges that, inferentially, there is always some limit to mixing possible in a natural atmosphere.

5. Setting a maximum value of 1000 s/m for R_a in the AENV model resulted in better agreement in overall deposition flux of 11 species relative to the ENVC model for the conditions tested. High R_a values would be associated with no mixing in the atmosphere (ideally stable night time conditions). An extremely high R_a value would not necessarily offer a reasonable representation of natural conditions. From a practical point of view, very large R_a values are not much

different than moderately large values since deposition velocity involves the inverse of the sum of all three resistances ($R_a + R_b + R_c$). When hourly deposition values for a month are summed, hourly conditions with small summed values for the three resistance factors (and hence correspondingly large deposition velocity and deposition flux values) are most important and drive the overall monthly summed deposition flux. Hence very large or moderately large R_a values (and correspondingly very small or moderately small deposition velocity and deposition fluxes) are unimportant. This limit is recommended for future use in the AENV model.

6. The Monin-Obukhov length (L) is used in calculation of the stability function which is ultimately used to calculate R_a. This length represents the height above the surface in which convectively driven turbulence dominates over mechanically driven turbulence and it is indirectly a measure of the convective instability generated by the vertical heat flux through the surface layer. It is only meaningful in daytime convectively driven boundary layers. L is limited to a maximum and minimum value of -5 and 5 m for negative and positive values, respectively, in the ENVC model. A negative value represents atmospheric instability and a positive value represents stability. In general, as L approaches zero, R_a becomes larger and corresponding deposition velocity is smaller. The result of applying these limits to L is a slightly lower R_a and a slightly higher corresponding deposition velocity. Since it is higher R_a values that are affected, the nature of the change is similar to that of setting an upper limit on R_a. The effect of using these limits to L was to bring AENV model results closer to ENVC model results (same general effect caused by setting an upper limit to R_a). These limits are recommended for future use in the AENV model as small absolute L values represent extremes which are not representative in nature.

7. Wind speed values in the AENV model are allowed to vary to a minimum of 0.09 m/s, below which they are assigned a value of 0 m/s. In the ENVC model, wind speed values are only allowed to vary to a minimum of 1 m/s, below which they are assigned a value of 1 m/s. The direction of change observed by using a 1 m/s limit to lowest wind speed values used in the AENV model was to bring model results in closer agreement to ENVC model results. This limit is recommended for future use in the AENV model.

8. One potential limitation of the AENV model is a requirement to calculate surface roughness length (z_o) as a monthly average using hourly data where the wind speed is >6 m/s. At issue is a situation where only a small number of hourly values exist during a month in which the wind speed is >6 m/s. Greater uncertainty exists in the calculated average z_o value when computed from only a small number of hourly values. The following approach is recommended for future use in the AENV model to deal with this limitation in most cases –
   - Seven hourly observations is recommended as the minimum number of observations in which to use in a month for calculating z_o.

- The average z_o value of two surrounding months can be used for any month in which an insufficient number of observations (i.e., <7) exist.
- If two or more consecutive months have <7 observations for a surface cover whose characteristics are not expected to undergo substantial change from season to season (e.g., coniferous forest canopy), then an annual average z_o value can be used to represent surface roughness length for these months.

9. Wetness alters the characteristics of a surface to act a sink for depositing species (primarily gases). The AENV model requires an hourly measurement to represent the amount of wetness on a surface in determination of surface resistance (R_c). The model is set up to use field measurement data from surface wetness sensing equipment. However, past experience has indicated that this field equipment does not provide reliable measurement data in an Alberta setting due to the wide range of climatic conditions experienced. Alternatively, the model allows a relative humidity (RH) measurement cutoff (87%) to be used as a gross approximation to represent a surface as being wet. An evaluation of alternative RH cutoff values indicated little change in monthly summed deposition flux for 11 species. As a result, it is recommended that the current RH cutoff value be maintained in the model for future use.

10. A final issue was examined related to performance of the ENVC model. The ENVC model has an apparent limitation in the way it treats settling properties of species associated with large particles (i.e., NO_3^-, Na^+, K^+, Ca^{2+}, and Mg^{2+}). The model forces the treatment of settling for >24% of these particles (by mass) as being similar to settling properties of fine particles. This underestimates neutralization capacity offered by depositing particulates containing base cations; and overestimates total deposition flux to a surface when all depositing species are taken into account. This limitation was further investigated to show how large the effect was for the ENVC model. Because the ENVC model tends to estimate higher total deposition fluxes compared to the AENV model, better agreement among these two models was achieved when corrections were made to the ENVC model to address this limitation.

Table 19 summarizes recommended changes to the AENV model for future use. Figure 56 shows the net effect of implementing recommended changes to the AENV model relative to ENVC model results for a coniferous forest cover for the conditions tested.

Table 19 Recommended changes to AENV acid deposition inference model.

Parameter	Original AENV model condition	Revised condition evaluated	Revised condition recommended for future use in AENV model
aerodynamic boundary resistance (R_a) [m]	upper limit on R_a is undefined	upper limit capped at 1000 s/m for all surface covers except water (2000 s/m for water)	yes
	upper limit on R_a is undefined	lower limit capped at 5 s/m for all surface covers	yes
Monin-Obukhov length (L) [m]	undefined limits	upper limit of -5 m on negative side and lower limit of +5 m on positive side	yes
wind speed minimum (u) [m/s]	set to 0 m/s if <0.09 m/s	set to 1 m/s if <1 m/s	yes
surface roughness length (z_o) [m]	computed as monthly average using hourly data where the wind speed >6 m/s	use seven hourly observations as minimum number of observations in a month to calculate z_o and surrounding monthly average values for <7 observations	yes
surface wetness condition	uses relative humidity (RH) measurement cutoff of 87% as approximation to represent surface as being wet	uses alternative (higher/lower) relative humidity (RH) measurement cutoff as approximation to represent surface as being wet	no

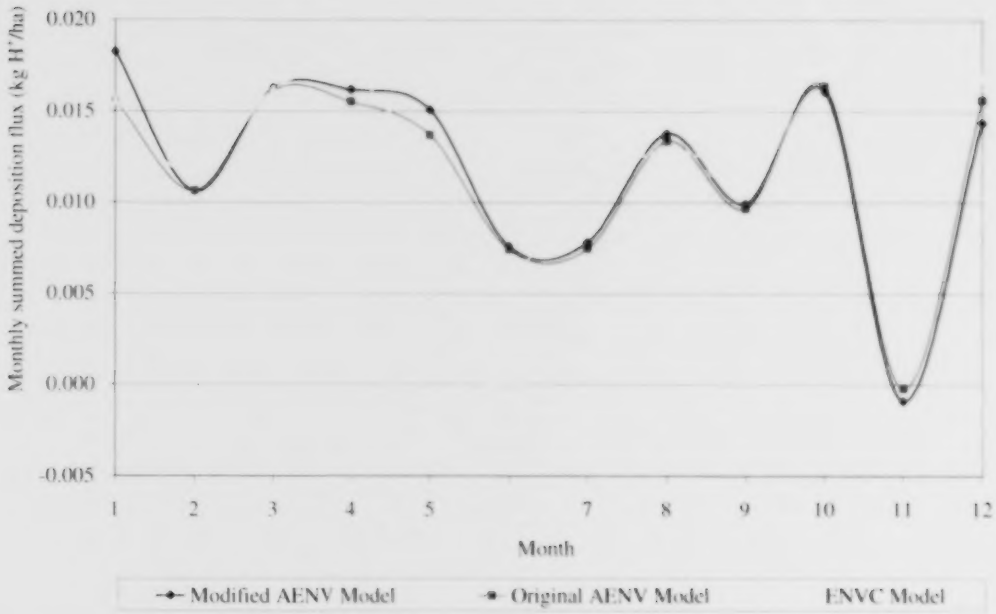

Figure 56 **Monthly summed deposition flux for 11 species using modified AENV model compared to original AENV model and ENVC model for a coniferous forest cover.**

7.0 REFERENCES

Alberta Environment (AENV). 1999. "Application of Critical, Target, and Monitoring Loads for the Evaluation and Management of Acid Deposition." Alberta Environment Publications No. T/472. Environmental Service, Environmental Sciences Division, Edmonton, AB. November, 1999.

Arimoto, R., Ray, B. J., Lewis, N. F., Tomza, U., and Duce, R. A. (1997). "Mass-particle size distributions of atmospheric dust and the dry deposition of dust to the remote ocean." *J. Geophys. Res. - Atmospheres*, 102(D13), 15867-15874.

Bates, D.L., 1996. Calculation and Analysis of Dry Acidic Deposition at Royal Park. Alberta Environment, Air Issues and Monitoring Branch, Edmonton, AB. 42 pp.

Brook, J. R., Zhang, L. M., Di-Giovanni, F., and Padro, J. (1999). "Description and evaluation of a model of deposition velocities for routine estimates of air pollutant dry deposition over North America. Part I: model development." *Atmos. Environ.*, 33(30), 5037-5051.

Businger, J. A. (1986). "Evaluation of the accuracy with which dry deposition can be measured with current micrometeorological techniques." *J. Climate Appl. Meteorol.*, 25(8), 1100-1124.

Cheng, L., Gates, D. L., and Myrick, B. (2001). "Acidic Deposition Monitoring and Calculations in Alberta, Draft 5." Alberta Environment, Edmonton, AB.

Concord Environmental Corporation (CEC) (1993). "Summary of Surface and Upper Air Data from the FSRIA Fort Saskatchewan Meteorological Station 1989 – 1992." Prepared for Alberta Environment, Environmental Quality Monitoring Branch in conjunction with Fort Saskatchewan Regional Industrial Association, CEC, Calgary, AB.

Draaijers, G. P. J., VanLeeuwen, E. P., DeJong, P. G. H., and Erisman, J. W. (1997). "Base cation deposition in Europe .1. Model description, results and uncertainties." *Atmos. Environ.*, 31(24), 4139-4157.

Dulac, F., Buatmenard, P., Arnold, M., Ezat, U., and Martin, D. (1987). "Atmospheric input of trace-metals to the western Mediterranean-Sea 1. Factors controlling the variability of atmospheric concentrations." *J. Geophys. Res. - Atmospheres*, 92(D7), 8437-8453.

Erisman, J. W., Draaijers, G., Duyzer, J., Hofschreuder, P., VanLeeuwen, N., Romer, F., Ruijgrok, W., Wyers, P., and Gallagher, M. (1997). "Particle deposition to forests - Summary of results and application." *Atmos. Environ.*, 31(3), 321-332.

Hedin, L. O., Granat, L., Likens, G. E., Buishand, T. A., Galloway, J. N., Butler, T. J., and Rodhe, H. (1994). "Steep declines in atmospheric base cations in regions of Europe and North-America." *Nature*, 367(6461), 351-354.

Hicks, B. B., Baldocchi, D. D., Meyers, T. P., Hosker, R. P., and Matt, D. R. (1987). "A preliminary multiple resitance routine for deriving dry deposition velocities from measured quantities." *Wat., Air, Soil Pollut.*, 36(3-4), 311-330.

Hoff, R. M., Leaitch, W. R., Fellin, P., and Barrie, L. A. (1983). "Mass size distributions of chemical-constituents of the winter Arctic aerosol." *J. Geophys. Res. - Oceans and Atmospheres*, 88(NC15), 947-956.

Holsen, T. M., and Noll, K. E. (1992). "Dry Deposition of Atmospheric Particles - Application of Current Models to Ambient Data." *Environ. Sci. Technol.*, 26(9), 1807-1815.

Lovett, G.M. (1994). "Atmospheric deposition of nutrients and pollutants in North America: an ecological perspective." *Ecol. Appl.*, 4, 629-650.

Mahrt, L., Vickers, D., Sun, J. L., Jensen, N. O., Jorgensen, H., Pardyjak, E., and Fernando, H. (2001). "Determination of the surface drag coefficient." *Bound.-Layer Meteorol.*, 99(2), 249-276.

Meyers, T. P., Finkelstein, P., Clarke, J., Ellestad, T. G., and Sims, P. F. (1998). "A multilayer model for inferring dry deposition using standard meteorological measurements." *J. Geophys. Res. - Atmospheres*, 103(D17), 22645-22661.

Meyers, T. P., Hall, M. E., Lindberg, S. E., and Kim, K. (1996). "Use of the modified Bowen-ratio technique to measure fluxes of trace gases." *Atmos. Environ.*, 30(19), 3321-3329.

Milford, J. B., and Davidson, C. I. (1985). "The Sizes of Particulate Trace-Elements in the Atmosphere - a Review." *J. Air Pollut. Control Assoc.*, 35(12), 1249-1260.

Niyogi, D. D. S., Alapaty, K., and Raman, S. (2003). "A photosynthesis-based dry deposition modeling approach." *Wat., Air, Soil Pollut.*, 144(1), 171-194.

Panofsky, H. A. (1974). "Atmospheric Boundary-Layer Below 150 Meters." *Annu. Rev. Fluid Mech.*, 6 147-177.

Peters, L. K., Berkowitz, C. M., Carmichael, G. R., Easter, R. C., Fairweather, G., Ghan, S. J., Hales, J. M., Leung, L. R., Pennell, W. R., Potra, F. A., Saylor, R. D., and Tsang, T. T. (1995). "The current state and future-direction of Eulerian models in simulating the tropospheric chemistry and transport of trace species – a review." *Atmos. Environ.*, 29(2), 189-222.

Ruijgrok, W., Davidson, C. I., and Nicholson, K. W. (1995). "Dry deposition of particles – implications and recommendations for mapping of deposition over Europe." *Tellus Series B-Chem. Phys. Meteorol.*, 47(5), 587-601.

Ruijgrok, W., Tieben, H., and Eisinga, P. (1997). "The dry deposition of particles to a forest canopy: A comparison of model and experimental results." *Atmos. Environ.*, 31(3), 399-415.

Sehmel, G. A. (1980). "Particle and gas dry deposition – a review." *Atmos. Environ.*, 14(9), 983-1011.

Slinn, W. G. N. (1982). "Predictions for particle deposition to vegetative canopies." *Atmos. Environ.*, 16(7), 1785-1794.

Smith, R. I., Fowler, D., Sutton, M. A., Flechard, C., and Coyle, M. (2000). "Regional estimation of pollutant gas dry deposition in the UK: model description, sensitivity analyses and outputs." *Atmos. Environ.*, 34(22), 3757-3777.

Venkatram, A., Karamchandani, P. K., and Misra, P. K. (1988). "Testing a comprehensive acid deposition model." *Atmos. Environ.*, 22(4), 737-747.

Voldner, E. C., Barrie, L. A., and Sirois, A. (1986). "A Literature-Review of Dry Deposition of Oxides of Sulfur and Nitrogen with Emphasis on Long-Range Transport Modeling in North-America." *Atmos. Environ.*, 20(11), 2101-2123.

Walcek, C. J., Brost, R. A., Chang, J. S., and Wesely, M. L. (1986). "SO_2, Sulfate and HNO_3 Deposition Velocities Computed using Regional Land-use and Meteorological Data." *Atmos. Environ.*, 20(5), 949-964.

WBK and Associates Inc. (WBK). (2008). "Dry Deposition Monitoring Method In Alberta, Phase II." Prepared for Alberta Environment, Edmonton, AB. March 2006. 59 pp.

Wesely, M. L., and Hicks, B. B. (2000). "A review of the current status of knowledge on dry deposition." *Atmos. Environ.*, 34(12-14), 2261-2282.

Wesely, M. L., and Hicks, B. B. (1977). "Some Factors that Affect Deposition Rates of Sulfur-Dioxide and Similar Gases on Vegetation." *J. Air Pollut. Control Assoc.*, 27(11), 1110-1116.

Whitby, K. T. (1978). "Physical characteristics of sulfur aerosols." *Atmos. Environ.*, 12(1-3), 135-159.

Wiman, B. L. B., and Agren, G. I. (1985). "Aerosol depletions and deposition in forests – a model analysis." *Atmos. Environ.*, 19(2), 335-347.

Wolff, G. T. (1984). "On the nature of nitrate in coarse Continental aerosols." *Atmos. Environ.*, 18(5), 977-981.

Zhang, L., Brook, J. R., and Vet, R. (2003). "A revised parameterization for gaseous dry deposition in air-quality models." *Atmos. Chem. Physics*, 3 2067-2082.

Zhang, L. M., Brook, J. R., and Vet, R. (2002a). "On ozone dry deposition - with emphasis on non-stomatal uptake and wet canopies." *Atmos. Environ.*, 36(30), 4787-4799.

Zhang, L., M. Moran, P. Makar, J. Brook, and S. Gong. (2002b). "Modelling gaseous dry deposition in AURAMS – A Unified Regional Air-quality Modelling System." *Atmos. Environ.*, 36, 537–560.

Zhang, L. M., Gong, S. L., Padro, J., and Barrie, L. (2001a). "A size-segregated particle dry deposition scheme for an atmospheric aerosol module." *Atmos. Environ.*, 35(3), 549-560.

Zhang, L. M., Moran, M. D., and Brook, J. R. (2001b). "A comparison of models to estimate in-canopy photosynthetically active radiation and their influence on canopy stomatal resistance." *Atmos. Environ.*, 35(26), 4463-4470.

APPENDIX A ENVIRONMENT CANADA CALCULATION METHODS FOR GASES AND PARTICULATES

(after Brook et al., 1999; Zhang et al., 2003, 2002a, 2002b, 2001a, and 2001b)

Parameters (for gases):

V_d:	deposition velocity (m/s)
R_a:	aerodynamic resistance (s/m)
R_b:	boundary-layer resistance (s/m)
R_c:	surface resistance (s/m)
k:	von Karman constant (0.4)
u_*:	friction velocity (m/s)
u:	horizontal wind speed at reference height (m/s)
L:	Monin-Obukhov length
H:	sensible heat flux
z:	reference height (10m)
z_0:	surface roughness length (m)
ψ_H:	stability function
Ri:	Bulk Richardson number
g:	gravitational acceleration (9.81 m/s^2)
T_2:	temperature at reference height (°K)
T_{2p}:	potential temperature at reference height (°K)
T_s:	surface temperature (°K)
T_d:	temperature difference (°K)
P:	surface pressure (kPa)
T_{avg}:	temperature average, $T_{avg} = (T_{2p} + T_s)/2$
SR:	solar radiation (w/m^2)
RH:	relative humidity (%)
$Prec$:	precipitation (mm/hour)
$FCLD$:	fraction of cloud covering (%)
$\cos\theta$:	cosine of solar zenith angle
$\cos\alpha$:	cosine of sun/leaf angle, set as 0.5
Di:	molecular diffusivity
Dv:	water diffusivity
Vi:	thermal diffusivity
MW:	Molecular Weight, $MW_{air} = 29$
W_{st}:	fraction of stomatal blocking under wet conditions

R_{st}:	stomatal resistance
R_m:	mesophyll resistance (dependent only on chemical species)
R_{ac}:	in-canopy aerodynamic resistance (not chemical species-dependent)
R_g:	ground resistance (scaled from SO_2 and O_3's R_g)
R_{cut}:	cuticle uptake resistance (scaled from SO_2 and O_3's R_{cut})
$G_s(PAR)$:	unstressed leaf stomatal conductance
PAR:	Photosynthetic Active Radiation
$f(T)$:	conductance-reducing effects of air temperature T (°C)
$f(D)$:	conductance-reducing effects of water-vapour-pressure deficit D
D:	water-vapour-pressure deficit
$f(\psi)$:	conductance-reducing effects of water stress ψ
ψ:	water stress
ψ_{c1} and ψ_{c2}:	leaf-water-potential dependency
$E^*(T)$:	saturation water vapour pressure (kPa) at air temperature T (°K)
E:	ambient water vapour pressure (kPa)
f_{snow}:	snow cover fraction
Sd:	snow depth (cm)
Sd_{max}:	maximum snow depth (cm)
R_{cutw0}:	reference values of wet cuticle resistance, see Table A1 for $R_{cutw0}(O_3)$
$R_{cutw0}(SO_2)$:	50 s/m or 100 s/m for rain or dew conditions, respectively
R_{cutd0}:	reference values of dry cuticle resistance, see Table A1
LAI:	Leaf Area Index
LUC:	Land Use Category (26 LUCs in gas model)
SC:	SeasonalCategory (5 in particulate model)

Deposition Velocity:

$$V_d = \frac{1}{R_a + R_b + R_c}$$

Aerodynamic Resistance (R_a):

ENVC adapts the Acid Deposition and Oxidant Model (ADOM) formulated by Pleim et. al. (1984) as cited in Zhang et al. (2001b) and further investigated by Padro et al. (1990) as cited in Zhang et al. (2001b).

$R_a = \frac{1}{ku_*}[0.74\ln(z/z_0) - \psi_H]$, with a lower limit of 5 and an upper limit of 1000 (upper limit of 2000 if water or lake as land use)

Friction velocity:

$$u_* = \begin{cases} \dfrac{ku}{\ln\left(\dfrac{z}{z0}\right)(1+4.7Ri)} & Stable,\ Ri > 0 \\ \dfrac{ku}{\ln\left(\dfrac{z}{z0}\right)}\sqrt{1-\dfrac{9.4Ri}{1+7.4\left[k/\ln\left(\dfrac{z}{z0}\right)\right]^2\sqrt{|Ri|}}} & Unstable,\ Ri < 0 \end{cases}$$

Bulk Richardson number:

$Ri = \frac{gzT_d}{T_v u^2}$, with a fixed value of 1×10^{-15} if SR>0 and Ri>0

Temperature difference:

$T_d = T_{2p} - T_s$, with an upper limit of -10^{-10} for negative values and a lower limit of 10^{-10} for positive values

Stability function:

$$\psi_H = \begin{cases} -4.7\dfrac{z}{L} & stable,\ 0 < \dfrac{z}{L} < 1 \\ 0.74 \times 2\ln\left\{\dfrac{1+\sqrt{1-9\dfrac{z}{L}}}{2}\right\} & unstable,\ -1 < \dfrac{z}{L} < 0 \end{cases}$$

Monin-Obukhov length:

$L = \frac{T_{avg} u_*^3}{kHg}$, with an upper limit of -5 on the negative side and a lower limit of +5 on the positive side

Sensible heat flux:

$$H = \begin{cases} \left\{\frac{uT_d}{0.74}\right\}\left\{\frac{k}{\ln(z/z0)}\right\}^2\left\{\frac{1}{(1+4.7Ri)^2}\right\} & Stable,\ Ri>0 \\ \left\{\frac{uT_d}{0.74}\right\}\left\{\frac{k}{\ln(z/z0)}\right\}^2\left\{1-\frac{9.4Ri}{1+5.3[k/\ln(z/z0)]^2\sqrt{|Ri|}}\right\} & Unstable,\ Ri<0 \end{cases}$$

<u>Sub Layer Resistance (R_b)</u>:

$$R_b = \frac{5}{u_*}\left(\frac{Vi}{Di}\right)^{2/3}$$

Thermal diffusivity:

$$Vi = \frac{145.8\times10^{-4}T_{avg}^{3/2}}{T_{avg}+110.4}$$

Molecular diffusivity:

$$Di = \frac{0.001T_v^{7/4}\sqrt{\frac{1}{MW_{gas}}+\frac{1}{MW_{air}}}}{(D_{air}^{1/3}+D_{gas}^{1/3})^2}$$

$$D_{gas} = 0.369MW_{gas} + 6.29$$
$$D_{air} = 0.369MW_{air} + 6.29$$

<u>Total Surface Resistance (R_c)</u>:

$\frac{1}{R_c} = \frac{1-Wst}{R_{st}+R_m} + \frac{1}{R_{ac}+R_g} + \frac{1}{R_{cut}}$, with a lower limit of 10 s/m

Fraction of stomatal blocking under wet conditions:

$$Wst = \begin{cases} 0 & SR \le 200 Wm^{-2} \\ (SR - 200)/800 & 200 < SR \le 600 Wm^{-2} \\ 0.5 & SR > 600 Wm^{-2} \end{cases}$$

Stomatal resistance:

$$R_{st} = \frac{1}{G_s(PAR) f(T) f(D) f(\psi) D_i / D_v}$$

Water diffusivity:

$$D_v = \frac{0.001 T_a^{7/4} \sqrt{\frac{1}{MW_{water}} + \frac{1}{MW_{air}}}}{\left(D_{air}^{1/3} + D_{water}^{1/3}\right)^2}$$

Unstressed leaf stomatal conductance:

$$G_s(PAR) = F_{sun} / r_{st}(PAR_{sun}) + F_{shade} / r_{st}(PAR_{shade})$$

$$F_{sun} = 2\cos\theta\left[1 - e^{-0.5LAI/\cos\theta}\right]$$
$$F_{shade} = LAI - F_{sun}$$

$$r_{st}(PAR) = r_{st\,min}(1 + b_{rs} / PAR)$$

$$PAR_{shade} = \begin{cases} R_{diff} e^{(-0.5LAI^{0.7})} + 0.07 R_{dir}(1.1 - 0.1LAI) e^{-\cos\theta} & LAI < 2.5 \quad or \quad SR < 200 wm^{-2} \\ R_{diff} e^{(-0.5LAI^{0.5})} + 0.07 R_{dir}(1.1 - 0.1LAI) e^{-\cos\theta} & LAI > 2.5 \quad and \quad SR > 200 wm^{-2} \end{cases}$$

$$PAR_{sun} = \begin{cases} R_{dir}\cos\alpha / \cos\theta + PAR_{shade} & LAI < 2.5 \quad or \quad SolarRad < 200 wm^{-2} \\ R_{dir}^{0.8}\cos\alpha / \cos\theta + PAR_{shade} & LAI > 2.5 \quad and \quad SolarRad > 200 wm^{-2} \end{cases}$$

Conductance-reducing effects of air temperature T:

$$f(T) = \frac{T - T_{min}}{T_{opt} - T_{min}} \left[\frac{T_{max} - T}{T_{max} - T_{opt}} \right]^{br} \quad \text{where } br = \frac{T_{max} - T_{opt}}{T_{opt} - T_{min}}$$

Conductance-reducing effects of water-vapour-pressure deficit D:

$f(D) = 1 - b_{leaf} D$, with a lower limit of 0.1 and a upper limit of 1

Water-vapour-pressure deficit:

$$D = E^*(T) - E$$

Saturation vapor pressure:

$$E^*(T) = 0.6108e^{\frac{(17.27(T - 273.16)}{T - 35.86}} \quad \text{(in units of mb in code)}$$

Ambient water vapour pressure:

$$E = E^*(T)RH$$

Conductance-reducing effects of water stress:

$$f(\psi) = \begin{cases} (\psi - \psi_{c2})/(\psi_{c1} - \psi_{c2}) & \psi < \psi_{c1} \\ 1 & \psi \geq \psi_{c1} \end{cases}$$

where $\psi = -0.72 - 0.0013SR$, with a lower limit of 0.1 and upper limit of 1

Mesophyll resistance:

Values of R_m for all dry-depositing species in AURAMS gas-phase chemical mechanism listed in Table A1.

In-canopy aerodynamic resistance:

$$R_{ac} = \frac{R_{ac,0} LAI^{1/4}}{u_*^2}$$

where

R_{ac0}: reference value for in-canopy aerodynamic resistance (Table A1)
LAI: Leaf area index (Table A2)

For some LUCs, a range of R_{ac0} values is given to reflect the change of canopy structure at different times of the growing season. R_{ac0} values for any day of the year based on minimum and maximum LAI values given as:

$$R_{ac0}(t) = R_{ac0}(\min) + \frac{LAI(t) - LAI(\min)}{LAI(Max) - LAI(\min)} \times \left[R_{ac0}(\max) - R_{ac0}(\min)\right]$$

Ground resistance:

$$\frac{1}{R_g(i)} = \frac{\alpha(i)}{R_g(SO_2)} + \frac{\beta(i)}{R_g(O_3)}$$

where

$$R_g(O_3) = \begin{cases} 2000\ s\ m^{-1} & LUC\ 1-3\ and\ Snow\ Surface \\ 200\ s\ m^{-1} & LUC\ 4-19,\ 25\ and\ 26 \\ 500\ s\ m^{-1} & LUC\ 20-24 \end{cases}$$

For snow surface, $R_g(O_3)$ adjusted by including a snow cover fraction(f_{snow}):

$$\frac{1}{R_g(O_3)} = \frac{1-2f_{snow}}{R_g(LUC)} + \frac{2f_{snow}}{R_{snow}}$$

where

$f_{snow} = \frac{sd}{sd_{max}}$, note – both f_{snow} and $2f_{snow}$ have a lower limit of 0 and upper limit of 1

$R_{snow} = 2000$ s/m

$$R_g(SO_2) = \begin{cases} 20\ s\ m^{-1} & LUC\ 1\ and\ 3 \\ 70(2-T) & LUC\ 2,\ T\ as\ Surface\ Temperature\ (°C) \\ 50 & LUC\ 4-26,\ Rain \\ 100 & LUC\ 4-26,\ Dew \\ R_{gd},\ (Table\ 1) & LUC\ 4-26,\ Not\ Rain\ or\ Dew,\ T \geq -1°C \\ \min(2R_{gd}, R_{gd}e^{0.2(-1-T)}) & LUC\ 4-26,\ Not\ Rain\ or\ Dew,\ T < -1°C \end{cases}$$

with a lower limit of 100 s/m and upper limit of 500 s/m (limit only applies to LUC2)

For snow surface, $R_g(SO_2)$ are adjusted by snow cover fraction(f_{snow}):

$$\frac{1}{R_g(SO_2)} = \frac{1-2f_{snow}}{R_g(LUC)} + \frac{2f_{snow}}{R_{snow}}$$

where

$f_{snow} = \frac{sd}{sd_{max}}$, note – both f_{snow} and $2f_{snow}$ have a lower limit of 0 and upper limit of 1

$R_{snow} = 70(2-T)$, T as °C

Canopy cuticle resistance:

$$R_{cut} = \begin{cases} \frac{R_{cutw0}}{LAI^{1/2}u_*} & Rain\ or\ Dew \\ \frac{R_{cutd0}}{e^{0.03RH}LAI^{1/4}u_*} & Not\ Rain \\ \min(2R_{cut}, R_{cut}e^{0.2(-1-T)}) & T<-1°C \end{cases}$$

where

$R_{cutw0}(O_3)$ listed in Table A1.
$R_{cutw0}(SO_2)$ = 50 s/m or 100 s/m for rain or dew conditions, respectively.
R_{cutd0} listed in Table A1.

with a lower limit of 100 s/m and 20 s/m for SO_2 dry and wet conditions, respectively

For snow surface, R_{cut} are adjusted by including a snow cover fraction (f_{snow})

$$\frac{1}{R_{cut}} = \frac{1-f_{snow}}{R_{cut}} + \frac{f_{snow}}{R_{snow}}$$

where

$$R_{snow} = \begin{cases} 2000 & O_3 \\ 70(2-T) & SO_2 \end{cases}$$

Roughness length:

$$z_0(t) = z_0(\min) + \frac{LAI(t) - LAI(\min)}{LAI(Max) - LAI(\min)} \times [z_0(\max) - z_0(\min)]$$

Rain or Dew conditions:

$$Condition = \begin{cases} Rain & T > 273.15°K \ and \ \Pr ec. > 0.1mm/hr \\ Dew & T > 273.15°K \ and \ u^* > u^*_{\min} \end{cases}$$

where:

$$u^*_{\min} = \frac{1.5Coedew}{DQ}$$

where:

$$Coedew = \begin{cases} 0.3 & FCLD < 0.25 \\ 0.2 & 0.25 \le FCLD < 0.75 \\ 0.1 & 0.75 \le FCLD \le 1 \end{cases}$$

and

$DQ = 0.0622(1 - RH)E^*(T_s)$, with a lower limit of 0.0001

Parameters (for particulates):

(Variables for computing R_a were not included)

V_d:	deposition velocity (m/s)
R_a:	aerodynamic resistance (s/m)
R_s:	surface resistance (s/m)
$u*$:	friction velocity (m/s)
u:	horizontal wind speed at reference height (m/s)
g:	gravitational acceleration (9.81 m/s^2)
T_2:	temperature at reference height (°K)
LAI:	Leaf Area Index
LUC:	Land Use Category (15 LUCs in particle model)
SC:	Season Category (5 SCs in particle model, listed in Table A5)
ρ :	density of particle
dp:	particle diameter
C:	correction factor for small particles

μ:	dynamic viscosity of air
ν:	kinematic viscosity of air
C:	Cunningham slip correction factor
E_B:	collection efficiency from Brownian diffusion
E_{IM}:	collection efficiency from impaction
E_{IN}:	collection efficiency from interception
R1:	correction factor representing fraction of particles that sticks to surface
Sc:	Schmidt number
D:	Brownian diffusivity
St:	Stokes number
K:	Boltzmann constant (gm cm^2/s^2-°K)
P:	surface pressure (kPa)
λ:	mean free path of air molecules

Deposition Velocity:

$$V_d = V_g + \frac{1}{R_a + R_s}$$

Assumes SO_4^{2-} and NH_4^+ have the same V_d; and NO_3^-, Ca^{2+}, Mg^{2+}, Na^+, and K^+ have the same V_d as described in Cheng et al. (2001).

Mass median diameter (MMD) and geometric standard deviation (GSD) for SO_4^{2-} chosen as 0.35 µm and 2.0 µm, respectively as reported in Wesely et al. (1985).

MMD and GSD for Na^+ are taken as 5.12 µm and 2.64 µm, respectively as reported in Ruijgrok et al (1997).

Gravitational settling velocity:

$$V_g = \frac{\rho d_p^2 g C}{18\mu}$$

Cunningham slip correction factor:

$$C = 1 + \frac{2\lambda}{d_p}(1.257 + 0.4e^{-0.55 d_p / \lambda})$$

Aerodynamic Resistance:

R_a is computed with the same approach as the gas model, but the parameters are adapted from Table A4.

Surface Resistance:

$$R_s = \frac{1}{\varepsilon_0 u_* (E_B + E_{IM} + E_{IN}) R_1}, \text{ with a lower limit of 5}$$

where ε_0 is an empirical constant chosen as 3 for all LUCs

Collection efficiency from Brownian diffusion:

$$E_B = Sc^{-\gamma}$$

where γ lies between $^1/_2$ and $^2/_3$ with larger values for rougher surfaces. (Table A4)

Schmidt number:

$$Sc = \nu / D$$

Collection efficiency from impaction:

$$E_{IM} = \left(\frac{St}{\alpha + St} \right)^{\beta}$$

where
a: constant varying with LUC (Table A4)
b: constant, chosen as 2

Stokes number:

$$St = \begin{cases} \dfrac{V_g u_*^2}{\nu} & \textit{smooth surface, LUC 8, 9, 12, 13, and 14} \\ \dfrac{V_g u_* A}{g} & \textit{vegetated surface, LUCs other than above} \end{cases}$$

where A is the characteristic radius varying with LUC and season (Table A4)

Collection efficiency from interception:

$E_{IN} = \frac{1}{2}\left(\frac{d_p}{A}\right)^2$, with a upper limit of 0.6

where A is the characteristic radius varying with LUC and season (Table A4)

Correction factor representing fraction of particles that sticks to the surface:

$R_1 = \exp(-St^{1/2})$, with a low limit of 0.5

Mean free path of air molecules:

$$\lambda = 6.54\times10^{-8}\frac{\mu}{1.818\times10^{-5}}\frac{101.3}{P}\left(\frac{T_2}{293.15}\right)^{1/2}$$

Brownian diffusivity:

$$D = \frac{CKT_2}{3\pi d_p \mu}$$

Dynamic viscosity of air:

$$\mu = \frac{145.8\times10^{-8}T_2^{3/2}}{T_2 + 110.4}$$

Kinematic viscosity of air:

$$\nu = \frac{\mu}{\rho_{air}}$$

Bin division:

For I = 1 to 40,

$$binsize = 0.001 * I^{2.5}$$

Units required for input parameters to Visual Basic Program

hourly pollutant concentration:	$\mu g/m^3$
hourly cloud fraction:	tenths (converted to decimal within program)
hourly pressure:	kPa (converted to mb within program)
hourly snow depth:	cm
hourly precipitation:	mm
hourly solar radiation:	W/m^2
hourly relative humidity:	% (converted to decimal within program)
hourly wind speed:	km/hr (converted to m/s within program)
hourly temperature:	°C (converted to K within program)

Table A1LUC and all related parameters (all resistance have units of s/m; na = not applicable; f(u) = function of wind speed).

	LUC	R_{sto}	R_{sto} O_3	R_{sto} O_3	R_{sto} SO_2	R_{ns} SO_2	r_{stmin} (s/m)	b_n (Wm^{-2})	T_{min} (°C)	T_{max} (°C)	T_{opt} (°C)	b_{vpd} (kPa^{-1})	Ψ_{f1} (Mpa)	Ψ_{f2} (Mpa)	z_0 (m)	Sd_{max} (cm)
1	water	0	na	na	na	20	na	na	na	na	na	na	na	na	f(u)	na
2	ice	0	na	na	na	[illegible]	na	na	na	na	na	na	na	na	0.01	1
3	inland lake	0	na	na	na	20	na	na	na	na	na	na	na	na	f(u)	na
4	evergreen needleleaf trees	100	4000	200	2000	200	250	44	−5	40	15	0.31	−2	−2.5	0.9	200
5	evergreen broadleaf trees	250	6000	400	2500	100	150	40	0	45	30	0.27	−1	−5.0	2.0	400
6	deciduous needleleaf trees	60–100	4000	200	2000	200	250	44	−5	40	15	0.31	−2	−2.5	0.4–0.9	200
7	deciduous broadleaf trees	100–250	6000	400	2500	200	150	43	0	45	27	0.36	−1.9	−2.5	0.4–1.0	200
8	tropical broadleaf trees	300	6000	400	2500	100	150	40	0	45	30	0.27	−1	−5.0	2.5	400
9	drought deciduous trees	100	8000	400	6000	300	250	44	0	45	25	0.31	−1	−4.0	0.6	200
10	evergreen broadleaf shrubs	60	6000	400	2000	200	150	40	0	45	30	0.27	−2	−4.0	0.2	50
11	deciduous shrubs	20–60	5000	300	2000	200	150	44	−5	40	15	0.27	−2	−4.0	0.05–0.2	50
12	thorn shrubs	40	5000	300	2000	200	250	44	0	45	25	0.27	−2	−3.5	0.2	50
13	short grass and forbs	20	4000	200	1000	200	150	50	5	40	30	0	−1.5	−2.5	0.04	5
14	long grass	10–40	4000	200	1000	200	100	20	5	45	25	0	−1.5	−2.5	0.02–0.1	20
15	crops	10–40	4000	200	1500	200	120	40	5	45	27	0	−1.5	−2.5	0.02–0.1	10
16	rice	10–40	4000	200	1500	50	120	40	5	45	27	0	−1.5	−2.5	0.02–0.1	10
17	sugar	10–40	4000	200	2000	200	120	50	5	45	25	0	−1.5	−2.5	0.02–0.1	10
18	maize	10–50	5000	300	2000	200	250	65	5	45	25	0	−1.5	−2.5	0.02–0.1	10
19	cotton	10–40	5000	300	2000	200	125	65	10	45	30	0	−1.5	−2.5	0.02–0.2	10
20	irrigated crops	20	4000	200	2000	50	150	40	5	45	25	0	−1.5	−2.5	0.05	10
21	urban	40	6000	400	4000	300	200	42	0	45	22	0.31	−1.5	−3	1.0	50
22	tundra	0	6000	400	2000	300	150	25	−5	40	20	0.24	0	−1.5	0.03	2
23	swamp	20	5000	300	1500	50	150	40	0	45	20	0.27	−1.5	−2.5	0.1	10
24	Desert	0	na	na	na	700	na	na	na	na	na	na	na	na	0.04	2
25	mixed wood forests	100	4000	200	2500	200	150	44	−3	42	21	0.34	−2	−2.5	0.6–0.9	200
26	Transitional forest	100	4000	200	2500	200	150	43	0	45	25	0.31	−2	−3	0.6–0.9	200

Table A2 LAI(i) values dependent upon Land Use Category (LUC) ("i" represents month number, "i=14" and "i=15" represent minimum and maximum value, respectively).

No.	LUC	1	2	3	4	5	6	7	8	9	10	11	12	13	14	15
1	water	0	0	0	0	0	0	0	0	0	0	0	0	0	0	0
2	ice	0	0	0	0	0	0	0	0	0	0	0	0	0	0	0
3	inland lake	0	0	0	0	0	0	0	0	0	0	0	0	0	0	0
4	evergreen needleleaf trees	5	5	5	5	5	5	5	5	5	5	5	5	5	5	5
5	evergreen broadleaf trees	6	6	6	6	6	6	6	6	6	6	6	6	6	6	6
6	deciduous needleleaf trees	0.1	0.1	0.5	1.0	2.0	4.0	5.0	5.0	4.0	2.0	1.0	0.1	0.1	0.1	5.0
7	deciduous broadleaf trees	0.1	0.1	0.5	1.0	2.0	4.0	5.0	5.0	4.0	2.0	1.0	0.1	0.1	0.1	5.0
8	tropical broadleaf trees	6	6	6	6	6	6	6	6	6	6	6	6	6	6	6
9	drought deciduous trees	4	4	4	4	4	4	4	4	4	4	4	4	4	4	4
10	evergreen broadleaf shrubs	3	3	3	3	3	3	3	3	3	3	3	3	3	3	3
11	deciduous shrubs	0.5	0.5	1.0	1.0	1.5	2.0	3.0	3.0	2.0	1.5	1.0	0.5	0.5	0.5	3.0
12	thorn shrubs	3	3	3	3	3	3	3	3	3	3	3	3	3	3	3
13	short grass and forbs	1	1	1	1	1	1	1	1	1	1	1	1	1	1	1
14	long grass	0.5	0.5	0.5	0.5	0.5	0.5	1.0	2.0	2.0	1.5	1.0	1.0	0.5	0.5	2.0
15	crops	0.1	0.1	0.1	0.5	1.0	2.0	3.0	3.5	4.0	0.1	0.1	0.1	0.1	0.1	4.0
16	rice	0.1	0.1	0.1	0.5	1.0	2.5	4.0	5.0	6.0	0.1	0.1	0.1	0.1	0.1	6.0
17	sugar	0.1	0.1	0.1	0.5	1.0	3.0	4.0	4.5	5.0	0.1	0.1	0.1	0.1	0.1	5.0
18	maize	0.1	0.1	0.1	0.5	1.0	2.0	3.0	3.5	4.0	0.1	0.1	0.1	0.1	0.1	4.0
19	cotton	0.1	0.1	0.1	0.5	1.0	3.0	4.0	4.5	5.0	0.1	0.1	0.1	0.1	0.1	5.0
20	irrigated crops	1	1	1	1	1	1	1	1	1	1	1	1	1	1	1
21	urban	0.1	0.1	0.1	0.1	0.5	1.0	1.0	1.0	1.0	1.0	0.4	0.1	0.1	0.1	1.0
22	tundra	1.0	1.0	0.5	0.1	0.1	0.1	0.1	1.0	2.0	1.5	1.5	1.0	1.0	0.1	2.0
23	swamp	4	4	4	4	4	4	4	4	4	4	4	4	4	4	4
24	Desert	0	0	0	0	0	0	0	0	0	0	0	0	0	0	0
25	mixed wood forests	3.0	3.0	3.0	4.0	4.5	5.0	5.0	5.0	4.0	3.0	3.0	3.0	3.0	3.0	5.0
26	Transitional forest	3.0	3.0	3.0	4.0	4.5	5.0	5.0	5.0	4.0	3.0	3.0	3.0	3.0	3.0	5.0

Table A3Species-specific chemical and physical parameters.[a]

No.	Symbol	Name	Depn Mmts	MW	H (M atm^{-1})	H* (M atm^{-1})	pe^{0} (W)	Rm	a	b
1	SO_2	Sulphur dioxide	Yes	64	(1.1-1.5) x 10^{0}	2.65 x 10^{5}	75.5 to -7.6	0	1	0
2	H_2SO_4	Sulphuric acid	No	98	2.1 x 10^{5}	>2.1 x 10^{5}	4.9 to -4.3	0	1	1
F	NO	Nitric oxide	Yes	30	(1.4-1.9) x10^{-3}	H	27.8 to 3.0	Not considered		
3	NO_2	Nitrogen dioxide	Yes	46	(0.7-4.1) x 10^{-2}	H	28.4 to 8.2	0	0	0.8
4	O_3	Ozone	Yes	48	(0.9-1.3) x 10^{-2}	H	28.1 to 18.6	0	0	1
5	H_2O_2	Hydrogen peroxide	Yes	34	(0.7-1.4) x 10^{5}	H	24.8 to 9.7	0	1	1
6	HNO_3	Nitric acid	Yes	63	(0.1-2.6) x 10^{6}	3.2 x 1013	14.1 to 8.9	0	10	10
7	HONO	Nitrous acid	Yes	47	(3.7-5.0) x 10^{1}	2.6 x 105	17.5 to 14.8	0	2	2
8	HNO_4	Pernitric acid	No	79	(0.1-1) x 10^{5}	>1 x 107	No data	0	5	5
9	NH_3	Ammonia	Yes	17	(1.0-7.8) x 10^{1}	1.1 x 104	Not applicable	0	1	0
10	PAN	Peroxyacetylnitrate	Yes	121	(2.8-5.0) x 10^{0}	H	30.2 to -1.5	0	0	0.6
11	PPN	Peroxypropylnitrate	No	135	2.9 x 10^{0}	H	37.8 to -2.3	0	0	0.6
12	APAN	Aromatic acylnitrate	No	183	No data	5	46.9 to 11.2	0	0	0.8
13	MPAN	Peroxymethacrylic nitric anhydride	No	147	1.7 x 10^{0}	H	3.1	0	0	0.3
14	HCHO	Formaldehyde	Yes	30	(0.3-1.4) x 10^{4}	4.9 x 103	3.0 to -0.1	0	0.8	0.2
15	MCHO	Acetaldehyde	No	44	(1.0-1.7) x 10^{1}	≥15	-1.0 to -3.9	100	0	0.05
16	PALD	C3 carbonyls	No	58	(2.4-3.7) x 10^{0}	H	-1.3 to -1.8	100	0	0.05
17	C4A	C4–C5 carbonyls	No	72	(0.9-1.8) x 10^{1}	H	-1.3 to -1.8	100	0	0.05
18	C7A	C6–C8 carbonyls	No	128	(0.4-11) x 10^{1}	H	-1.5	100	0	0.05
19	ACHO	Aromatic carbonyls	No	106	(3.5-4.2) x 10^{1}	H	-1.0 to -2.5	100	0	0.05
20	MVK	Methyl-vinyl-ketone	No	70	(2.1-4.4) x 10^{1}	H	0.2	0	0	0.05
21	MACR	Methacrolein	No	70	(4.3-6.5) x 10^{0}	H	-1.2	100	0	0.05
22	MGLY	Methylgloxal	No	72	(0.4-3.2) x 10^{4}	H	-0.7	0	0.01	0
23	MOH	Methyl alcohol	No	32	(1.4-2.3) x 10^{2}	≥H	3.0	0	0.6	0.1
24	ETOH	Ethyl alcohol	No	46	(1.2-2.3) x 10^{2}	≥H	-1.3 to -2.9	0	0.6	0
25	POH	C3 alcohol	No	60	(0.9-1.7) x 10^{2}	≥H	-0.3	0	0.4	0
26	CRES	Cresol	No	104	8.3 x 10^{2}	H	-2.5	0	0.01	0
27	FORM	Formic acid	Yes	46	(0.9-8.9) x 10^{3}	9.8 x 10^{6}	1.9 to -6.4	0	2	0
28	ACAC	Acetic acid	Yes	60	(0.8-9.3) x 10^{3}	9.6 x 10^{5}	-3.1 to -9.6	0	1.5	0
29	ROOH	Organic peroxides	Yes	48	(0.1-3.1) x 10^{2}	H	4.2 to 3.6	0	0.1	0.8
30	ONIT	Organic nitrates	No	77	2.0 x 10^{0}	H	10.5 to -5.0	100	0	0.5
31	INIT	Isoprene nitrate	No	147	2.0 x 10^{0}	H	No data	100	0	0.5

[a] Values for Henry's Law constant (H) were obtained from Howard and Meylan (1997) and Sander (1999).

Table A4Parameters related to LUC and SC in particle model.

NO.	Land use categories Description (LUC)	Z_0 (m)					A (mm)						
		SC 1	SC 2	SC 3	SC4	SC 5	SC 1	SC 2	SC 3	SC 4	SC 5		
1	Evergreen}needleleaf trees	0.8	0.9	0.9	0.9	0.8	2	2	2	2	2	1	0.56
2	Evergreen broadleaf trees	2.65	2.65	2.65	2.65	2.65	5	5	5	5	5	0.6	0.58
3	Deciduous needleleaf trees	0.85	0.85	0.8	0.55	0.6	2	2	5	5	2	1.1	0.56
4	Deciduous broadleaf trees	1.05	1.05	0.95	0.55	0.75	5	5	10	10	5	0.8	0.56
5	Mixed broadleleaf and needleaf trees	1.15	1.15	1.15	1.15	1.15	5	5	5	5	5	0.8	0.56
6	Grass	0.1	0.1	0.05	0.02	0.05	2	2	5	5	2	1.2	0.54
7	Crops, mixed farming	0.1	0.1	0.02	0.02	0.05	2	2	5	5	2	1.2	0.54
8	Desert	0.04	0.04	0.04	0.04	0.04	na	na	na	na	na	50	0.54
9	Tundra	0.03	0.03	0.03	0.03	0.03	na	na	na	na	na	50	0.54
10	Shrubs and interrupted wood-lands	0.1	0.1	0.1	0.1	0.1	10	10	10	10	10	1.3	0.54
11	Wet land with plants	0.03	0.03	0.02	0.02	0.03	10	10	10	10	10	2	0.54
12	Ice cap and glacier	0.01	0.01	0.01	0.01	0.01	na	na	na	na	na	50	0.54
13	Inland water	f (u)	f (u)	f(u)	f(u)	f (u)	na	na	na	na	na	100	0.5
14	Ocean	f (u)	f (u)	f(u)	f(u)	f (u)	na	na	na	na	na	100	0.5
15	Urban	1	1	1	1	1	10	10	10	10	10	1.5	0.56

Table A5 Latitude values applied for the determination of Seasonal categories (SC) used in particle model.

NO.	Seasonal categories (SC)	Month											
		12	1	2	3	4	5	6	7	8	9	10	11
1	Midsummer with lush vegetation.	<30			<35			<55	<70	<45	<35		
2	Autumn with cropland that has not been harvested.									45-80	35-65	35-45	35-40
3	Late autumn after frost, no snow.										65-80	45-65	40-50
4	Winter, snow on ground and sub-freezing.				>40	>45	>60	>70	>80			>65	>50
5	Transitional spring with partially green short annuals.	30-35			35-40	35-45	35-60	55-70	70-80				

APPENDIX B ALBERTA ENVIRONMENT CALCULATION METHODS FOR GASES AND PARTICULATES

(after Cheng et al., 2001 and WBK, 2008)

Parameters:

B	defined equation described herein
C	concentration ($\mu g/m^3$)
D	diffusion coefficient of the substance of interest (cm^2/s)
F	dry deposition flux ($\mu g/m^2/s$)
g	gravitational acceleration (9.81 m/s^2)
H	sensible heat flux (w/m^2)
k	von Karman constant (0.4)
L	Monin-Obukhov length scale
PAI	Potential Acid Input (kg H^+/ha/yr)
Pr	Prandtl number for air (0.72)
R_a	aerodynamic resistance (s/m)
R_b	boundary-layer resistance (s/m)
R_c	surface resistance (s/m)
R_i	Bulk Richardson number
RH	relative humidity
Sc	Schmidt number
SW	soil wetness
T_d	temperature difference between 10 and 2 m ($T_{10} - T_2$)
T_2	temperature at 2 m (Kelvin)
u	wind speed (m/s)
u^*	friction velocity (m/s)
V_d	deposition velocity (m/s)
[X]	concentration of X chemical species deposited (kg/ha/yr)
z	reference height (10 m)
z_0	surface roughness length (m)
η	dynamic viscosity of air (18.0×10^{-6} N-s/m^2 at 1 atm and 25°C)
ρ	density of air (1.18 kg/m^3 at 1 atm and 25°C)
σ_θ	standard deviation of wind direction (rad)
ψ	integrated stability correction term

Equations:

$$\mathbf{PAI_{dry}} = \frac{[SO_2]}{64} + \frac{[NO_2]}{46} + \frac{[HNO_2]}{47} + \frac{[HNO_3]}{63} + 2\frac{[SO_4^{2-}]}{96} + \frac{[NO_3^-]}{62} + \frac{[NH_4^+]}{18} - \left(\frac{[K^+]}{39} + \frac{[Na^+]}{23} + 2\frac{[Ca^{2+}]}{40} + 2\frac{[Mg^{2+}]}{24}\right)$$

deposition concentrations units in kg/ha/yr

$$\mathbf{F = V_d C}$$

$$\mathbf{V_d} = \frac{1}{(R_a + R_b + R_c)}$$

Summary of Species Specific Deposition Velocity Formulae:

$$V_{d(SO_2)} = \frac{1}{R_a + R_{b(SO_2)} + R_{c(SO_2)}}$$

$$V_{d(NO_2)} = \frac{1}{R_a + R_{b(NO_2)} + R_{c(NO_2)}}$$

$$V_{d(HNO_3)} = \frac{1}{R_a + R_{b(SO_2)}}$$

$$V_{d(HNO_2)} = \frac{1}{R_a + R_{b(HNO_2)}}$$

R_c is treated as being negligible for nitric and nitrous acid.

$$V_{d(SO_4^{2-}, NH_4^+)} = \frac{1}{R_a + R_{b(SO_4^{2-})}}$$

$$V_{d(NO_3^-, Ca^{2+}, Mg^{2+}, K^+, Na^+)} = \frac{1}{R_a + (0.5 \times R_{b(SO_4^{2-})})}$$

Aerodynamic Resistance (R_a):

$$R_a = \frac{1}{ku^*}\left\{\ln\frac{z}{z_0} - \psi\left(\frac{z}{L}\right)\right\}$$ (R_a is infinite and $V_d = 0$ when u and T_d are zero)

Friction velocity:

$u^* = \frac{u\sigma_\theta}{1.9}$ (this relationship is used as an initial estimate of u^* to calculate z_0, a more precise value of u^* is calculated after z_0 is obtained – refer to below)

$z_o = z\, e^{-\left(\frac{0.4u}{u^*}\right)}$ (calculated as a monthly average using data where the wind speed is >6 m/s)

A more precise value of u^* calculated after z_o is obtained (based on atmospheric conditions):

$$u^* = ku\left\{\ln\left(\frac{z}{z_0}\right)(1+4.7Ri)\right\}^{-1} \qquad \textit{Stable conditions} \mathbf{R_i} > 0$$

$$u^* = \frac{ku}{\ln\left(\frac{z}{z_0}\right)\sqrt{1-\left\{\frac{9.4Ri}{1+(7.4B)}\right\}}} \qquad \textit{Unstable conditions} \mathbf{R_i} < 0$$

$$u^* = \frac{ku}{\ln\left(\frac{z}{z_0}\right)} \qquad \textit{Neutral conditions } \mathbf{R_i} = 0$$

Bulk Richardson number

$$R_i = \frac{gzT_d}{T_z u^2}$$

Stability function (based on atmospheric conditions):

$$\psi = -\frac{5z}{L} \qquad \textit{Stable conditions}$$

$$\psi = 2\ln\left\{\frac{1}{2}\left(1+\sqrt{1-\frac{15z}{L}}\right)\right\} \qquad \textit{Unstable conditions}$$

$$\psi = 0 \qquad \textit{Neutral conditions}$$

Monin-Obukhov length:

$$L = \frac{T_z u^{*3}}{kHg}$$

Sensible heat flux (based on atmospheric conditions):

$$H = \left\{\frac{uT_d}{0.74}\right\}\left\{\frac{k}{\ln\left(\frac{z}{z_0}\right)}\right\}^2\left\{\frac{1}{(1+4.7Ri)^2}\right\} \quad \textit{Neutral and Stable conditions}$$

$$H = \left\{\frac{uT_d}{0.74}\right\}\left\{\frac{k}{\ln\left(\frac{z}{z_0}\right)}\right\}^2\left\{1-\frac{9.4Ri}{(1+5.3B)}\right\} \quad \textit{Unstable conditions}$$

$$\text{Where } B = 9.4\left[\frac{k}{\ln\left(z/z_0\right)}\right]^2\left[|R_i|\frac{z}{z_0}\right]^{1/2}$$

Boundary Layer Resistance (R_b):

R_b (gases):

$$R_b = \frac{2}{ku_*}\left(\frac{\eta}{\rho D}\times\frac{1}{\mathrm{Pr}}\right)^{2/3}$$

$$R_b = \frac{7.22}{u_*} \text{ for } SO_2 \text{ and } HNO_3$$

$$R_b = \frac{6.18}{u_*} \text{ for } NO_2$$

$$R_b = \frac{6.09}{u_*} \text{ for } HNO_2$$

R_b (particulates):

R_b values for particulate sulphate are obtained from scientific literature for daytime and nighttime as a function of surface type and weighted according to average day length for each month at a mid-Alberta latitude location (54°N latitude) after Cheng and Angle (1993) as cited in Cheng et al. (2001).

Table B1 Boundary-Layer Resistance (s/cm) for Fine Particulate (SO_4^{2-}, $NH4^+$), Day Length Weighted Averages at 54°N Latitude for the Middle of Each Month.

Surface Type	Winter (Dec, Jan, Feb)		Spring (Mar, Apr, May)		Summer (Jun, July, Aug)		Autumn (Sep, Oct, Nov)	
	Dry	Wet	Dry	Wet	Dry	Wet	Dry	Wet
Deciduous Forest	16.9	0	5.4	0	1.3	0	3.2	0
Coniferous Forest	2.5	0	2.7	0	1.9	0	2.3	0
Wetland/Swamp*	20.4	0	3.8	0	2.6	0	3.2	0
Grassland*	20.4	0	5.6	0	3.9	0	4.7	0
Cropland*	20.4	0	9.0†	0	3.9	0	7.9‡	0
Urban§	33.9	0	10.9	0	2.6	0	6.3	0
Open Water	0	0	0	0	0	0	0	0
Snow/Ice	20.4	0	-	-	-	-	-	-

* in winter, wetland, grassland, and cropland treated as a snow surface. † bare soil and active growth.
‡ bare soil and senescent growth. § consists of a mixture of deciduous forest and buildings.

Table B2 Boundary-Layer Resistance (s/cm) for Coarse Particulate (NO_3^-, Na, K, Ca, Mg) Day Length Weighted Averages at 54°N Latitude for the Middle of Each Month.

Surface Type	Winter (Dec, Jan, Feb)		Spring (Mar, Apr, May)		Summer (Jun, July, Aug)		Autumn (Sep, Oct, Nov)	
	Dry	Wet	Dry	Wet	Dry	Wet	Dry	Wet
Deciduous Forest	8.45	0	2.7	0	0.65	0	1.6	0
Coniferous Forest	1.25	0	1.35	0	0.95	0	1.15	0
Wetland/Swamp*	10.2	0	1.9	0	1.3	0	1.6	0
Grassland*	10.2	0	2.8	0	1.95	0	2.35	0
Cropland*	10.2	0	4.5†	0	1.95	0	3.95‡	0
Urban§	16.95	0	5.45	0	1.3	0	3.15	0
Open Water	0	0	0	0	0	0	0	0
Snow/Ice	10.2	0	-	-	-	-	-	-

* in winter, wetland, grassland, and cropland treated as a snow surface. † bare soil and active growth.
‡ bare soil and senescent growth. § consists of a mixture of deciduous forest and buildings.

Day length Weighted Seasonal Average R_b = $\frac{day\ length}{24hrs}\left(R_{b\ day}\right)+\left(1-\frac{day\ length}{24hrs}\left(R_{b\ night}\right)\right)$

Day length = $0.133\left\{\cos^{-1}\left(-\tan(55^{\circ})\times\tan(Solar\ Declination)\right)\right\}$

Solar Declination = $23.45\left\{\sin\left(\frac{360\times(284+Julian\ Day)}{365}\right)\right\}$

Surface Resistance (R_c):

Bulk surface resistance values are used from literature as a function of surface type, surface wetness, and incident radiation. Day length weighted average R_c values for SO_2 and NO_2 are used from Voldner et al. (1986), Arrit et al. (1987) and Walcek et al. (1986) as cited in Cheng et al. (2001):

Table B3 Day Length Weighted Averages Bulk Surface Resistance (s/cm) for Sulphur Dioxide (SO_2):

Surface Type	Winter (Dec, Jan, Feb)		Spring (Mar, Apr, May)		Summer (Jun, July, Aug)		Autumn (Sep, Oct, Nov)	
	Dry	Wet	Dry	Wet	Dry	Wet	Dry	Wet
Deciduous Forest	10	10	4.7	0	3.5	0	7.9	0.4
Coniferous Forest	5	5	4.1	0	3.5	0	4.9	0.2
Wetland/Swamp*	7	1	0.5	0	0.7	0	1	0.1
Grassland*	7	1	1	0	1.3	0	2	0.1
Cropland*	7	1	0†	0	2	0	2‡	0.1
Urban§	10	2	10	0	10	0	10	0.1
Open Water	0	0	0	0	0	0	0	0
Snow/Ice	7	1	-	-	-	-	-	-

* in winter, wetland, grassland, and cropland treated as a snow surface. † bare soil and active growth.
‡ bare soil and senescent growth. § consists of a mixture of deciduous forest and buildings.

Table B4 Day Length Weighted Averages Bulk Surface Resistance (s/cm) for Nitrogen Dioxide (NO_2):

Surface Type	Winter (Dec, Jan, Feb)		Spring (Mar, Apr, May)		Summer (Jun, July, Aug)		Autumn (Sep, Oct, Nov)	
	Dry	Wet	Dry	Wet	Dry	Wet	Dry	Wet
Deciduous Forest	20.0	70.0	3.3	70.0	2.2	70.0	4.7	70.0
Coniferous Forest	10.0	70.0	2.7	70.0	2.2	70.0	3.3	70.0
Wetland/Swamp*	50.0	70.0	12.1	70.0	11.5	70.0	12.9	70.0
Grassland*	50.0	70.0	3.3	70.0	3.3	70.0	6.6	70.0
Cropland*	50.0	70.0	3.3†	70.0	4.6	70.0	7.9‡	70.0
Urban§	10.0	70.0	10.0	70.0	10.0	70.0	10.0	70.0
Open Water	70.0	70.0	70.0	70.0	70.0	70.0	70.0	70.0
Snow/Ice	50.0	70.0	-	-	-	-	-	-

* in winter, wetland, grassland, and cropland treated as a snow surface. † bare soil and active growth.
‡ bare soil and senescent growth. § consists of a mixture of deciduous forest and buildings.

R_c (HNO_3): 10 s/m (for all seasons and all surfaces)
R_c (HNO_2): 10 s/m (for all seasons and all surfaces)
R_c (NH_3): 28 s/m (dry conditions)
9 s/m (wet conditions)
201 s/m (when T_2<0°C)

R_c (particulates): 0 s/m

R_c is calculated based on surface wetness criteria, such that it either represents a "total dry condition," "total wet condition," or "weighted wet condition" using the following flowchart, and relative humidity (RH) and surface wetness (SW) criteria:

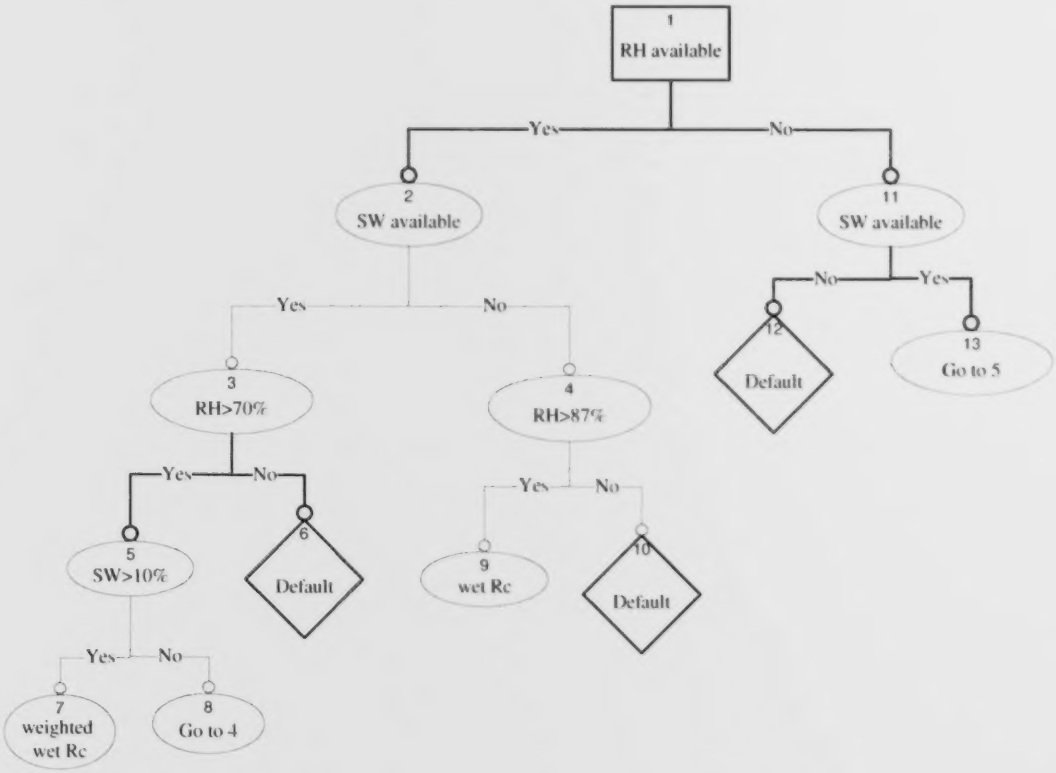

Figure B1Flowchart for calculating Rc (Adapted from Bates (1996)

Default = R_c value for dry conditions
Wet R_c = R_c value for wet conditions
Weighted Wet R_c = Time weighted wet R_c

$$\textbf{Time weighted wet } R_c = \left(\frac{SW}{100} \times wet\ Rc\right) + \left[\left(1 - \frac{SW}{100}\right) \times dry\ Rc\right]$$

Calculation of V_d in the absence of meteorological data:

Missing hourly meteorological data are treated in the following manner:

- 1 hour of meteorological data missing → the average resistance of the hours before and after are used to represent the missing hour
- consecutive hours of meteorological data missing → each hour's calculated median resistance for the month is used to represent the missing hours

Units required for input parameters to Visual Basic Program

hourly pollutant concentration: $\mu g/m^3$

hourly wind speed:	km/hr (converted to m/s within program)
hourly wind direction std. dev.:	degrees (converted to radians within program)
hourly temperature:	°C (converted to K in program)
hourly delta temperature:	°C
hourly relative humidity:	% (converted to decimal within program)
hourly surface wetness:	%

APPENDIX C MONTHLY AVERAGE SPECIES CONCENTRATIONS

Table C1 Monthly average chemical concentrations.

	gaseous chemicals			(µg/m^3)	particulate chemicals						(µg/m^3)
month	SO2	NO2	HNO2	HNO3	SO4	NH4	NO3	Na	K	Ca	Mg
Month 1	2.9	19.1	0.76	1.46	1.03	0.65	0.30	0.14	0.09	0.19	0.04
Month 2	3.7	18.6	0.14	0.62	1.01	0.46	0.15	0.10	0.01	0.26	0.04
Month 3	3.3	10.9	0.07	0.61	2.35	0.69	0.17	0.12	0.01	0.35	0.03
Month 4	4.3	9.4	0.11	0.74	0.95	0.49	0.14	0.07	0.03	0.81	0.04
Month 5	3.2	6.1	0.13	0.41	0.67	0.31	0.05	0.04	0.02	0.38	0.05
Month 6	2.3	3.7	0.01	0.19	0.53	0.25	0.04	0.02	0.03	0.47	0.04
Month 7	3.9	5.0	0.02	0.25	0.50	0.23	0.08	0.05	0.06	0.79	0.07
Month 8	4.2	7.0	0.06	0.31	0.70	0.34	0.07	0.05	0.04	0.61	0.07
Month 9	1.7	7.1	0.11	0.21	0.59	0.29	0.05	0.06	0.04	0.23	0.04
Month 10	2.6	10.7	0.27	1.24	0.97	0.43	0.07	0.05	0.04	0.88	0.06
Month 11	1.0	14.4	0.14	0.19	0.79	0.66	0.48	0.10	0.07	1.92	0.06
Month 12	4.9	21.7	0.80	0.34	0.68	0.34	0.38	0.10	0.09	0.55	0.05

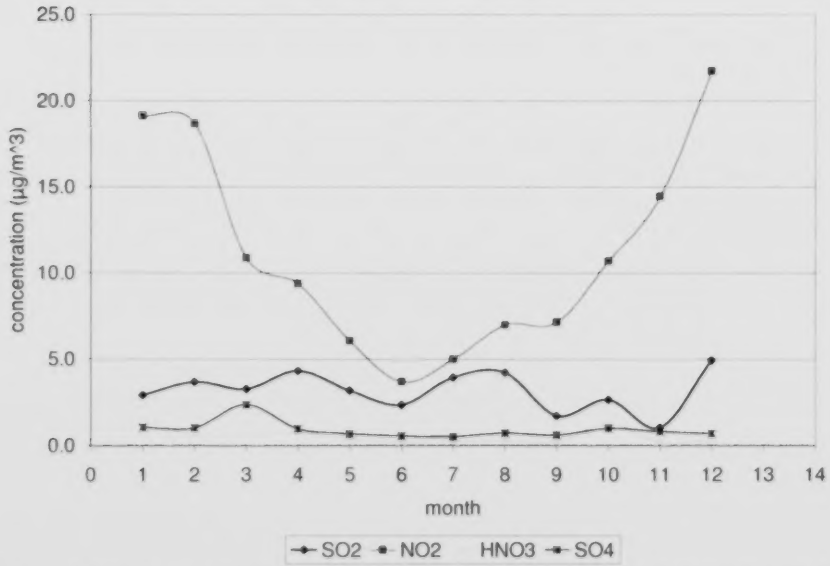

Figure C1 Monthly averaged chemical concentrations for the largest N and S contributors.

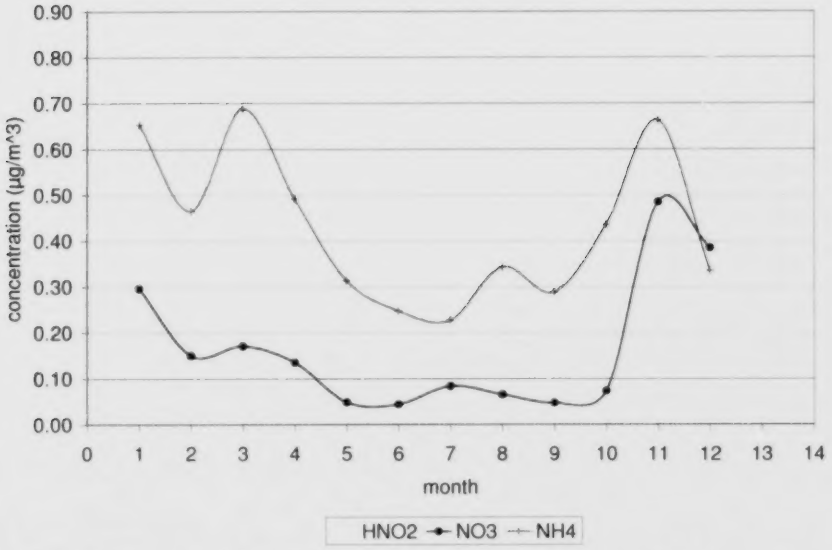

Figure C2Monthly averaged chemical concentrations for remaining N species.

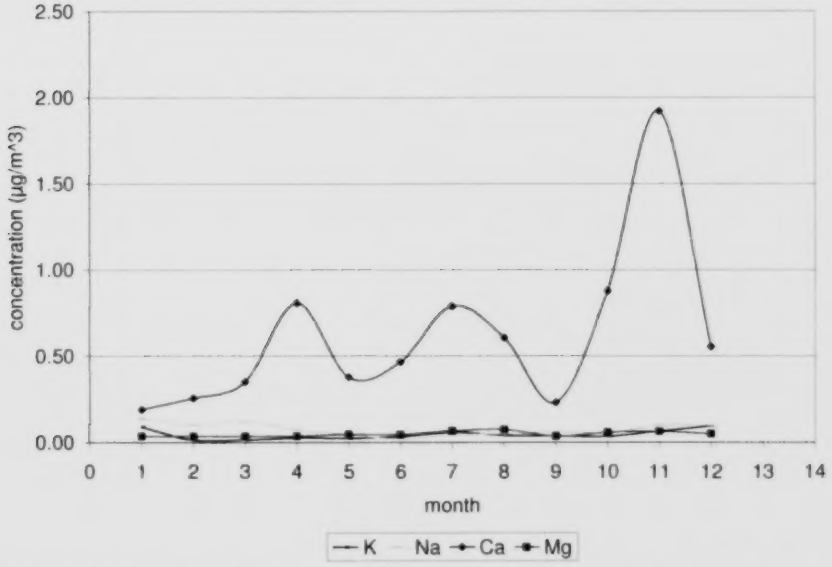

Figure C3Monthly averaged chemical concentrations for base cations.

APPENDIX D TABLES FOR MONTHLY DEPOSITION VELOCITIES OF COMPONENT CHEMICALS

Table D1Monthly average deposition velocities for SO_2 – coniferous forest (cm/s).

month	AENV	ENVC	difference
Month 1	0.09	0.14	-0.06
Month 2	0.10	0.12	-0.03
Month 3	0.13	0.23	-0.11
Month 4	0.17	0.34	-0.16
Month 5	0.25	0.37	-0.12
Month 6	0.49	0.36	0.13
Month 7	0.40	0.30	0.11
Month 8	0.35	0.29	0.06
Month 9	0.38	0.38	0.01
Month 10	0.36	0.35	0.01
Month 11	0.12	0.19	-0.07
Month 12	0.13	0.18	-0.05

Table D2Monthly average deposition velocities for NO_2 – coniferous forest (cm/s).

month	AENV	ENVC	difference
Month 1	0.05	0.08	-0.04
Month 2	0.05	0.07	-0.02
Month 3	0.09	0.15	-0.06
Month 4	0.18	0.22	-0.04
Month 5	0.20	0.24	-0.04
Month 6	0.25	0.24	0.01
Month 7	0.24	0.20	0.04
Month 8	0.24	0.19	0.05
Month 9	0.15	0.23	-0.08
Month 10	0.11	0.20	-0.09
Month 11	0.08	0.11	-0.03
Month 12	0.07	0.10	-0.03

Table D3 Monthly average deposition velocities for HNO_2 – coniferous forest (cm/s).

month	AENV	ENVC	difference
Month 1	0.94	0.32	0.62
Month 2	1.15	0.27	0.87
Month 3	1.68	0.50	1.18
Month 4	1.78	0.68	1.10
Month 5	2.17	0.73	1.45
Month 6	2.04	0.69	1.35
Month 7	1.83	0.58	1.24
Month 8	1.73	0.57	1.17
Month 9	2.14	0.76	1.38
Month 10	1.51	0.69	0.82
Month 11	1.29	0.42	0.87
Month 12	1.07	0.39	0.67

Table D4 Monthly average deposition velocities for HNO_3 – coniferous forest (cm/s).

month	AENV	ENVC	difference
Month 1	0.88	0.86	0.02
Month 2	1.07	0.82	0.25
Month 3	1.57	1.25	0.32
Month 4	1.68	1.59	0.09
Month 5	2.05	1.58	0.47
Month 6	1.92	1.51	0.41
Month 7	1.71	1.33	0.38
Month 8	1.63	1.30	0.32
Month 9	2.01	1.59	0.42
Month 10	1.42	1.32	0.09
Month 11	1.21	1.11	0.10
Month 12	1.00	1.05	-0.04

Table D5 Monthly average deposition velocities for SO_4^{2-}/NH_4^+ – coniferous forest (cm/s).

month	AENV	ENVC	difference
Month 1	0.17	0.09	0.08
Month 2	0.19	0.09	0.10
Month 3	0.20	0.12	0.08
Month 4	0.25	0.15	0.10
Month 5	0.23	0.14	0.09
Month 6	0.35	0.13	0.22
Month 7	0.34	0.10	0.24
Month 8	0.33	0.10	0.23
Month 9	0.29	0.11	0.18
Month 10	0.25	0.10	0.16
Month 11	0.26	0.10	0.16
Month 12	0.24	0.09	0.15

Table D6 Monthly average deposition velocities for $NO_3^-/Na^+/K^+/Ca^{2+}/Mg^{2+}$ – coniferous forest (cm/s)

month	AENV	ENVC	difference
Month 1	0.30	0.30	0.00
Month 2	0.35	0.26	0.09
Month 3	0.38	0.38	-0.01
Month 4	0.46	0.51	-0.05
Month 5	0.44	0.48	-0.04
Month 6	0.64	0.41	0.23
Month 7	0.63	0.29	0.33
Month 8	0.60	0.32	0.28
Month 9	0.54	0.36	0.17
Month 10	0.45	0.30	0.16
Month 11	0.46	0.31	0.15
Month 12	0.42	0.28	0.15

Table D7Small and large particle deposition velocities for AENV LUCs.

	deciduous forest	coniferous forest	wetland/swamp	grassland	cropland	urban	water	snow/ice
	small	small	small	small	small	small	small	small
Month 1	0.03	0.17	0.03	0.03	0.03	0.02	2.85	0.03
Month 2	0.03	0.19	0.03	0.03	0.03	0.02	3.49	0.03
Month 3	0.10	0.20	0.14	0.10	0.06	0.05	5.97	
Month 4	0.13	0.25	0.18	0.13	0.08	0.07	4.84	
Month 5	0.12	0.23	0.17	0.12	0.08	0.06	8.21	
Month 6	0.49	0.35	0.26	0.18	0.18	0.26	6.70	
Month 7	0.48	0.34	0.26	0.18	0.18	0.26	5.77	
Month 8	0.46	0.33	0.25	0.17	0.17	0.25	5.28	
Month 9	0.21	0.29	0.21	0.15	0.09	0.11	8.05	
Month 10	0.19	0.25	0.19	0.13	0.08	0.10	4.67	
Month 11	0.19	0.26	0.19	0.14	0.09	0.11	3.22	
Month 12	0.04	0.24	0.04	0.04	0.04	0.02	2.33	0.04
	large	large	large	large	large	large	large	large
Month 1	0.06	0.30	0.05	0.05	0.05	0.03	2.85	0.05
Month 2	0.06	0.35	0.05	0.05	0.05	0.03	3.49	0.05
Month 3	0.20	0.38	0.28	0.19	0.12	0.10	5.97	
Month 4	0.25	0.46	0.34	0.24	0.15	0.13	4.84	
Month 5	0.23	0.44	0.32	0.23	0.14	0.12	8.21	
Month 6	0.88	0.64	0.49	0.34	0.34	0.49	6.70	
Month 7	0.86	0.63	0.48	0.34	0.34	0.48	5.77	
Month 8	0.82	0.60	0.46	0.32	0.32	0.46	5.28	
Month 9	0.40	0.54	0.40	0.28	0.17	0.22	8.05	
Month 10	0.34	0.45	0.34	0.25	0.16	0.19	4.67	
Month 11	0.35	0.46	0.35	0.25	0.16	0.20	3.22	
Month 12	0.08	0.42	0.07	0.07	0.07	0.04	2.33	0.07

APPENDIX E MONTHLY AVERAGED DIURNAL DEPOSITION VELOCITIES FOR SO_2, NO_2, AND HNO_3

SO_2

January

February

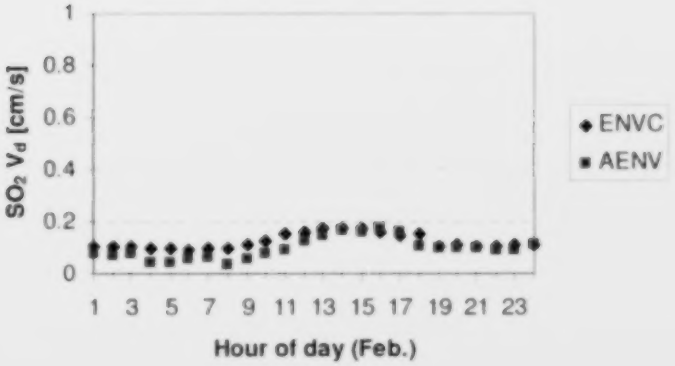

March

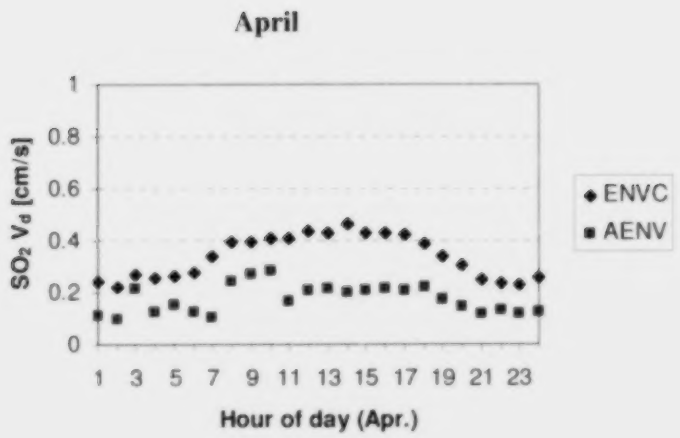
April
1
0.8
0.6
0.4
0.2
0
SO2 Vd [cm/s]
1 3 5 7 9 11 13 15 17 19 21 23
Hour of day (Apr.)
ENVC
AENV

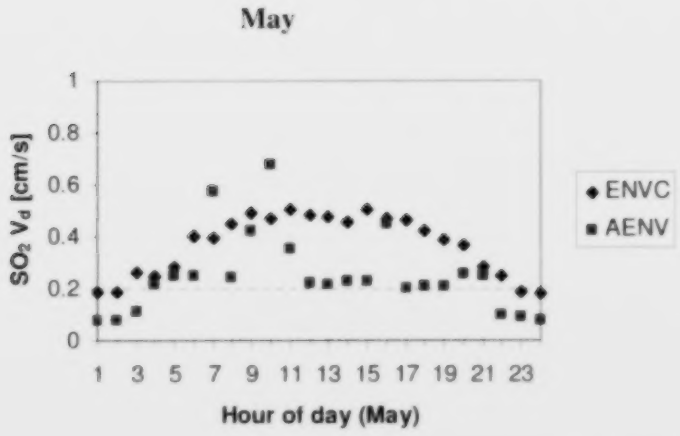
May
1
0.8
0.6
0.4
0.2
0
SO2 Vd [cm/s]
1 3 5 7 9 11 13 15 17 19 21 23
Hour of day (May)
ENVC
AENV

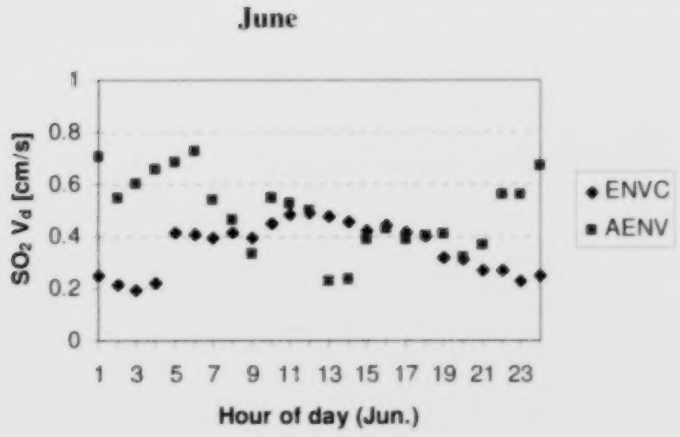
June
1
0.8
0.6
0.4
0.2
0
SO2 Vd [cm/s]
1 3 5 7 9 11 13 15 17 19 21 23
Hour of day (Jun.)
ENVC
AENV

July

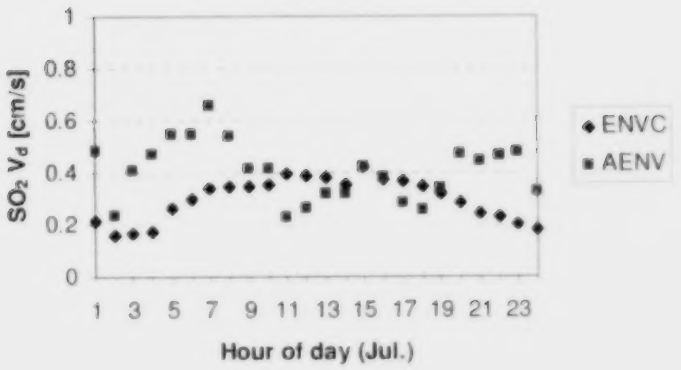

August

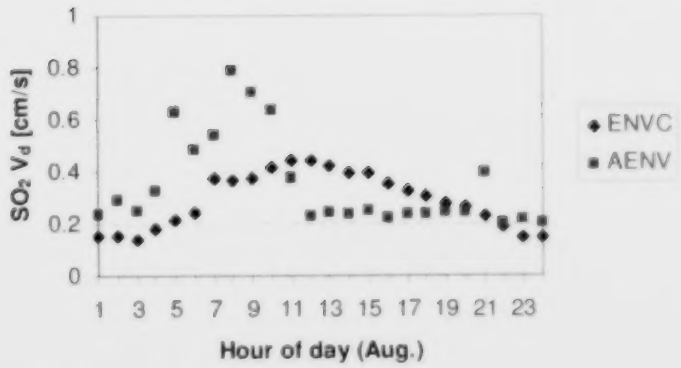

September

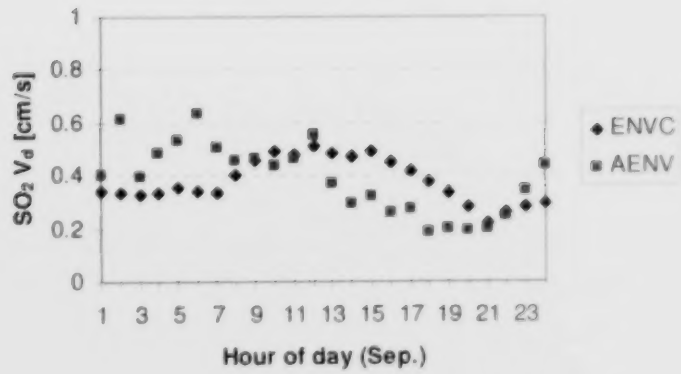

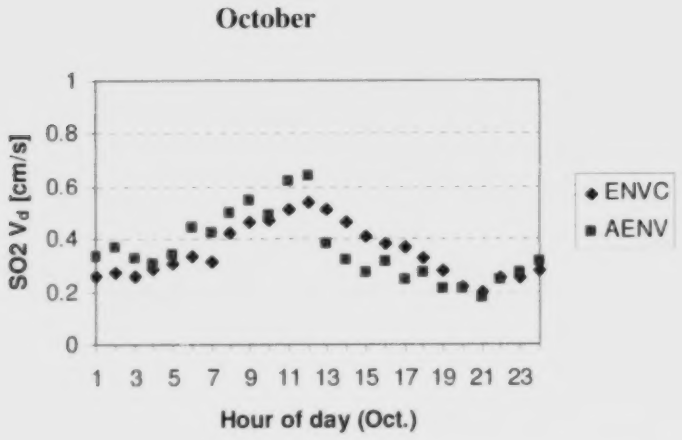
October
SO2 Vd [cm/s]
1
0.8
0.6
0.4
0.2
0
1 3 5 7 9 11 13 15 17 19 21 23
Hour of day (Oct.)
ENVC
AENV

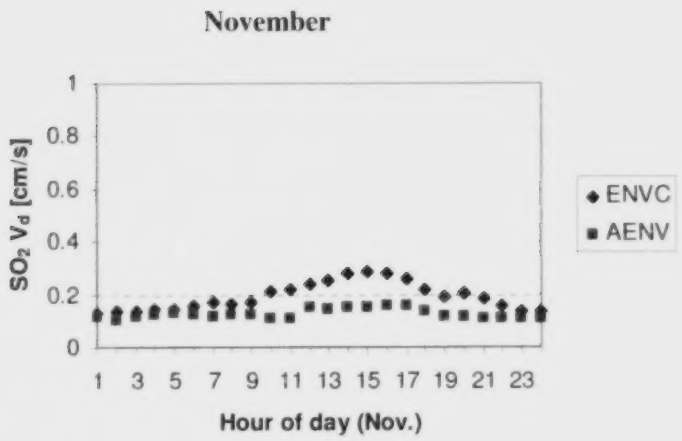
November
SO2 Vd [cm/s]
1
0.8
0.6
0.4
0.2
0
1 3 5 7 9 11 13 15 17 19 21 23
Hour of day (Nov.)
ENVC
AENV

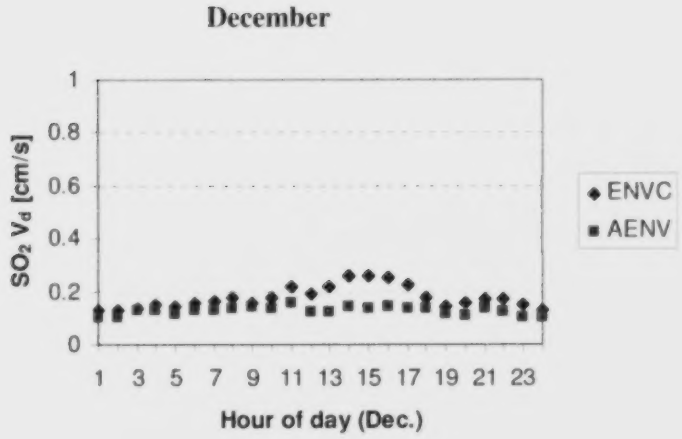
December
SO2 Vd [cm/s]
1
0.8
0.6
0.4
0.2
0
1 3 5 7 9 11 13 15 17 19 21 23
Hour of day (Dec.)
ENVC
AENV

NO_2

January

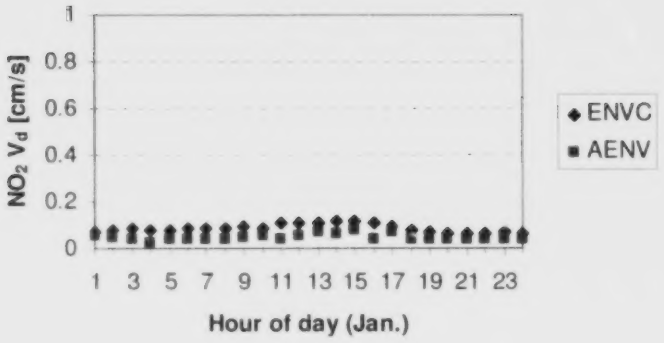

February

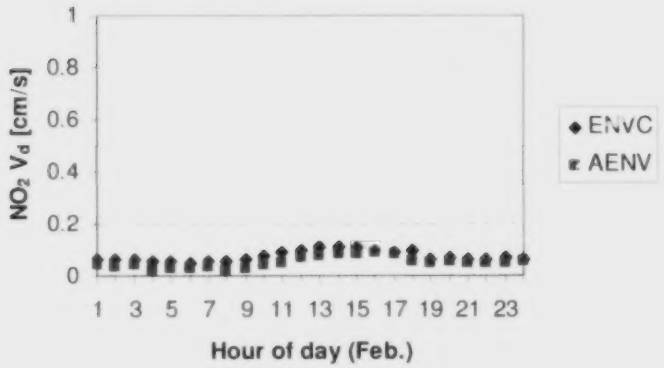

March

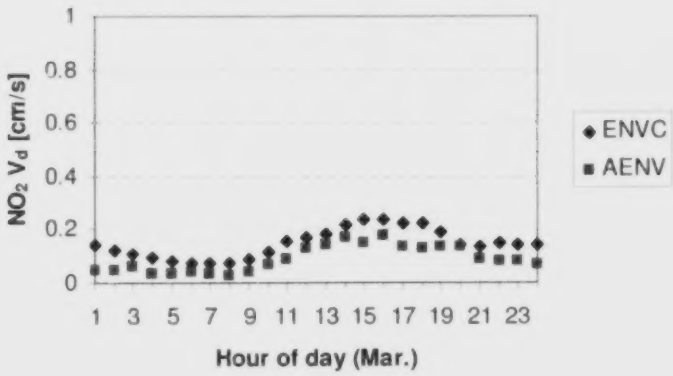

April

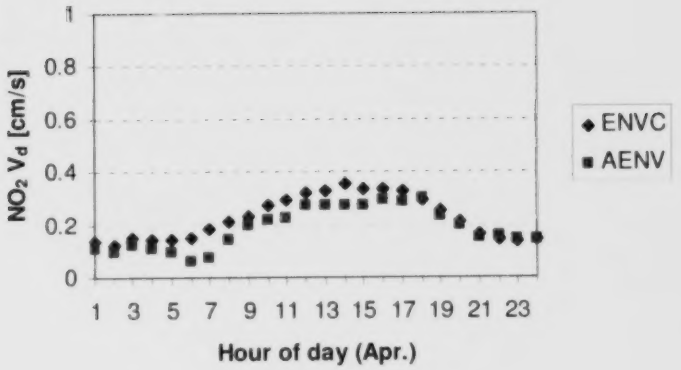

May

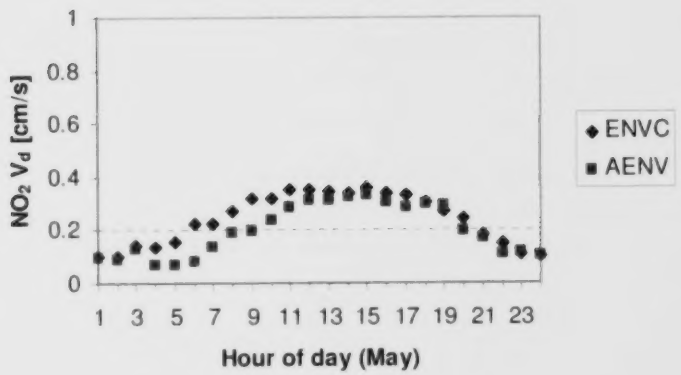

June

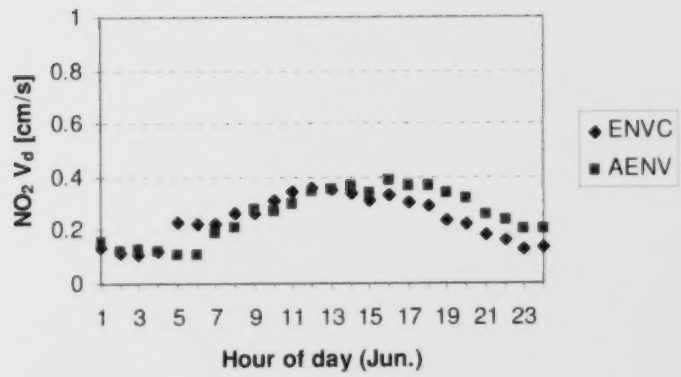

July

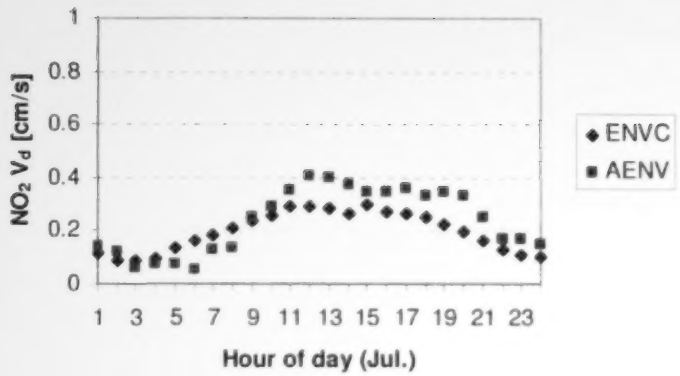

August

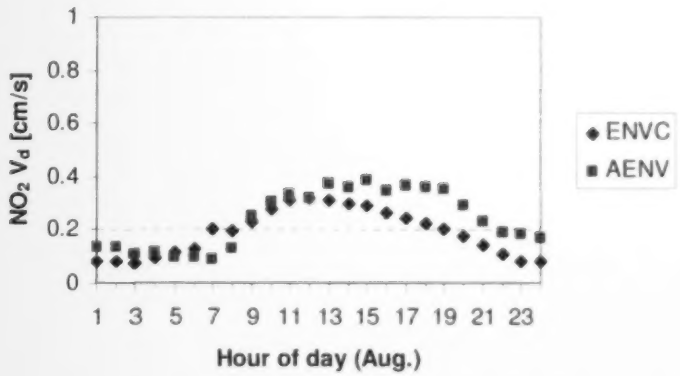

September

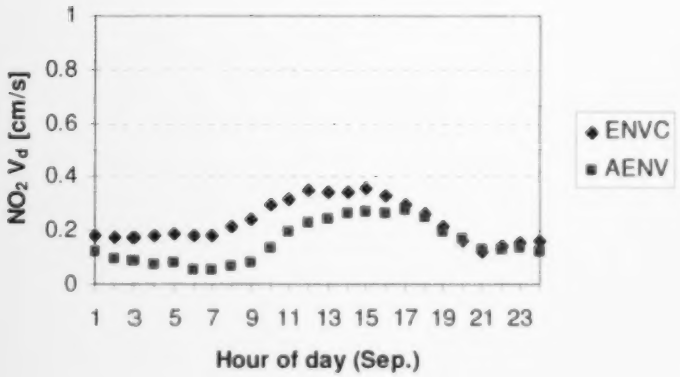

October

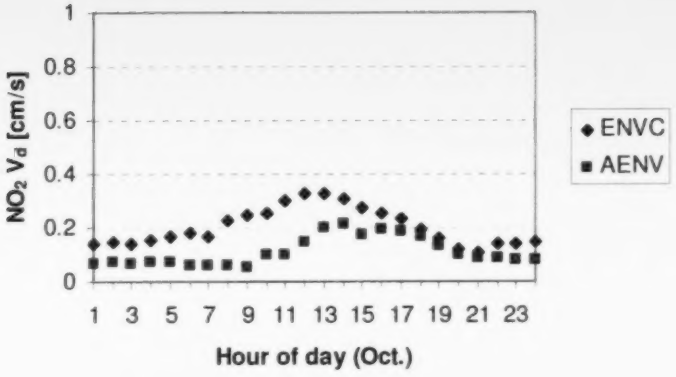

November

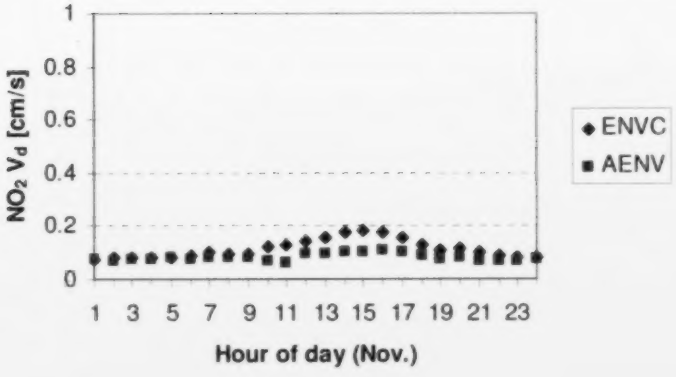

December

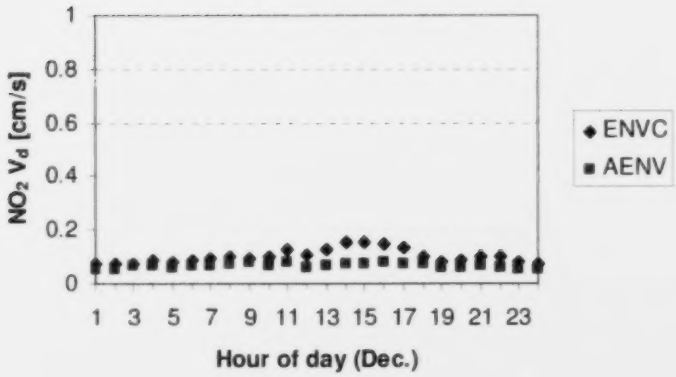

HNO_3

January

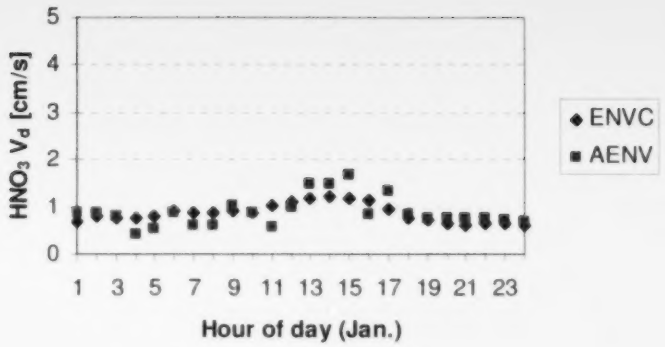

February

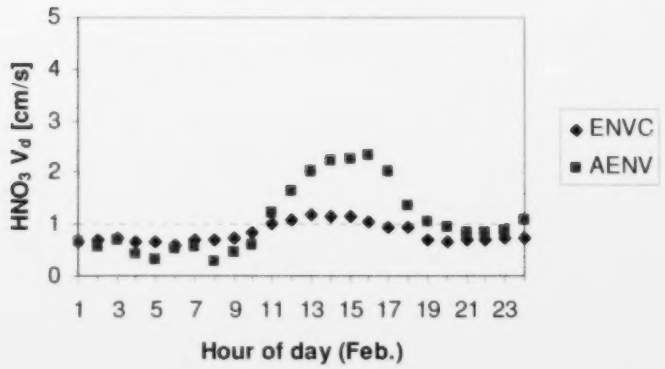

March

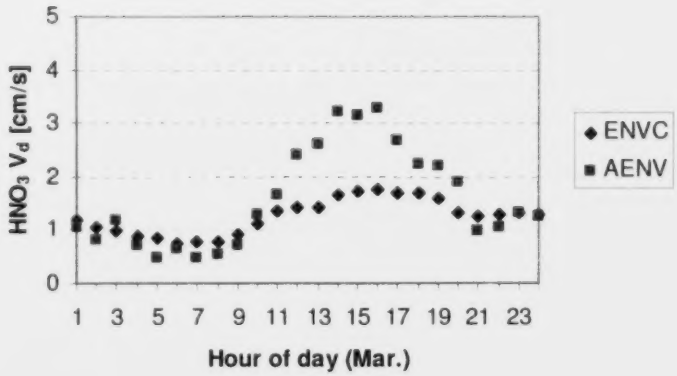

April

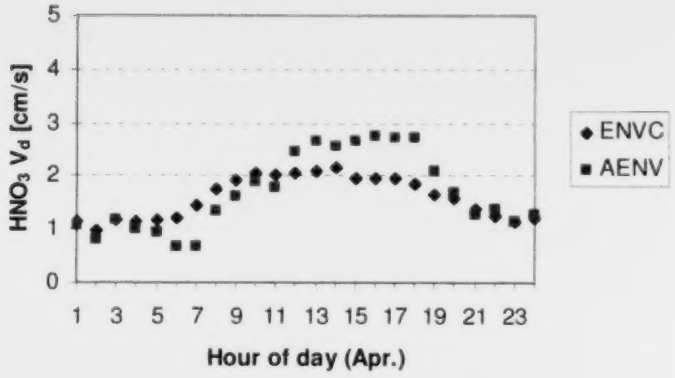

May

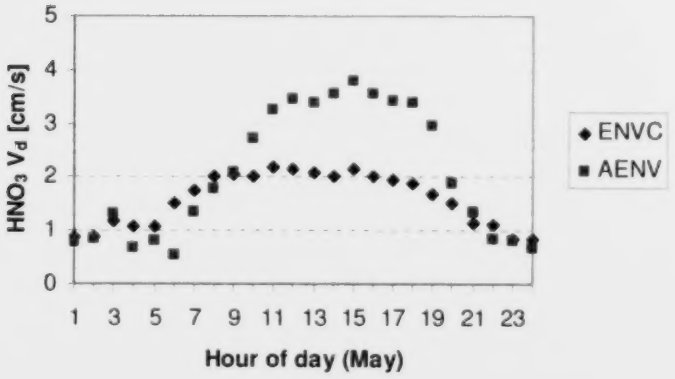

June

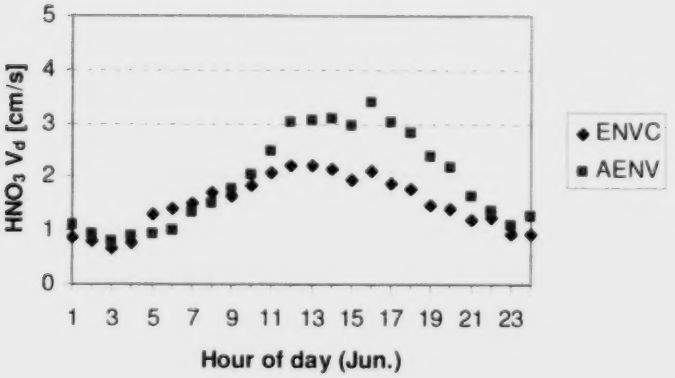

July

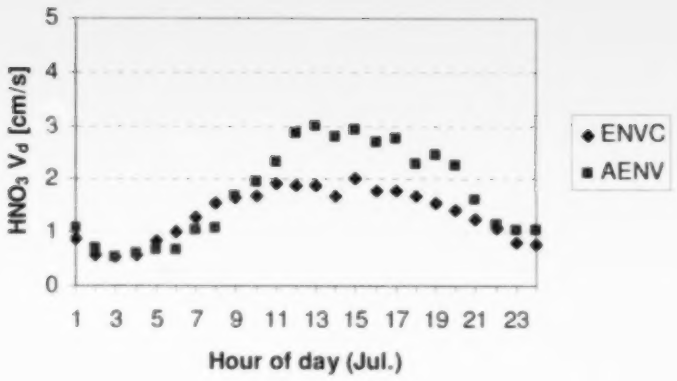

August

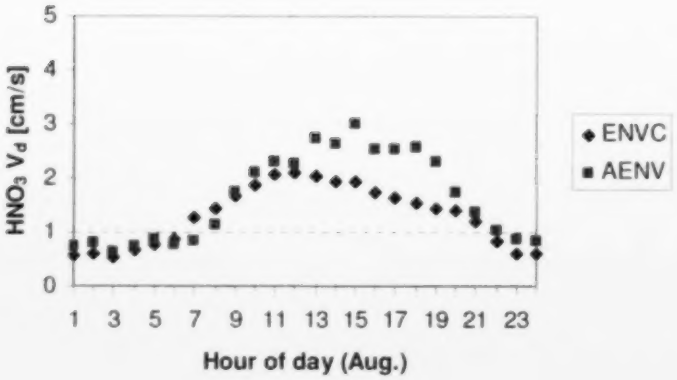

September

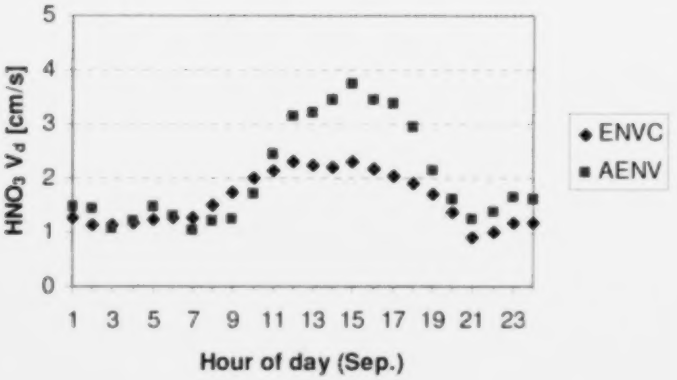

October

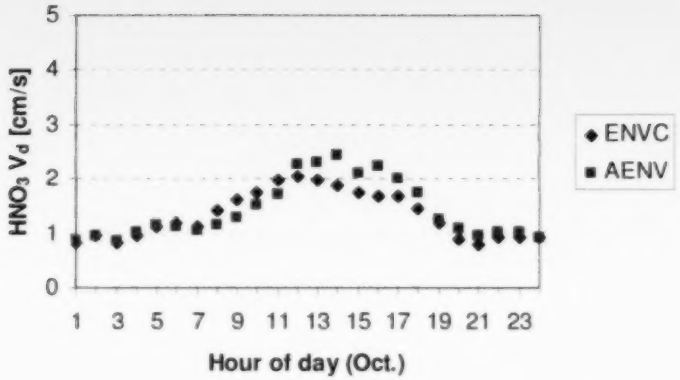

November

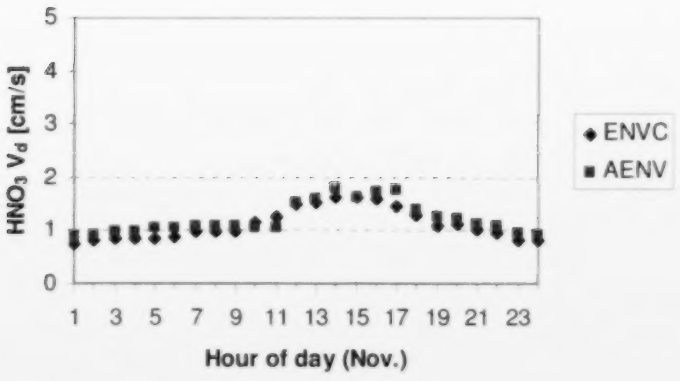

December

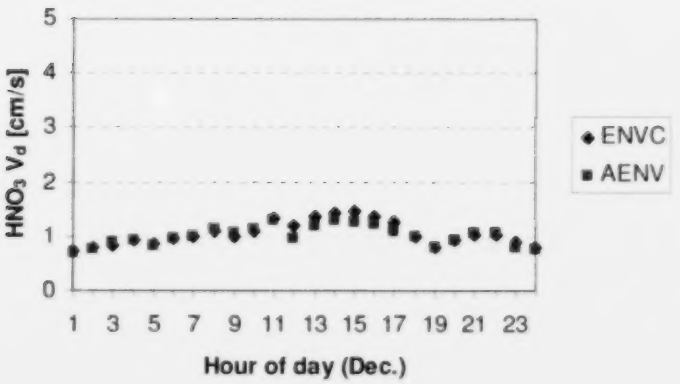

APPENDIX F COUNTS FOR RESISTANCE FACTORS

Table F1 Number of times hourly calculated R_a, R_b, or R_c was the largest (dominant) resistance factor in AENV model for SO_2.

	value of total R (s/m)	<10	10-100	100-300	300-1000	>1000
	dep vel Vd (cm/s)	>10.0	1.0-10.0	0.3-1.0	0.1-0.3	<0.1
jan	total resistance	0	0	0	346	397
	Ra	0	0	0	0	194
	Rb	0	0	0	0	0
	Rc	0	0	0	346	6
feb	total resistance	0	0	0	351	321
	Ra	0	0	0	0	102
	Rb	0	0	0	0	0
	Rc	0	0	0	351	3
mar	total resistance	0	3	0	421	320
	Ra	0	0	0	0	123
	Rb	0	3	0	0	0
	Rc	0	0	0	421	2
apr	total resistance	0	6	1	520	193
	Ra	0	2	1	4	89
	Rb	0	4	0	0	0
	Rc	0	0	0	516	0
may	total resistance	0	16	1	479	248
	Ra	0	3	1	5	167
	Rb	0	13	0	0	0
	Rc	0	0	0	474	1
jun	total resistance	0	60	9	475	176
	Ra	0	10	9	22	157
	Rb	0	50	0	0	0
	Rc	0	0	0	453	0
jul	total resistance	0	66	27	457	194
	Ra	0	3	21	19	129
	Rb	0	63	6	0	0
	Rc	0	0	0	438	0
aug	total resistance	0	55	14	461	214
	Ra	0	13	14	18	165
	Rb	0	42	0	0	0
	Rc	0	0	0	443	0
sep	total resistance	0	81	31	414	194
	Ra	0	4	28	27	146
	Rb	0	30	3	0	0
	Rc	0	47	0	387	0
oct	total resistance	0	96	42	353	253
	Ra	0	20	42	25	233
	Rb	0	28	0	0	0
	Rc	0	48	0	328	0
nov	total resistance	0	0	0	483	237
	Ra	0	0	0	0	191
	Rb	0	0	0	0	0
	Rc	0	0	0	483	4
dec	total resistance	0	0	0	525	219
	Ra	0	0	0	0	161
	Rb	0	0	0	0	0
	Rc	0	0	0	525	8

Table F2 Number of times hourly calculated R_a, R_b, or R_c was the largest (dominant) resistance factor in ENVC model for SO_2.

	value of total R (s/m)	<10	10-100	100-300	300-1000	>1000
	dep vel Vd (cm/s)	>10.0	1.0-10.0	0.3-1.0	0.1-0.3	<0.1
jan	total resistance	0	3	68	300	372
	Ra	0	0	0	0	0
	Rb	0	0	0	0	0
	Rc	0	3	68	300	372
feb	total resistance	0	0	8	339	325
	Ra	0	0	0	0	0
	Rb	0	0	0	0	0
	Rc	0	0	8	339	325
maar	total resistance	0	8	157	359	220
	Ra	0	0	0	0	0
	Rb	0	0	0	0	0
	Rc	0	8	157	359	220
apr	total resistance	0	10	301	312	97
	Ra	0	0	0	0	0
	Rb	0	0	0	0	0
	Rc	0	10	301	312	97
may	total resistance	0	30	311	271	132
	Ra	0	0	0	0	0
	Rb	0	0	0	0	0
	Rc	0	30	311	271	132
jun	total resistance	0	19	299	306	96
	Ra	0	0	0	0	0
	Rb	0	0	0	0	0
	Rc	0	19	299	306	96
jjul	total resistance	0	0	275	356	113
	Ra	0	0	0	0	0
	Rb	0	0	0	0	0
	Rc	0	0	275	356	113
aug	total resistance	0	5	258	342	139
	Ra	0	0	0	0	0
	Rb	0	0	0	0	0
	Rc	0	5	258	342	139
sep	total resistance	0	22	320	270	108
	Ra	0	0	0	0	0
	Rb	0	0	0	0	0
	Rc	0	22	320	270	108
oct	total resistance	0	12	317	264	151
	Ra	0	0	0	0	0
	Rb	0	0	0	0	0
	Rc	0	12	317	264	151
nov	total resistance	0	1	117	355	247
	Ra	0	0	0	0	0
	Rb	0	0	0	0	0
	Rc	0	1	117	355	247
dec	total resistance	0	1	89	385	269
	Ra	0	0	0	0	0
	Rb	0	0	0	0	0
	Rc	0	1	89	385	269

Table F3 Number of times hourly calculated R_a, R_b, or R_c was the largest (dominant) resistance factor in AENV model for NO_2.

	value of total R (s/m)	<10	10-100	100-300	300-1000	>1000
	dep vel Vd (cm/s)	>10.0	1.0-10.0	0.3-1.0	0.1-0.3	<0.1
jan	total resistance	0	0	0	0	743
	Ra	0	0	0	0	173
	Rb	0	0	0	0	0
	Rc	0	0	0	0	375
feb	total resistance	0	0	0	0	672
	Ra	0	0	0	0	98
	Rb	0	0	0	0	0
	Rc	0	0	0	0	361
mar	total resistance	0	0	75	33	636
	Ra	0	0	0	2	110
	Rb	0	0	0	0	0
	Rc	0	0	75	31	332
apr	total resistance	0	0	159	213	348
	Ra	0	0	0	13	87
	Rb	0	0	0	0	0
	Rc	0	0	159	200	157
may	total resistance	0	0	300	136	308
	Ra	0	0	0	16	157
	Rb	0	0	0	0	0
	Rc	0	0	300	120	71
jun	total resistance	0	0	397	70	253
	Ra	0	0	0	22	145
	Rb	0	0	0	0	0
	Rc	0	0	397	48	89
jul	total resistance	0	0	403	43	298
	Ra	0	0	0	17	120
	Rb	0	0	0	0	0
	Rc	0	0	403	26	115
aug	total resistance	0	0	395	59	290
	Ra	0	0	0	14	145
	Rb	0	0	0	0	0
	Rc	0	0	395	45	97
sep	total resistance	0	0	0	390	330
	Ra	0	0	0	7	120
	Rb	0	0	0	0	0
	Rc	0	0	0	383	163
oct	total resistance	0	0	0	271	473
	Ra	0	0	0	6	196
	Rb	0	0	0	0	0
	Rc	0	0	0	265	258
nov	total resistance	0	0	0	66	654
	Ra	0	0	0	2	173
	Rb	0	0	0	0	0
	Rc	0	0	0	64	440
dec	total resistance	0	0	0	0	751
	Ra	0	0	0	0	137
	Rb	0	0	0	0	0
	Rc	0	0	0	0	558

Table F4 Number of times hourly calculated R_a, R_b, or R_c was the largest (dominant) resistance factor in ENVC model for NO_2.

	value of total R (s/m)	<10	10-100	100-300	300-1000	>1000
	dep vel Vd (cm/s)	>10.0	1.0-10.0	0.3-1.0	0.1-0.3	<0.1
jan	total resistance	0	0	17	199	527
	Ra	0	0	0	0	0
	Rb	0	0	0	0	0
	Rc	0	0	17	199	527
feb	total resistance	0	0	2	184	486
	Ra	0	0	0	0	0
	Rb	0	0	0	0	0
	Rc	0	0	2	184	486
mar	total resistance	0	0	72	344	328
	Ra	0	0	0	0	0
	Rb	0	0	0	0	0
	Rc	0	0	72	344	328
apr	total resistance	0	0	161	390	169
	Ra	0	0	0	0	0
	Rb	0	0	0	0	0
	Rc	0	0	161	390	169
may	total resistance	0	0	197	364	183
	Ra	0	0	0	0	0
	Rb	0	0	0	0	0
	Rc	0	0	197	364	183
jun	total resistance	0	0	188	379	153
	Ra	0	0	0	0	0
	Rb	0	0	0	0	0
	Rc	0	0	188	379	153
jul	total resistance	0	0	97	463	184
	Ra	0	0	0	0	0
	Rb	0	0	0	0	0
	Rc	0	0	97	463	184
aug	total resistance	0	0	92	434	218
	Ra	0	0	0	0	0
	Rb	0	0	0	0	0
	Rc	0	0	92	434	218
sep	total resistance	0	0	170	383	167
	Ra	0	0	0	0	0
	Rb	0	0	0	0	0
	Rc	0	0	170	383	167
oct	total resistance	0	0	144	398	202
	Ra	0	0	0	0	0
	Rb	0	0	0	0	0
	Rc	0	0	144	398	202
nov	total resistance	0	0	29	302	389
	Ra	0	0	0	0	0
	Rb	0	0	0	0	0
	Rc	0	0	29	302	389
dec	total resistance	0	0	15	277	452
	Ra	0	0	0	0	0
	Rb	0	0	0	0	0
	Rc	0	0	15	277	452

Table F5 Number of times hourly calculated R_a, R_b, or R_c was the largest (dominant) resistance factor in AENV model for HNO_3.

	value of total R (s/m)	<10	10-100	100-300	300-1000	>1000
	dep vel Vd (cm/s)	>10.0	1.0-10.0	0.3-1.0	0.1-0.3	<0.1
jan	total resistance	0	257	73	41	372
	Ra	0	22	58	40	175
	Rb	0	210	15	1	0
	Rc	0	25	0	0	0
feb	total resistance	0	291	46	21	314
	Ra	0	8	29	21	98
	Rb	0	261	17	0	0
	Rc	0	22	0	0	0
mar	total resistance	0	383	29	24	308
	Ra	0	16	26	24	113
	Rb	0	267	3	0	0
	Rc	0	100	0	0	0
apr	total resistance	0	469	44	16	191
	Ra	0	35	36	16	87
	Rb	0	351	8	0	0
	Rc	0	83	0	0	0
may	total resistance	0	438	44	30	232
	Ra	0	48	43	30	152
	Rb	0	211	1	0	0
	Rc	0	179	0	0	0
jun	total resistance	0	461	54	37	168
	Ra	0	49	54	37	149
	Rb	0	319	0	0	0
	Rc	0	93	0	0	0
jul	total resistance	0	463	59	35	187
	Ra	0	7	35	35	122
	Rb	0	377	24	0	0
	Rc	0	79	0	0	0
aug	total resistance	0	447	63	27	207
	Ra	0	22	51	27	158
	Rb	0	374	12	0	0
	Rc	0	51	0	0	0
sep	total resistance	0	447	50	36	187
	Ra	0	18	46	36	139
	Rb	0	284	4	0	0
	Rc	0	145	0	0	0
oct	total resistance	0	377	77	51	239
	Ra	0	61	74	51	219
	Rb	0	252	3	0	0
	Rc	0	64	0	0	0
nov	total resistance	0	373	94	33	220
	Ra	0	57	87	33	178
	Rb	0	305	7	0	0
	Rc	0	11	0	0	0
dec	total resistance	0	367	139	47	191
	Ra	0	360	139	47	141
	Rb	0	0	0	0	0
	Rc	0	7	0	0	0

Table F6 Number of times hourly calculated R_a, R_b, or R_c was the largest (dominant) resistance factor in ENVC model for HNO_3.

	value of total R (s/m)	<10	10-100	100-300	300-1000	>1000
	dep vel Vd (cm/s)	>10.0	1.0-10.0	0.3-1.0	0.1-0.3	<0.1
jan	total resistance	0	237	299	116	91
	Ra	0	12	45	53	68
	Rb	0	3	0	0	0
	Rc	0	222	254	63	23
feb	total resistance	0	205	336	67	64
	Ra	0	3	4	39	42
	Rb	0	0	0	0	0
	Rc	0	202	332	28	22
mar	total resistance	0	400	198	80	66
	Ra	0	4	16	51	37
	Rb	0	37	0	0	0
	Rc	0	359	182	29	29
apr	total resistance	0	478	161	56	25
	Ra	0	22	35	50	25
	Rb	0	54	0	0	0
	Rc	0	402	126	6	0
may	total resistance	0	462	154	80	48
	Ra	0	43	65	64	47
	Rb	0	56	0	0	1
	Rc	0	363	89	16	0
jun	total resistance	0	433	202	69	16
	Ra	0	70	109	64	16
	Rb	0	16	0	0	0
	Rc	0	347	93	5	0
jul	total resistance	0	431	197	101	15
	Ra	0	54	89	101	15
	Rb	0	27	0	0	0
	Rc	0	350	108	0	0
aug	total resistance	0	437	160	135	12
	Ra	0	48	87	135	12
	Rb	0	19	0	0	0
	Rc	0	370	73	0	0
sep	total resistance	0	446	134	129	11
	Ra	0	62	103	129	11
	Rb	0	43	0	0	0
	Rc	0	341	31	0	0
oct	total resistance	0	380	199	117	48
	Ra	0	152	163	114	48
	Rb	0	19	0	0	0
	Rc	0	209	36	3	0
nov	total resistance	0	334	229	88	69
	Ra	0	13	62	80	69
	Rb	0	6	0	0	0
	Rc	0	315	167	8	0
dec	total resistance	0	339	288	75	42
	Ra	0	7	42	69	42
	Rb	0	9	0	0	0
	Rc	0	323	246	6	0

Table F7 Number of times hourly calculated R_a, R_b, or R_c was the largest (dominant) resistance factor in AENV model for HNO_3 for total resistance <100 s/m.

	value of total R (s/m)	<15	15-25	25-40	40-65	65-100
	dep vel Vd (cm/s)	>6.7	4.0-6.7	2.5-4.0	1.5-2.5	1.0-1.5
jan	total resistance	0	19	67	103	68
	Ra	0	0	0	3	19
	Rb	0	0	61	100	49
	Rc	0	19	6	0	0
feb	total resistance	0	7	111	121	52
	Ra	0	0	0	1	7
	Rb	0	0	96	120	45
	Rc	0	7	15	0	0
mar	total resistance	0	74	173	103	33
	Ra	0	0	0	3	13
	Rb	0	0	147	100	20
	Rc	0	74	26	0	0
apr	total resistance	0	29	197	162	81
	Ra	0	0	0	3	32
	Rb	0	0	143	159	49
	Rc	0	29	54	0	0
may	total resistance	0	146	189	69	34
	Ra	0	0	0	17	31
	Rb	0	0	156	52	3
	Rc	0	146	33	0	0
jun	total resistance	0	58	242	123	38
	Ra	0	0	4	17	28
	Rb	0	0	203	106	10
	Rc	0	58	35	0	0
jul	total resistance	0	51	183	171	58
	Ra	0	0	0	0	7
	Rb	0	0	155	171	51
	Rc	0	51	28	0	0
aug	total resistance	0	31	197	168	51
	Ra	0	0	0	2	20
	Rb	0	0	177	166	31
	Rc	0	31	20	0	0
sep	total resistance	0	124	179	105	39
	Ra	0	0	0	1	17
	Rb	0	0	158	104	22
	Rc	0	124	21	0	0
oct	total resistance	0	42	155	112	68
	Ra	0	0	0	12	49
	Rb	0	0	133	100	19
	Rc	0	42	22	0	0
nov	total resistance	0	1	121	164	87
	Ra	0	0	0	15	42
	Rb	0	0	111	149	45
	Rc	0	1	10	0	0
dec	total resistance	0	3	25	177	162
	Ra	0	0	21	177	162
	Rb	0	0	0	0	0
	Rc	0	3	4	0	0

Table F8 Number of times hourly calculated R_a, R_b, or R_c was the largest (dominant) resistance factor in ENVC model for HNO_3 for total resistance <100 s/m.

	value of total R (s/m)	<15	15-25	25-40	40-65	65-100
	dep vel Vd (cm/s)	>6.7	4.0-6.7	2.5-4.0	1.5-2.5	1.0-1.5
jan	total resistance	0	11	19	73	134
	Ra	0	0	0	4	8
	Rb	0	0	0	2	1
	Rc	0	11	19	67	125
feb	total resistance	0	0	1	75	129
	Ra	0	0	0	2	1
	Rb	0	0	0	0	0
	Rc	0	0	1	73	128
mar	total resistance	0	9	75	155	161
	Ra	0	0	0	0	4
	Rb	0	0	15	18	4
	Rc	0	9	60	137	153
apr	total resistance	0	15	138	170	155
	Ra	0	0	0	5	17
	Rb	0	0	34	15	5
	Rc	0	15	104	150	133
may	total resistance	0	27	138	166	131
	Ra	0	0	5	17	21
	Rb	0	0	38	13	5
	Rc	0	27	95	136	105
jun	total resistance	0	11	135	150	137
	Ra	0	0	18	22	30
	Rb	0	0	12	4	0
	Rc	0	11	105	124	107
jul	total resistance	0	9	78	186	158
	Ra	0	0	1	14	39
	Rb	0	0	6	11	10
	Rc	0	9	71	161	109
aug	total resistance	0	4	81	199	153
	Ra	0	0	0	17	31
	Rb	0	0	9	5	5
	Rc	0	4	72	177	117
sep	total resistance	0	35	132	162	117
	Ra	0	0	1	23	38
	Rb	0	0	15	14	14
	Rc	0	35	116	125	65
oct	total resistance	0	9	114	150	107
	Ra	0	0	17	76	59
	Rb	0	0	18	1	0
	Rc	0	9	79	73	48
nov	total resistance	0	0	58	145	131
	Ra	0	0	0	7	6
	Rb	0	0	5	1	0
	Rc	0	0	53	137	125
dec	total resistance	0	1	42	131	165
	Ra	0	0	0	5	2
	Rb	0	0	6	3	0
	Rc	0	1	36	123	163

APPENDIX G BREAKDOWN OF CHEMICALS CONTRIBUTING TO DIFFERENCES IN DEPOSITION CAUSED BY PERCENT CHANGES OF RESISTANCES (R_A, R_B, AND R_C)

Light yellow, gold, and orange highlighting in tables shown below indicate small, medium, and large differences in deposition (in H^+ equivalents), respectively.

Table G1 Influence of ±10% and ±50% change in R_a on total deposition (in H^+ equivalents) as a result of sensitivity testing of AENV model.

	base case total	absolute difference from base case (g H+/ha)			
Ra		0.5	0.9	1.1	1.5
Month 1	16.9	2.6	0.4	-0.4	-1.7
Month 2	11.7	1.0	0.2	-0.2	-0.7
Month 3	17.0	1.3	0.2	-0.2	-0.9
Month 4	15.9	1.7	0.3	-0.3	-1.2
Month 5	14.0	1.5	0.2	-0.2	-1.0
Month 6	7.5	0.7	0.1	-0.1	-0.5
Month 7	7.6	0.3	0.0	0.0	-0.2
Month 8	13.6	1.1	0.2	-0.2	-0.7
Month 9	9.8	0.7	0.1	-0.1	-0.5
Month 10	16.8	2.4	0.4	-0.4	-1.6
Month 11	0.2	-0.1	0.0	0.0	0.1
Month 12	16.3	2.3	0.4	-0.3	-1.5

Table G2 Influence of ±10% and ±50% change in R_a on HNO_2 deposition (in H^+ equivalents) as a result of sensitivity testing of AENV model.

	base case	absolute difference from base case (g H+/ha)			
month	(g H+/ha)	0.5	0.9	1.1	1.5
Month 1	3.2	0.8	0.1	-0.1	-0.5
Month 2	0.8	0.2	0.0	0.0	-0.1
Month 3	0.6	0.1	0.0	0.0	-0.1
Month 4	1.0	0.3	0.0	0.0	-0.2
Month 5	1.7	0.3	0.1	0.0	-0.2
Month 6	0.2	0.0	0.0	0.0	0.0
Month 7	0.3	0.1	0.0	0.0	0.0
Month 8	0.5	0.1	0.0	0.0	-0.1
Month 9	1.1	0.2	0.0	0.0	-0.1
Month 10	2.5	0.5	0.1	-0.1	-0.4
Month 11	1.2	0.3	0.1	0.0	-0.2
Month 12	4.8	1.5	0.2	-0.2	-0.9

Table G3 Influence of ±10% and ±50% change in R_a on HNO_3 deposition (in H^+ equivalents) as a result of sensitivity testing of AENV model.

	base case	absolute difference from base case (g H+/ha)			
month	(g H+/ha)	0.5	0.9	1.1	1.5
Month 1	4.8	1.1	0.2	-0.2	-0.7
Month 2	2.5	0.5	0.1	-0.1	-0.3
Month 3	4.1	0.7	0.1	-0.1	-0.5
Month 4	4.6	1.0	0.2	-0.2	-0.7
Month 5	3.8	0.6	0.1	-0.1	-0.4
Month 6	1.7	0.3	0.1	0.0	-0.2
Month 7	1.9	0.4	0.1	-0.1	-0.3
Month 8	2.0	0.4	0.1	-0.1	-0.3
Month 9	1.4	0.2	0.0	0.0	-0.2
Month 10	8.3	1.5	0.3	-0.2	-1.1
Month 11	1.0	0.2	0.0	0.0	-0.2
Month 12	1.5	0.4	0.1	-0.1	-0.3

Table G4 Influence of ±10% and ±50% change in R_b on total deposition (in H^+ equivalents) as a result of sensitivity testing of AENV model.

	base case total	absolute difference from base case (g H+/ha)			
Rb		0.5	0.9	1.1	1.5
Month 1	16.9	3.2	0.5	-0.4	-1.9
Month 2	11.7	1.8	0.3	-0.2	-1.0
Month 3	17.0	3.7	0.5	-0.4	-1.8
Month 4	15.9	0.1	0.1	-0.1	-0.6
Month 5	14.0	0.8	0.2	-0.2	-0.8
Month 6	7.5	-0.7	0.0	0.0	0.0
Month 7	7.6	-3.4	-0.4	0.3	1.0
Month 8	13.6	-0.6	0.0	0.0	-0.2
Month 9	9.8	0.6	0.1	-0.1	-0.5
Month 10	16.8	0.5	0.2	-0.2	-1.1
Month 11	0.2	-5.8	-0.7	0.6	2.2
Month 12	16.3	0.6	0.2	-0.2	-0.7

Table G5 Influence of ±10% and ±50% change in R_b on HNO_3 deposition (in H^+ equivalents) as a result of sensitivity testing of AENV model.

	base case	absolute difference from base case (g H+/ha)			
month	(g H+/ha)	0.5	0.9	1.1	1.5
Month 1	4.8	1.3	0.2	-0.2	-0.8
Month 2	2.5	0.7	0.1	-0.1	-0.4
Month 3	4.1	1.0	0.2	-0.2	-0.7
Month 4	4.6	1.1	0.2	-0.2	-0.7
Month 5	3.8	0.8	0.1	-0.1	-0.6
Month 6	1.7	0.4	0.1	-0.1	-0.3
Month 7	1.9	0.5	0.1	-0.1	-0.3
Month 8	2.0	0.5	0.1	-0.1	-0.3
Month 9	1.4	0.3	0.1	-0.1	-0.2
Month 10	8.3	1.9	0.3	-0.3	-1.3
Month 11	1.0	0.2	0.0	0.0	-0.2
Month 12	1.5	0.4	0.1	-0.1	-0.2

Table G6 Influence of ±10% and ±50% change in R_b on SO_4^{2-} deposition (in H^+ equivalents) as a result of sensitivity testing of AENV model.

	base case	absolute difference from base case (g H+/ha)			
month	(g H+/ha)	0.5	0.9	1.1	1.5
Month 1	1.0	0.7	0.1	-0.1	-0.3
Month 2	1.0	0.8	0.1	-0.1	-0.3
Month 3	2.9	2.4	0.3	-0.2	-0.9
Month 4	1.3	1.1	0.1	-0.1	-0.4
Month 5	0.9	0.8	0.1	-0.1	-0.3
Month 6	1.0	0.8	0.1	-0.1	-0.3
Month 7	1.0	0.8	0.1	-0.1	-0.3
Month 8	1.3	1.0	0.1	-0.1	-0.4
Month 9	0.9	0.8	0.1	-0.1	-0.3
Month 10	1.3	1.0	0.1	-0.1	-0.4
Month 11	1.2	0.9	0.1	-0.1	-0.3
Month 12	1.0	0.7	0.1	-0.1	-0.3

Table G7 Influence of ±10% and ±50% change in R_b on NH_4^+ deposition (in H^+ equivalents) as a result of sensitivity testing of AENV model.

	base case	absolute difference from base case (g H+/ha)			
month	(g H+/ha)	0.5	0.9	1.1	1.5
Month 1	1.7	1.1	0.1	-0.1	-0.4
Month 2	1.3	1.0	0.1	-0.1	-0.4
Month 3	2.2	1.8	0.2	-0.2	-0.7
Month 4	1.8	1.5	0.2	-0.1	-0.5
Month 5	1.2	1.0	0.1	-0.1	-0.4
Month 6	1.2	1.0	0.1	-0.1	-0.4
Month 7	1.2	0.9	0.1	-0.1	-0.3
Month 8	1.7	1.3	0.2	-0.1	-0.5
Month 9	1.2	1.0	0.1	-0.1	-0.4
Month 10	1.5	1.2	0.1	-0.1	-0.4
Month 11	2.7	2.0	0.2	-0.2	-0.8
Month 12	1.2	0.9	0.1	-0.1	-0.3

Table G8 Influence of ±10% and ±50% change in R_b on Ca^{2+} deposition (in H^+ equivalents) as a result of sensitivity testing of AENV model.

	base case	absolute difference from base case (g H+/ha)			
month	(g H+/ha)	0.5	0.9	1.1	1.5
Month 1	-1.3	-0.5	-0.1	0.1	0.2
Month 2	-2.0	-0.9	-0.1	0.1	0.3
Month 3	-3.3	-1.4	-0.2	0.1	0.5
Month 4	-8.5	-3.7	-0.4	0.4	1.4
Month 5	-4.2	-1.9	-0.2	0.2	0.7
Month 6	-6.6	-2.8	-0.3	0.3	1.1
Month 7	-12.0	-5.1	-0.6	0.5	2.0
Month 8	-8.5	-3.6	-0.4	0.4	1.4
Month 9	-3.1	-1.4	-0.2	0.1	0.5
Month 10	-9.0	-3.9	-0.5	0.4	1.5
Month 11	-22.0	-9.0	-1.1	1.0	3.7
Month 12	-5.5	-2.2	-0.3	0.2	0.9

Table G9 Influence of ±10% and ±50% change in R_c on total deposition (in H^+ equivalents) as a result of sensitivity testing of AENV model.

	base case total	absolute difference from base case (g H+/ha)			
Rc		0.5	0.9	1.1	1.5
Month 1	16.9	6.7	0.9	-0.7	-2.9
Month 2	11.7	6.5	0.8	-0.7	-2.6
Month 3	17.0	8.6	1.1	-0.9	-3.5
Month 4	15.9	10.6	1.3	-1.1	-4.4
Month 5	14.0	8.5	1.1	-0.9	-3.6
Month 6	7.6	5.8	0.7	-0.6	-2.4
Month 7	7.6	9.4	1.1	-1.0	-3.6
Month 8	13.6	10.4	1.3	-1.1	-4.2
Month 9	9.8	6.6	0.8	-0.7	-2.6
Month 10	16.8	8.9	1.2	-1.0	-4.1
Month 11	0.2	6.2	0.8	-0.6	-2.4
Month 12	16.3	9.8	1.2	-1.0	-4.0

Table G8 Influence of ±10% and ±50% change in R_b on Ca^{2+} deposition (in H^+ equivalents) as a result of sensitivity testing of AENV model.

	base case	absolute difference from base case (g H+/ha)			
month	(g H+/ha)	0.5	0.9	1.1	1.5
Month 1	-1.3	-0.5	-0.1	0.1	0.2
Month 2	-2.0	-0.9	-0.1	0.1	0.3
Month 3	-3.3	-1.4	-0.2	0.1	0.5
Month 4	-8.5	-3.7	-0.4	0.4	1.4
Month 5	-4.2	-1.9	-0.2	0.2	0.7
Month 6	-6.6	-2.8	-0.3	0.3	1.1
Month 7	-12.0	-5.1	-0.6	0.5	2.0
Month 8	-8.5	-3.6	-0.4	0.4	1.4
Month 9	-3.1	-1.4	-0.2	0.1	0.5
Month 10	-9.0	-3.9	-0.5	0.4	1.5
Month 11	-22.0	-9.0	-1.1	1.0	3.7
Month 12	-5.5	-2.2	-0.3	0.2	0.9

Table G9 Influence of ±10% and ±50% change in R_c on total deposition (in H^+ equivalents) as a result of sensitivity testing of AENV model.

	base case total	absolute difference from base case (g H+/ha)			
Rc		0.5	0.9	1.1	1.5
Month 1	16.9	6.7	0.9	-0.7	-2.9
Month 2	11.7	6.5	0.8	-0.7	-2.6
Month 3	17.0	8.6	1.1	-0.9	-3.5
Month 4	15.9	10.6	1.3	-1.1	-4.4
Month 5	14.0	8.5	1.1	-0.9	-3.6
Month 6	7.6	5.8	0.7	-0.6	-2.4
Month 7	7.6	9.4	1.1	-1.0	-3.6
Month 8	13.6	10.4	1.3	-1.1	-4.2
Month 9	9.8	6.6	0.8	-0.7	-2.6
Month 10	16.8	8.9	1.2	-1.0	-4.1
Month 11	0.2	6.2	0.8	-0.6	-2.4
Month 12	16.3	9.8	1.2	-1.0	-4.0

Table G10 Influence of ±10% and ±50% change in R_c on SO_2 deposition (in H^+ equivalents) as a result of sensitivity testing of AENV model.

	base case	absolute difference from base case (g H+/ha)			
month		0.5	0.9	1.1	1.5
Month 1	1.2	0.9	0.1	-0.1	-0.3
Month 2	1.6	1.3	0.2	-0.1	-0.5
Month 3	2.2	1.8	0.2	-0.2	-0.6
Month 4	3.1	2.7	0.3	-0.3	-1.0
Month 5	2.6	2.3	0.3	-0.2	-0.8
Month 6	3.0	1.8	0.2	-0.2	-0.6
Month 7	4.5	3.6	0.4	-0.3	-1.3
Month 8	5.1	3.2	0.4	-0.3	-1.2
Month 9	2.1	1.3	0.2	-0.1	-0.5
Month 10	2.1	1.3	0.2	-0.1	-0.5
Month 11	0.6	0.5	0.1	-0.1	-0.2
Month 12	2.7	2.1	0.3	-0.2	-0.8

Table G11 Influence of ±10% and ±50% change in R_c on NO_2 deposition (in H^+ equivalents) as a result of sensitivity testing of AENV model.

	base case	absolute difference from base case (g H+/ha)			
month	(g H+/ha)	0.5	0.9	1.1	1.5
Month 1	6.4	4.7	0.6	-0.5	-1.8
Month 2	6.1	4.8	0.6	-0.5	-1.8
Month 3	7.3	5.8	0.7	-0.6	-2.2
Month 4	9.5	7.0	0.9	-0.7	-2.7
Month 5	6.8	5.0	0.6	-0.5	-1.9
Month 6	5.1	3.7	0.5	-0.4	-1.5
Month 7	7.0	5.4	0.7	-0.5	-2.1
Month 8	9.2	6.8	0.8	-0.7	-2.7
Month 9	5.7	4.7	0.6	-0.5	-1.7
Month 10	7.0	5.4	0.7	-0.5	-2.0
Month 11	6.9	5.3	0.6	-0.5	-2.0
Month 12	8.9	7.1	0.8	-0.7	-2.6

Table G10 Influence of ±10% and ±50% change in R_c on SO_2 deposition (in H^+ equivalents) as a result of sensitivity testing of AENV model.

	base case	absolute difference from base case (g H+/ha)			
month		0.5	0.9	1.1	1.5
Month 1	1.2	0.9	0.1	-0.1	-0.3
Month 2	1.6	1.3	0.2	-0.1	-0.5
Month 3	2.2	1.8	0.2	-0.2	-0.6
Month 4	3.1	2.7	0.3	-0.3	-1.0
Month 5	2.6	2.3	0.3	-0.2	-0.8
Month 6	3.0	1.8	0.2	-0.2	-0.6
Month 7	4.5	3.6	0.4	-0.3	-1.3
Month 8	5.1	3.2	0.4	-0.3	-1.2
Month 9	2.1	1.3	0.2	-0.1	-0.5
Month 10	2.1	1.3	0.2	-0.1	-0.5
Month 11	0.6	0.5	0.1	-0.1	-0.2
Month 12	2.7	2.1	0.3	-0.2	-0.8

Table G11 Influence of ±10% and ±50% change in R_c on NO_2 deposition (in H^+ equivalents) as a result of sensitivity testing of AENV model.

	base case	absolute difference from base case (g H+/ha)			
month	(g H+/ha)	0.5	0.9	1.1	1.5
Month 1	6.4	4.7	0.6	-0.5	-1.8
Month 2	6.1	4.8	0.6	-0.5	-1.8
Month 3	7.3	5.8	0.7	-0.6	-2.2
Month 4	9.5	7.0	0.9	-0.7	-2.7
Month 5	6.8	5.0	0.6	-0.5	-1.9
Month 6	5.1	3.7	0.5	-0.4	-1.5
Month 7	7.0	5.4	0.7	-0.5	-2.1
Month 8	9.2	6.8	0.8	-0.7	-2.7
Month 9	5.7	4.7	0.6	-0.5	-1.7
Month 10	7.0	5.4	0.7	-0.5	-2.0
Month 11	6.9	5.3	0.6	-0.5	-2.0
Month 12	8.9	7.1	0.8	-0.7	-2.6

APPENDIX H DEPOSITION CONTRIBUTIONS FOR SPECIES ASSOCIATED WITH LARGE PARTICLES

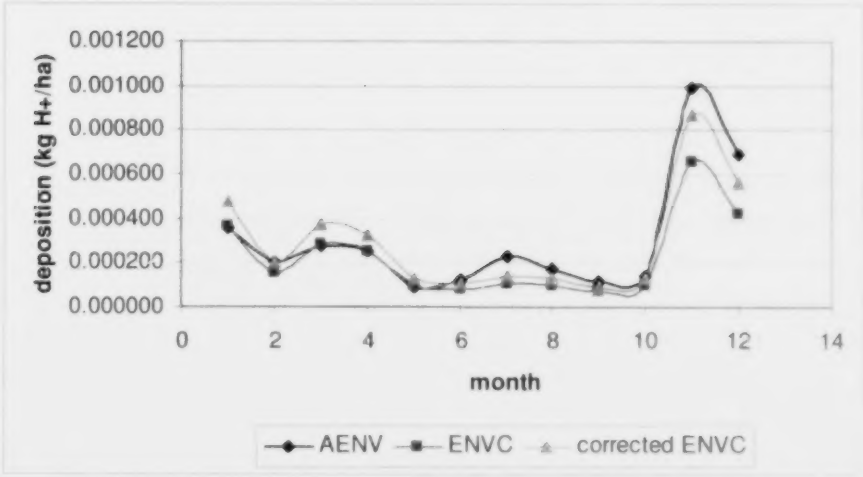

Figure H1 Monthly summed deposition flux for NO_3^- for AENV model base case, ENVC model, and ENVC model corrected for large particle size distribution for a coniferous forest cover.

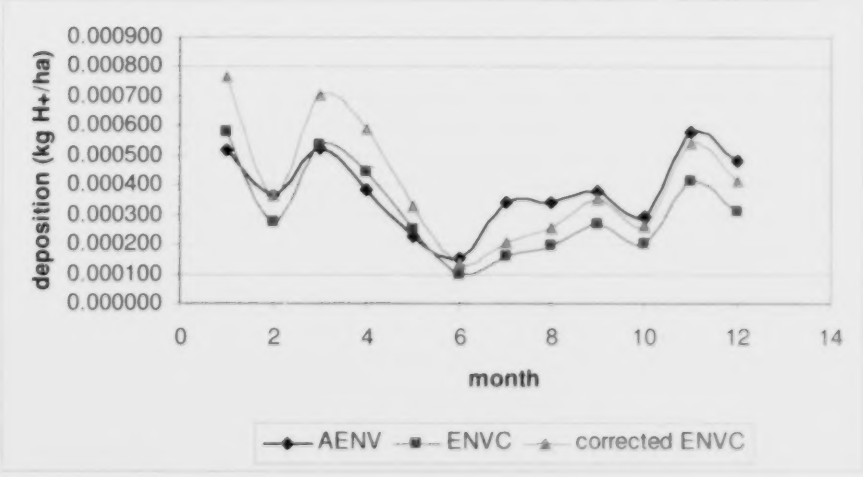

Figure H2 Monthly summed deposition flux for Na^+ for AENV model base case, ENVC model, and ENVC model corrected for large particle size distribution for a coniferous forest cover.

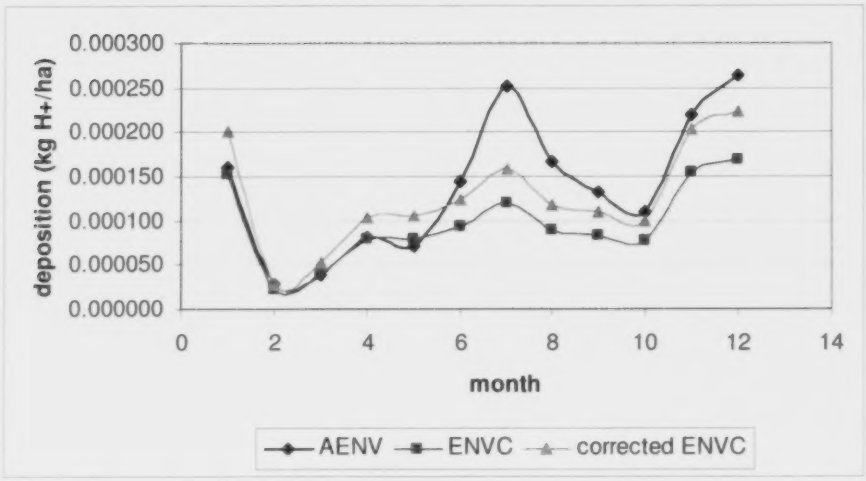

Figure H3 Monthly summed deposition flux for K^+ for AENV model base case, ENVC model, and ENVC model corrected for large particle size distribution for a coniferous forest cover.

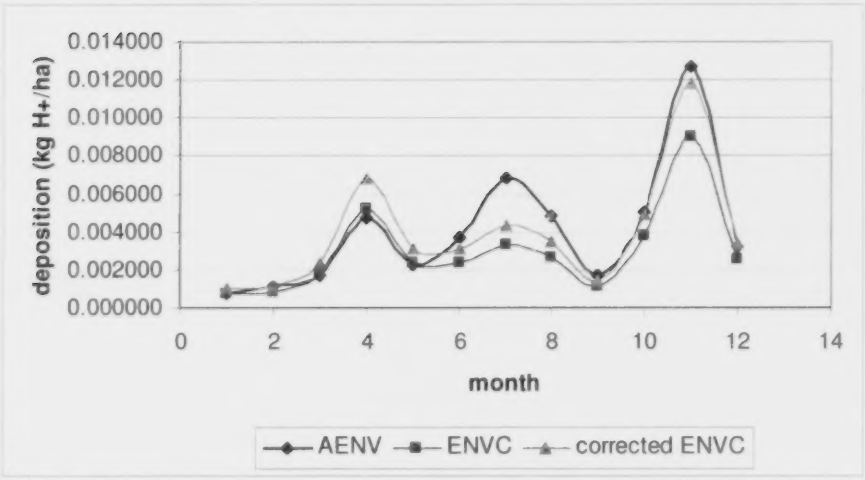

Figure H4 Monthly summed deposition flux for Ca^{2+} for AENV model base case, ENVC model, and ENVC model corrected for large particle size distribution for a coniferous forest cover.

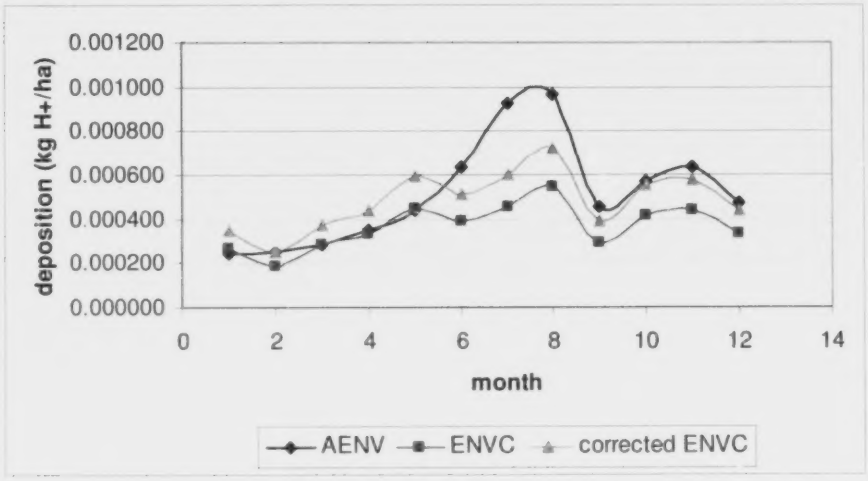

Figure H5 Monthly summed deposition flux for Mg^{2+} for AENV model base case, ENVC model, and ENVC model corrected for large particle size distribution for a coniferous forest cover.